



VIRUS ADSORPTION TO COLLOIDS IN WATER: INTERACTIONS BETWEEN
BACTERIOPHAGE MS2, KAOLINITE, AND FIBERGLASS

THESIS

Ashlee N. Ellis, Captain, USAF

AFIT-ENV-MS-19-M-171

DEPARTMENT OF THE AIR FORCE
AIR UNIVERSITY

AIR FORCE INSTITUTE OF TECHNOLOGY

Wright-Patterson Air Force Base, Ohio

DISTRIBUTION STATEMENT A. APPROVED FOR PUBLIC RELEASE;
DISTRIBUTION UNLIMITED.

The views expressed in this thesis are those of the author and do not reflect the official policy or position of the United States Air Force, Department of Defense, or the United States Government.

AFIT-ENV-MS-19-M-171

VIRUS ADSORPTION TO COLLOIDS IN WATER: INTERACTIONS BETWEEN
BACTERIOPHAGE MS2, KAOLINITE, AND FIBERGLASS

THESIS

Presented to the Faculty

Department of Systems and Engineering Management

Graduate School of Engineering and Management

Air Force Institute of Technology

Air University

Air Education and Training Command

In Partial Fulfillment of the Requirements for the
Degree of Master of Science in Engineering Management

Ashlee N. Ellis, BS

Captain, USAF

March 2019

DISTRIBUTION STATEMENT A.
APPROVED FOR PUBLIC RELEASE; DISTRIBUTION UNLIMITED.

VIRUS ADSORPTION TO COLLOIDS IN WATER: INTERACTIONS BETWEEN
BACTERIOPHAGE MS2, KAOLINITE, AND FIBERGLASS

Ashlee N. Ellis, BS

Captain, USAF

Committee Membership:

Approved:

Dr. Willie F. Harper, Jr., P.E. (Chair)

Date

Lt Col Andrew J. Hoisington, PhD, P.E. (Member)

Date

Dr. Yun Xing, PhD. (Member)

Date

Abstract

Virus adsorption to colloidal particles is an important issue in the water quality community, and it is a particularly important issue for conventional wastewater treatment plants that accept biohazardous waste. Colloids impact the transport of viruses in engineered treatment systems, and they also provide protection against oxidants and other destructive mechanisms. This study evaluated the adsorption of bacteriophage MS2 to colloidal suspensions of kaolinite (KAO) and fiberglass (FG). A series of laboratory batch tests were carried out over a range of experimental conditions to determine kinetic rate constants and characterize bond strength, and computational experiments were done to assess both adsorption and aggregation of MS2. First order removal rate constants were faster by an order of magnitude than previously reported values, and between $2.5 - 2.8 \text{ min}^{-1}$ and $0.4 - 2.8 \text{ min}^{-1}$ for KAO and FG, respectively. By the first sampling time following inoculation, significant MS2 adsorption was observed across all experimental conditions. Qualitative evidence of MS2 adsorption was collected with a large panel of fluorescent and bright field microscopic images, which showed clusters of MS2 on and around the colloidal particles. At the end of the two-hour FG experiment, 55.2% - 80.8% of the adsorbed MS2 was tightly bound, meaning that it was not readily removed during the wash step. For KAO, 54.8% - 87.9% of the adsorbed MS2 was tightly bound. This implies MS2 has a stronger affinity for KAO than FG. MS2 aggregation was also observed experimentally and was predicted on the basis of XDLVO models. These results show that clusters of viruses can quickly and strongly attach to colloids in a dynamic system, potentially leading to colloidal particles transporting and protecting viruses. Water resource recovery facilities (WRRF) need to pay attention to colloidal particles when treating biohazardous wastes.

Acknowledgments

My sincerest gratitude for the opportunity to research this subject and the invaluable skills and knowledge I gained throughout the process from Dr. Harper, Dr. Yun Xing, Lt Col Hoisington, Dr. Magnuson, and Dr. Irina Drachuk. The exciting experience working with you all has ignited what will be a life-long interest in water studies, and I will use what you taught me to help the Air Force and others every chance I get. Finally, there is no way this thesis would have been possible without my daughter's sweet hug breaks; and, most importantly, my husband's superhero skills of taking care of life for our family this past year and a half. Cheers to all of our accomplishment!

Ashlee N. Ellis

Table of Contents

	Page
Abstract.....	v
Acknowledgments.....	vi
Table of Contents	vii
List of Figures.....	ix
List of Tables	xii
I. Introduction	1
1.1 Introduction.....	1
II. Literature Review	4
2.1 The Properties of MS2	4
2.2 Colloids	5
2.2.1 <i>Colloid Characteristics</i>	5
2.2.2 <i>The Presence of Colloids in Influent and Effluent Streams</i>	8
2.2.3 <i>Adsorption of Viruses to Colloids</i>	10
2.3 XDLVO Modeling	11
III. Methodology	15
3.1 Overview	15
3.2 Preparation of Bacteriophage MS2	15
3.3. Colloidal Stock Solutions.....	17
3.4 Batch Tests with MS2 and Colloidal Suspensions.....	18
3.5 Particle Physicochemical Analysis	20
3.6 XDLVO Modeling	21
IV. Results	24
4.1 MS2 Removal Kinetics	24
4.2 Bond Strength	41
4.3 Surface Attachment and Aggregation	57
V. Conclusions	71
5.1 Conclusions.....	71
Appendix A Statistically Significant Removal of MS2.....	73

Appendix B	Supernatant Raw Data.....	85
Appendix C	Washed Pellet Raw Data.....	93
Appendix D	XDLVO Parameters.....	99
Bibliography	101

List of Figures

	Page
Figure 1. Centrifuged MS2 and <i>E. coli</i>	16
Figure 2. Lysed cells in agar.....	17
Figure 3. MS2 removal in the presence of colloids: First experiment.....	25
Figure 4. MS2 removal in the presence of colloids: Second experiment.....	27
Figure 5. MS2 removal in the presence of colloids: Third experiment.....	29
Figure 6. XPS spectra of KAO.....	31
Figure 7. XPS spectra of FG.....	32
Figure 8. First experiment low concentration FG.....	35
Figure 9. First experiment low concentration FG after 30 minutes.....	36
Figure 10. Second experiment high concentration FG colloids after 120 minutes.....	37
Figure 11. First experiment low concentration KAO.....	38
Figure 12. Second experiment low concentration KAO after 30 minutes.....	39
Figure 13. Second experiment high concentration KAO colloids after 120 minutes.....	40
Figure 14. Bond strength profile: Experiment one low concentration FG.....	43
Figure 15. Bond strength profile: Experiment one high concentration FG.....	44
Figure 16. Bond strength profile: Experiment one low concentration KAO.....	45
Figure 17. Bond strength profile: Experiment one high concentration KAO.....	46
Figure 18. Bond strength profile: Experiment two low concentration FG.....	48
Figure 19. Bond strength profile: Experiment two high concentration FG.....	49
Figure 20. Bond strength profile: Experiment two low concentration KAO.....	50
Figure 21. Bond strength profile: Experiment two high concentration KAO.....	51

Figure 22. Bond strength profile: Experiment three low concentration FG	53
Figure 23. Bond strength profile: Experiment three high concentration FG	54
Figure 24. Bond strength profile: Experiment three low concentration KAO.....	55
Figure 25. Bond strength profile: Experiment three high concentration KAO.....	56
Figure 26. XDLVO interaction energy profiles: MS2-MS2, FG-MS2, and KAO-MS2 ..	58
Figure 27. XDLVO interaction energy profiles: MS2-MS2 varying surface-potentials ..	59
Figure 28. XDLVO energy profile: FG-MS2, holding constant FG surface-potential.....	60
Figure 29. XDLVO energy profile: KAO-MS2, KAO surface potential constant	61
Figure 30. AFM images: KAO without MS2 and with MS2.....	63
Figure 31. AFM images: FG without MS2 and with MS2	64
Figure 32. AFM image: FG with MS2.....	65
Figure 33. MS2 control experiment: declining slope.....	66
Figure 34. XDLVO energy profile: Different ionic strengths	69
Figure 35. XDLVO energy profiles: Positive MS2 surface-potential	70
Figure 36. Significant MS2 removal: Experiment one low concentration FG	73
Figure 37. Significant MS2 removal: Experiment one high concentration FG	74
Figure 38. Significant MS2 removal: Experiment one low concentration KAO.....	75
Figure 39. Significant MS2 removal: Experiment one high concentration KAO.....	76
Figure 40. Significant MS2 removal: Experiment two low concentration FG.....	77
Figure 41. Significant MS2 removal: Experiment two high concentration FG.....	78
Figure 42. Significant MS2 removal: Experiment two low concentration KAO	79
Figure 43. Significant MS2 removal: Experiment two high concentration KAO	80
Figure 44. Significant MS2 removal: Experiment three low concentration FG.....	81

Figure 45. Significant MS2 removal: Experiment three high concentration FG 82

Figure 46. Significant MS2 removal: Experiment three low concentration KAO 83

Figure 47. Significant MS2 removal: Experiment three high concentration KAO 84

List of Tables

	Page
Table 1. AFIT MS2 stock concentrations	17
Table 2. First Order Rate Constants from All Three Experiments	28
Table 3. XPS Surface Data (courtesy of Dr. Xing).....	33
Table 4. Experiment One Supernatant Raw Data	85
Table 5. Experiment Two Supernatant Raw Data	87
Table 6. Experiment Three Supernatant Raw Data	89
Table 7. Experiment Control Supernatant Raw Data.....	91
Table 8. Washed Pellet Raw Data Experiment One	93
Table 9. Washed Pellet Raw Data Experiment Two.....	95
Table 10. Washed Pellet Raw Data Experiment Three.....	97
Table 11. XDLVO Parameters and References	99

VIRUS ADSORPTION TO COLLOIDS IN WATER: INTERACTIONS OF BACTERIOPHAGE MS2, KAOLINITE, AND FIBERGLASS

I. Introduction

1.1 Introduction

The U.S. Environmental Protection Agency (EPA) National Homeland Security Research Center (NHSRC) is working with environmental engineering professionals to improve water infrastructure security (Arduino et al., 2015; Chattopadhyay & Taft, 2018; Water and Wastewater & Sector Strategic Roadmap Work Group, 2017). Small and large drinking and wastewater treatment plants have requested guidance from the EPA for treating high-consequence biological contaminants due to having limited resources for research. These contaminants include a wide range of dangerous whole cells, viruses, proteins, and metabolites. Small drinking water treatment systems make up more than 97% of the nation's 156,000 public water systems (EPA, n.d.). These agents may be natural or genetically modified, and they pose a serious threat to the public when mobilized as weapons or when present in wastes (Levy & Sidel, 2011; Water Environment Research Foundation, 2016). The EPA is interested in protecting the public and the environment from the harmful effects of biological contaminants.

Biologically contaminated wastewater can come from hospitals (Q. Wang, Wang, & Yang, 2018), accidents, or terrorist attacks (Roffey, Lantorp, Tegnell, & Elgh, 2002). Water resource recovery facilities (WRRF) may receive requests to accept biohazardous wastes, and before granting such requests, managers must carefully consider the possible effects on operations. Guidance on the handling of such waste streams is needed to aid WRRF in their decision to accept such wastes (Water Environment Research Foundation,

2016). WRRF operators must also prepare for situations that involve the deliberate and malicious introduction of bio-contaminants into the wastewater collection system (Arduino et al., 2015; Water Environment Research Foundation, 2016; Zoli, Steinberg, Grabowski, & Hermann, 2018). The protocols, policies, or regulations that are needed must be based upon scientifically-based facts related to the effect of the biological contaminant on the treatment system and public and environmental health. One important aspect of this issue concerns adsorption of biological contaminants to colloidal materials common to wastewaters. Colloids can transport and protect pathogens through the treatment process (Sakoda, Sakai, Hayakawa, & Suzuki, 1997). Transport of disease vectors through one of the 14,748 wastewater treatment plants in the United States (American Society of Civil Engineers, 2017) has potential to harm many people at once by neglecting to effectively treat water for pathogenic microbes before reintroducing it back into the environment.

Pathogens can also be present in source waters used for potable purposes. The Safe Drinking Water Act (SDWA) requires water treatment utilities to meet National Primary Drinking Water Regulations associated with both pathogens and particles, and historical data shows that SDWA violations are more frequent at small drinking water treatment plants (i.e. serving less than 10,000 people) because these facilities have limited resources (Benear & Olmstead, 2008; EPA, 2016). In these cases, people may be exposed to biologically contaminated drinking water when treatment is poor or in the event that poorly treated water is spiked with a bioweapon. Pathogens adsorbed to colloids in drinking water are more difficult to inactivate at the point of use and can harm public health (Stagg, Wallis, & Ward, 1977; Templeton, Andrews, & Hofmann, 2005).

There are also international and diplomatic reasons for the Department of Defense (DoD) to be concerned with protecting infrastructure and preventing accidents according to the U.S. Government Global Water Strategy (USAID, 2017). This strategy was endorsed by the president and outlines the involvement of the DoD to use its resources to reduce conflicts over water and protect water resources for high-priority countries. The DoD can use the conclusions from this research about the transport of viruses in water when diplomatically interacting with other nations.

MS2 bacteriophage are the focus of this research study, and they represent surrogates for viruses of potential interest in the water quality community. MS2 (family Leviviridae, genus Levivirus) is a 25 nm diameter, icosahedral, single-stranded ribonucleic acid (RNA) virus, and has been used as a surrogate for Ebola and for human enteric viruses (Fu & Li, 2016; Lin & Marr, 2017; Shishovs et al., 2016; Skripkin, Adhin, de Smit, & van Duin, 1990; Toropova, Basnak, Twarock, Stockley, & Ranson, 2008). MS2 is expected to adsorb to particles in water because of the hydrophobicity of the outer surface (Wiencek, Klapes, & Foegeding, 1990).

The objectives of this research are to:

- Determine removal rate constants associated with the adsorption of MS2 to colloidal suspensions of kaolinite (KAO) and fiberglass (FG)
- Characterize binding strength associated with virus adsorption
- Use Extended Derjaguin-Landau-Verwey-Overbeek (XDLVO) theory modeling to comparatively assess virus surface attachment and aggregation

II. Literature Review

2.1 The Properties of MS2

MS2 physiochemical properties (such as topography, size, shape, composition, surface charge, isoelectric point (IEP), hydrophobicity, surficial functional groups, and RNA genome with multilayer capsid) as well as solvent chemistry are the important properties in the literature for controlling MS2 kinetics in water with colloids because these factors determine the resulting surface complexation, surface charge, and hydrophobicity. MS2 is a commonly used surrogate for Ebola virus, Norwalk virus, enteroviruses, caliciviruses, astroviruses, and Hepatitis A and E viruses and other human enteric viruses because it is similar in genome type, structure and size and as a fecal indicator virus (Harwood, Jiang, & Sobsey, 2015; Hmaied & Jebri, 2013; Shin & Sobsey, 1998). It is icosahedral in shape and is approximately 25-27 nm in diameter (Armanious et al., 2016; Chrysikopoulos & Syngouna, 2012; Madigan & Martinko, 1996). It is a single-stranded RNA virus that infects coliform bacteria for lytic reproduction (Hmaied & Jebri, 2013). The IEP (the pH at which the particle has a neutral surface charge) for MS2 is 3.3-3.9 and its surface charge is -0.02 Volts in deionized water (DI water) (Armanious et al., 2016; Chrysikopoulos & Syngouna, 2012; Michen & Graule, 2010). The low IEP means that at neutral water pH, its surface charge will be negative and will likely repel negatively charged particles with which it will interact. Also, hydrophobicity of a substance is measured by the contact angle between its surface and water, and MS2 is known to have a contact angle of $33\pm 1^\circ$ (Chrysikopoulos & Syngouna, 2012; Park & Kim, 2015). Chrysikopoulos & Syngouna et al. (2012) asserted that substances with

contact angles $>90^\circ$ are hydrophobic and contact angles $<90^\circ$ are hydrophilic. MS2 has hydrophobic regions, but overall MS2 is more hydrophilic (Armanious et al., 2016).

The ionic strength of the solution influences the surface charge of the particle (Langlet, Gaboriaud, Duval, & Gantzer, 2008). MS2 has amino and carboxylic functional groups on the capsid surface which protrude from the surface of the virus into the solution, reducing the separation distance between the functional group and the ion, and allowing adsorption and aggregation despite like-charged surfaces when the ionic strength of the solute is increased (Langlet et al., 2008; Michen & Graule, 2010). However, ions can also screen particle surface charge and reduce aggregation as ionic strength is increased (Meissner, Prause, Bharti, & Findenegg, 2015). Surface charge, size, IEP, hydrophobicity and functional groups are important physicochemical properties of MS2 and the ionic strength of the solution influences its surface charge and potential to aggregate.

2.2 Colloids

2.2.1 Colloid Characteristics

Colloids have been defined as entities small enough to remain suspended in the water column but with supramolecular properties (e.g., electrical surface charge, Gustafsson & Gschwend, 1997). Typically, colloidal particles are between 1 nm and 1 μm in diameter (IUPAC, 2002). Nanoparticles (NP) are colloids in the size range of 1 to 100 nm (Khan, Saeed, & Khan, 2017). Other definitions have been proposed. Colloids have also been defined as a dispersed phase present in another phase (IUPAC, 2002), or as materials which permeate a filter of pore size between 0.1 and 1 μm while also being

retained by an ultrafilter with a nominal pore size of 100 kiloDaltons (IUPAC, 2002). These three definitions for colloid do not precisely overlap, but the practical understanding of colloids is that they remain dispersed and do not quickly settle out of water.

Colloids that occur in water are generated by surface erosion, precipitation, and biological processes (Stumm & Morgan., 1996). They are heterogeneous in size, shape, surface charge, structure, and chemical composition. There are three major types of colloids: inorganic colloids, humic substances, and large biopolymers such as polysaccharides and peptidoglycans (Buffle, Wilkinson, Stoll, Filella, & Zhang, 1998; Fanun, 2014). The inorganic colloids are composed of iron oxides, manganese oxides, silica oxides, metal phosphates, or aluminosilicates including clay and zeolites (Buffle et al., 1998; Fanun, 2014). The humic substances (fulvic compounds, humic acids, and humin) and large biopolymers are organic and may be naturally occurring or anthropogenic (R. Q. Wang, Gutierrez, Choon, & Croué, 2015). Some of the colloidal material in the environment is in the form of engineered nanoparticles (ENPs) which are now being used in sporting goods, tires, clothing, cosmetics, electronics, and in medical procedures (Keller & Lazareva, 2013; Nel, Xia, Madler, & Li, 2006; Shi et al., 2016). Numerous studies have shown that a wide range of organic and inorganic water pollutants can adsorb to colloids (Burakov et al., 2018; Hakim & Kobayashi, 2018; Hennebert, Avellan, Yan, & Aguerre-Chariol, 2013; Hiradate, Yonezawa, & Takesako, 2006; McNew, Kananizadeh, Li, & LeBoeuf, 2017).

Adsorption to colloids is influenced by surface properties such as surface charge, surface roughness, and hydrophobicity. Surface charge of the colloid and the water

pollutant in an aqueous solution will influence the amount of adsorption. Hur et al. (2015) studied the removal of metals using graphene oxide and found that if the system $\text{pH} < \text{IEP}$ of a colloid, then adsorption was observed to be lower than when the $\text{pH} > \text{IEP}$ due to protonation on the surface functional groups causing particles to be repelled from one another. Furthermore, the IEP of colloids spans the entire pH range and can have a heterogeneous surface charge (Kosmulski, 2009; Kumar et al., 2016; Zhou & Gunter, 1992). For example, Kumar et al. (2016) measured the surface charge of kaolinite on mica and sapphire and observed that along the basal planes of the kaolinite there was surface charge heterogeneity, although it was lower than the charge at the rims. Inorganic colloids (like aluminosilicates) are generally known to have a negative surface charge in neutral pH (Buffle et al., 1998). Organic biopolymer electrolytes can change shape based upon pH and ionic strength, and have unevenly distributed surface charge (Buffle et al., 1998). Humic substances are mainly represented by fulvic compounds in freshwaters, can have high charge density in neutral water, and a maximum IEP of 5 (Buffle et al., 1998; Hakim & Kobayashi, 2018; Hiradate et al., 2006; Kosmulski, 2009). Surface charge changes the electrostatic repulsion between colloids when in aqueous solution, pushing particles away from one another due to the layer of water; and, this is the hydration effect (Baalousha, Lead, von der Kammer, & Hofmann, 2009). Baalousha et al. (2009) also described the hydrophobic effect as the pushing of water molecules away from particles and adding attraction between even the like-charged particles. In a review by Jiang, Shang, Heijman, & Rietveld (2018) an article was discussed that showed high-silica manufactured zeolites were favorable to organic micro-pollutant adsorption because of their higher hydrophobicity. Inorganic colloids, like clays, are known to be hydrophobic,

but humic substances have hydrophobic moieties with an overall hydrophilic tendency (Buffle et al., 1998; Hoff & Akin, 2018). Biopolymers can be rigid or flexible and have hydrophobic regions on the surface (Buffle et al., 1998; Cunha & Gandini, 2010). Hydrophobicity is measured by the water contact angle formed with a surface, and hydrophobic materials are associated with high surface roughness (Cunha & Gandini, 2010). For example, Cunha et al. (2010) suggest surface morphologies can hinder water spreading. Jiang et al. (2018) and Cunha & Gandini (2010), when considered together, may suggest that the smoother the surface the more hydrophobic and the more observed adsorption. Inorganic colloids, like silica, have relatively smooth and angular surfaces (Kumar et al., 2016). These surface characteristics influence the adsorption of pollutants in water to colloids.

2.2.2 The Presence of Colloids in Influent and Effluent Streams

The presence of colloidal materials has been mentioned in numerous water and wastewater journal articles, textbooks, and technical reports (Chattopadhyay & Taft, 2018; Chaudhry, Holloway, Cath, & Nelson, 2015; Hashimoto, Matsuda, Inoue, & Ike, 2014; Hu et al., 2018; Levine et al., 1985; Li et al., 2016; Mattle et al., 2011; Walshe, Pang, Flury, Close, & Flintoft, 2010). Colloids include NP and these are of concern because they remain suspended in wastewater and have been measured in the effluent of wastewater treatment plants (WWTP). Environmentally relevant NP can be anthropogenic or naturally occurring. Common NP include humic substances (like polysaccharides) and metals (like titanium oxide, TiO₂). A recent study estimated that 10-30%, 3-17% and 4-19% of all NPs are discarded into water bodies in Asia, Europe and North America respectively (Keller & Lazareva, 2013). However, a relatively small

number of studies have characterized the concentrations of colloidal materials in the influent and effluent streams of full-scale water or wastewater treatment plants.

Hennebert et al. (2013) detected (but did not quantify) colloids present in 25 waste leachates that were to be sent to a WWTP. Hu et al. (2018) measured NP mixtures that occurred in the effluent of five WWTP, and the concentration ranged from 0.07-0.55mg/L. Their work showed that the treatment process does not remove all NP before the effluent is released back into the water environment. The NP mixtures included naturally occurring (polysaccharides and proteins) and anthropogenic (TiO₂) NP. Their results showed that NP uptake can cause damage to plant growth and that NP remain present in wastewater effluent. Also, Shi et al. (2016) detected (TiO₂) NP in the influent and effluent of two WWTP in Shijiazhuang, China. They found that the TiO₂ NP influent concentrations for the two WWTP were approximately 175 µg/L and 170 µg/L respectively, and the effluent concentrations for the two WWTP were 25 µg/L and 50 µg/L, respectively. Their results show that, while WWTP could remove NP, there remained amounts of NP present in the effluent. In another article concerning silver-based NP, Li et al. (2016) measured the influent concentration of a WWTP to be 0.73-11.5 ngL⁻¹, and the effluent concentration to be 0.7-11.1 ngL⁻¹. Their research also showed that NP are reduced, but are still present after treatment. The presence of colloids is ubiquitous in water and wastewater treatment systems, but there is a need for more quantitative characterization of the colloidal suspensions entering and leaving water treatment systems due to the possibility of transport and protection.

2.2.3 Adsorption of Viruses to Colloids

Many viruses adsorb to colloidal particle suspensions. Bacteriophage T4 adsorbed to the surface of KAO (Carlson et al., 1968). Bacteriophages T2, F2, T4 and the poliovirus adsorb to bentonite and KAO (Moore, Sagik, & J.F. Jr., 1975). Tong, Shen, Yang, & Kim (2012) mixed bacteriophage MS2 with bentonite and KAO suspensions and determined adsorption kinetics both with and without the presence of divalent cations. Gutierrez et al. (2009) measured the adsorption of rotavirus and MS2 to FG coated with hematite nanoparticles in 1mM NaCl solution, and observed adsorption capacities of 2.6×10^6 PFU/g rotavirus and approximately 2.41×10^{11} PFU/g MS2. Chattopadhyay & Puls (2000) used T2, MS2, and ϕ X174 bacteriophages with hectorite, KAO, and norman clay phyllosilicate clays in 0.01 M NaCl solution. They found that the amount of T2 phage which adsorbed onto hectorite, KAO, and norman clay was about 1.95×10^7 PFU/g, 1.85×10^7 PFU/g, and 1.86×10^7 PFU/g, respectively. They found that the amount of MS2 which adsorbed onto hectorite, KAO, and norman clay was about 1.87×10^7 PFU/g, 1.7×10^7 PFU/g, and 1.84×10^7 PFU/g, respectively. They found that the amount of ϕ X174 phage which adsorbed onto hectorite, KAO, and norman clay was about 1.86×10^7 PFU/g, 1.69×10^7 PFU/g, and 1.78×10^7 PFU/g, respectively. Additionally, Zhang & Zhang (2015) measured the adsorption of MS2 onto 100 mg/L of each nanoparticle, TiO₂ and NiO, in 10 mM NaCl and DI water. They found 1.7×10^8 PFU/g of MS2 and 10.3×10^8 PFU/g of MS2 adsorbed onto TiO₂ and NiO in 10 mM NaCl respectively; and, 10.6×10^8 PFU/g and 100.1×10^8 PFU/g onto TiO₂ and NiO in DI water respectively. It is clear that adsorption to colloids can impact the fate of viruses.

It is also well-known that viruses attached to colloidal particles are more difficult to inactivate. For example, Stagg, Wallis, & Ward (1977) showed that bacteriophages attached to clay were more resistant to HOCL than were freely suspended phages. Templeton, Andrews, & Hofmann (2005) investigated whether colloid-sized particles can enmesh and protect viruses from 254-nm ultraviolet (UV) light; their study used two viral surrogates (MS2 coliphage and bacteriophage T4) and three types of particles (KAO clay, humic acid powder, and activated sludge) and they found that particles less than 2 μm in diameter are large enough to protect viruses from UV light. Water quality professionals interested in virus inactivation must account for the presence of colloidal particles.

2.3 XDLVO Modeling

The theory developed by Derjaguin, Landau, Verwey, and Overbeek, DLVO Theory, and its extension, XDLVO theory, provide methods to model the energy that particles in water must overcome to be stable or flocculate using the interacting particle (i.e. surface charge and particle size) and solution properties (i.e. ionic strength) (Israelachvili, 2011). Stabilization of colloids in suspension means repulsion forces are keeping the colloids separated (Chang, 2007). At small separation distances, attractive van der Waals interaction forces dominate (Israelachvili, 2011). In an aqueous solution there are Lewis acid-base interaction forces, and the total interaction energy for the system is the sum of the repulsive electrostatic double-layer, attractive van der Waals, and Lewis acid-base interaction forces (Chrysikopoulos & Syngouna, 2012).

Chrysikopoulos & Syngouna (2012) showed the importance of including the Lewis acid-base interactions in the total energy and attachment of two viruses (MS2 and

φX174) onto two clay colloidal particles (KAO and montmorillonite) keeping constant the pH (7.0) and ionic strength (0.0001 M) of the DI water medium. Additionally, hydrophobic forces were found to positively mediate the Lewis acid-base interaction. DLVO theory assumes smooth, spherical, homogenous particles, unlike viruses which have various functional groups and porous, angular surfaces. Initially, two DLVO forces (van der Waals and electrostatic) were considered for calculating the potential energy. Then, the forces for Lewis acid-base interaction energy were included for calculating the XDLVO total interaction energy. In DLVO theory the total interaction energy between two substances in water is a function of interparticle distance.

The van der Waal variables are: Hamaker constant, the radius of the colloidal particle, the characteristic wavelength of the interaction, and minimum separation distance between the two approaching particles. The Hamaker constant, A_{123} , relates the three interacting substances' apolar components of their surface tensions. Chrysikopoulos & Syngouna (2012) used KAO and montmorillonite as the collectors. DI water was material 2. The viruses were considered material 1, the colloids. In a book by Carel van Oss (2006), the Hamaker constant is shown to depend upon the substance's number of atoms per unit volume and London's constant, $\beta=3/4\alpha^2\hbar\nu$. The α is the substance's polarizability. The $\hbar\nu$, distance times the velocity, is the substance's energy corresponding to the main dispersion. The Hamaker constant formula adapted to consider the physical properties of materials 1 and 3, and the London's and Hamaker constants becomes: $\beta_{12} = \sqrt{\beta_{11}\beta_{22}}$ and $A_{12} = \sqrt{A_{11}A_{22}}$. Chrysikopoulos & Syngouna (2012) provided the resulting values for the Hamaker constants: KAO-water-KAO was $3.1 \times 10^{-}$

²⁰ J, virus-water-virus was 7.5×10^{-21} J, and montmorillonite-water-montmorillonite was 2.2×10^{-10} J.

Another important point about DLVO theory is the shape of the interacting particles, which affects the interaction energy calculation. The characteristic wavelength of the interaction depends on the shapes of the two interacting particles in water. Clay particles are known to be flat and platy shaped (Berg, 2010). Chrysikopoulos & Syngouna (2012) used both a sphere-plate and sphere-sphere formulas for the interaction energy for van der Waal forces and compared the curves. The potential energy for sphere-plate showed a higher potential energy curve than sphere-sphere and MS2 showed higher potential energy for all four combinations (MS2-KAO, φX174-KAO, MS2-montmorillonite, φX174- montmorillonite). The DLVO interaction energy calculations for sphere-plate and sphere-sphere were similar in magnitude. Finally, the sphere-plate model was determined to be more appropriate, because of the size difference between the two particles. When the size difference between two particles is large, then the larger particle shape is considered a plate.

Chrysikopoulos & Syngouna (2012) continued with calculating the interaction energy of the two materials immersed in water by explaining the electrostatic double-layer forces interacting between the viruses and colloids. This force depends upon the relative dielectric constant of the medium, permittivity of free space, dielectric constant of the suspending liquid, the surface potential of the colloidal particle, the surface potential of the collector surface, the Debye-Huckel parameter, and the minimum separation distance between the two approaching particles. The Debye-Huckel parameter

depends upon the ionic strength, the Boltzmann constant, and the temperature-among other constant values. The hydrophobic force constant depends on the contact angles of the colloidal particle and water. Attinti et al. (2010) used Yoon's approach for calculating hydrophobic forces, similar to Chrysikopoulos & Syngouna (2012).

Chrysikopoulos & Syngouna (2012) compared energy profiles using DLVO forces only (using zeta potential instead of surface potential for the electrostatic forces) with energy profiles of acid-base alone and the XDLVO potential energy curves of all combinations of the curves. This showed that potential energy for DLVO overestimated the energy barrier that keeps the suspensions stable for all combinations (MS2-KAO, ϕ X174-KAO, MS2-montmorillonite, ϕ X174-KAO). XDLVO theory was more accurate and it was recommended it be used for water treatment applications.

In another article, Tong, Shen, Yang, & Kim (2012) examined and explained using DLVO theory the deposition of MS2 onto clay coated, poly-l-lysine (PLL) hydrobromide coated, and bare silica surfaces. Their results showed that the observed deposition was consistent with the DLVO interaction calculations and that increasing the ionic strength reduced the energy barrier for all three materials, suggesting that the more available ions in solution the lower the energy barrier that would need to be overcome for heteroaggregation. Attinti, Wei, Kniel, Sims, & Jin (2010) used DLVO and XDLVO theory to explain the interaction of viruses with saturated sands. They found that the observed strong attachment of viruses to the aluminum oxide-coated sand was likely due to the relatively smaller electrostatic repulsion and greater hydrophobic attraction.

III. Methodology

3.1 Overview

Colloidal suspensions of KAO and FG were mixed with bacteriophage MS2 in laboratory-scale batch tests carried out in triplicate. Time series samples were collected to measure the concentration of MS2 which remained in solution. Liquid and pellet samples were collected and prepared for microscopic analysis. Pellets obtained from the adsorption experiments were used for bond strength experiments. XDLVO modeling was carried out to help investigate MS2 aggregation and surface interactions with colloids. Two-tailed, student T-tests were used to determine statistical significance at the 95% confidence level ($\alpha = 0.05$).

3.2 Preparation of Bacteriophage MS2

MS2 bacteriophage was produced using a method from the US EPA (U.S. Environmental Protection Agency, 2001). Briefly, a small amount of MS2 stock (10^8 pfu/ml, a donation from EPA, Cincinnati) was added to an overnight growth stock of host bacteria, *Escherichia coli* (*E. coli*), with a final concentration of 400 pfu/ml or higher. The *E. coli* stock was then allowed to grow for 24-48 hours at 35 °C in an incubator (Lab-Line, Imperial III) for the phage to propagate. Afterwards, the liquid suspension was centrifuged (Eppendorf Centrifuge 5810 R at 4000 rpm for 20 minutes at 4°C) and syringe filtered to remove the *E. coli* debris. This method produced approximately $5\sim 9 \times 10^{10}$ pfu/ml phages. An additional purification step was performed to remove the organic compounds as these small molecules may interfere with the phage-colloid adsorption experiments. This was achieved by centrifuging the sample through a centrifugal unit

with a molecular weight cutoff of 100K (Amicon Ultra-15, MWCO 100K) (Figure 1). The phages were resuspended in sterile phosphate-buffered saline and stored at 4°C for future use. Purified MS2 were then incubated with SYTO™ 9 Green Fluorescent Nucleic Acid Stain (Thermo Fisher, S34854) for 30-60 minutes in the dark at a dye concentration of 4 µM (1:1250 dilution of the original stock) (Stuntz, 2018). MS2 were enumerated using the double-layer plate agar method (see Figure 2 and Table 1). The fluorescently labeled phages were used in the following experiments.

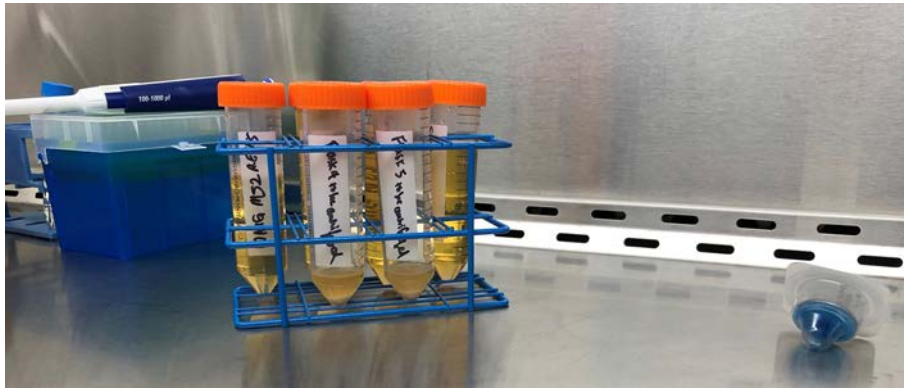


Figure 1. Centrifuged MS2 and *E. coli* showing larger cells in the bottom of the tube and an example of the FG filter used for purification in the bottom right corner

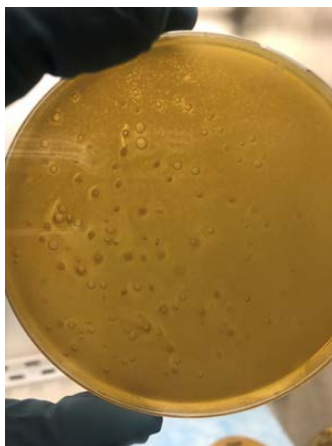


Figure 2. Lysed cells in agar appear as plaques

Table 1. AFIT MS2 stock concentrations

Stock	Concentration (pfu/ml)
Experiments 1 and 2	1.6×10^8
Experiment 3	3.5×10^7

3.3. Colloidal Stock Solutions

Two types of colloid suspensions were prepared, and two concentrations for each colloid type were prepared. KAO is a commonly found colloid in wastewater and FG has been used as a simulant of wastewater contamination. To make the KAO colloid stock solutions, KAO (Fisher Chemical, Catalog# K2-500, 1g for the high concentration stock and 0.2 g for the low concentration stock) were added to 1 liter of DI water, vigorously stirred with a magnetic stirrer for 30 minutes and allowed to settle overnight. The supernatant was then used as the colloid suspension. The KAO particles were less than $0.45 \mu\text{m}$ in size according to the manufacturer's label. The FG suspensions were made by

mixing 1 piece of FG filter (GE Healthcare, Catalog# 1827-042) with DI water in a blender (Waring Commercial, 717BB). For the higher concentration FG stock solution, one filter was blended with 150 ml of DI water and transferred to a 500 ml flask. The lower concentration of FG stock solution was mixed by adding an FG filter to 500 ml of DI water. The FG colloid suspensions were settled overnight, and the supernatant was used as the colloid suspension. The operationally defined colloid stock solution was obtained by allowing the solutions to settle overnight.

The pH and concentration of each colloid suspension were measured. Colloid concentrations were measured by turbidity (Bionate 3 Thermo Spectronic light-scattering spectrophotometer) and weight (Fisher Scientific scale) using the following procedure. First, 30 ml of each colloid suspension was centrifuged at 4000 rpm for 15 minutes, as much of the supernatant was removed without disturbing the pellet and the remaining colloid slurries were transferred to a pre-weighed microcentrifuge tube. The samples were then left in a chemical hood to dry for approximately three weeks. Once completely dried, the tubes were weighed again to calculate the dry weight of the colloids. These dry weight measurements were then used to calculate colloid stock concentrations.

3.4 Batch Tests with MS2 and Colloidal Suspensions

First, 20 ml samples of each colloidal solution were added to a 50 ml sterilized beaker with a plastic magnetic stirrer on a stirring plate. Next, 1 ml of the labeled MS2 was added to each beaker, the beakers were covered with foil to prevent photo-bleaching. The MS2-colloid mixtures were constantly stirred for 120 minutes and three 1 ml samples were withdrawn at immediately after adding MS2 to colloids, and after 15, 30,

60, and 120 minutes. Samples were taken in triplicate for each time point. The samples were centrifuged at 4000 rpm for 15 minutes to separate supernatant from the colloids. The supernatant, containing free floating MS2, was then measured for SYTO™ 9 green fluorescent dye using a Qubit 3.0 Fluorometer (Thermo Fisher Scientific) using blue light (470 nm) excitation. Fluorescence reduction in the supernatant compared to the initial total amount of green fluorescence added was used as a measure of MS2 removal from the liquid phase through either aggregation or adsorption onto the colloids. Supernatant fluorescence measurements used for statistical significance were normalized by dye and colloid concentration to allow comparisons. The fluorescence in the raw water was measured and the fluorescence measurements were adjusted. Also, for experiments 1 and 2 twelve samples of the amount of fluorescence of the MS2 stock were measured, and the average of them was used as the initial concentration of fluorescence used in the percent calculations. In experiment 3, three samples of the amount of fluorescence of the MS2 stock were measured, and the average of them was used as the initial concentration of fluorescence used in the percent calculations.

To determine whether MS2 phages adsorbed onto colloids were tightly bounded or loosely associated, a washing step was performed on the pellets. Briefly, pellet samples from the previous step were centrifuged one more time to remove residue supernatant. Afterwards, 1 ml of DI water was added to each pellet sample, the mixture was vigorously vortexed, and then each pellet was centrifuged again to separate the washed pellets from the washing solution. The washed solution was then measured with Qubit 3.0 Fluorometer for fluorescence. Supernatant of the washed pellet fluorescence measurements was used for statistical significance and was normalized by dye and

colloid concentration to allow comparisons. These measurements represent the amount of phages not tightly bound onto the colloids, but were loosely associated with colloid particles. The raw data for the washed pellet fluorescence is located in Appendix C (Table 8-Table 10).

Once the images (discussed in section 3.5) were obtained, unadsorbed MS2 was observed. A control experiment was performed to test for the possibility of MS2 aggregation. The control experiment followed the same procedure as the batch experiments, except that colloids were not added to the beaker of labelled MS2.

3.5 Particle Physicochemical Analysis

Fluorescent and light microscopy and atomic force microscopy (AFM) were used to gather particle size and topography observations, and X-ray photoelectron spectroscopy (XPS) was used to gather information about surface composition. ImageJ software was used to overlay the bright field and fluorescence images to check colocalization of the fluorescent MS2 and colloid particles using a Zeiss fluorescence microscope (filter set, excitation; 488 nm, emission: 520 nm). Imaging conditions (camera exposure time, excitation light intensity) were kept identical for all samples. High-degree of colocalization indicated adsorption of phages onto the colloid particles; poor colocalization would suggest a different virus removal mechanism (such as aggregation) other than adsorption. Additional image analysis with ImageJ and AFM provided colloid particle size and MS2 aggregates formation and size distribution. Attinti et al. (2010) used AFM to measure the interaction forces between a virus (Aichi virus) and sand in an aqueous solution; and, then DLVO and XDLVO theories and the retention

of virus on the sand columns were compared to the measured interaction forces from the AFM. AFM provides observations of topography, which aids in confirming adsorption. AFM methods can be done either by measuring deflections of a tip moving over a substrate or measuring deflections of a substrate touching a tip (Israelachvili, 2011). This method was used to observe the topography of KAO, FG, and MS2 particles, and was performed by Dr. Yun Xing. XPS analysis was also provided by Dr. Xing. It described the chemical composition of the surface of the KAO, FG, and MS2. XPS can offer many more physicochemical observations about particle size, the thickness and structure of coatings on nanoscale particles, and surficial functional groups (Baer & Engelhard, 2010). Together, AFM, microscopy, and XPS provided observations about physicochemical surface properties of the KAO, FG, and MS2 particles.

3.6 XDLVO Modeling

The XDLVO theory was used to interpret the MS2 aggregation and adsorption onto suspended particles. The model includes van der Waals forces (attractive energy), repulsive electrostatic forces (electrostatic repulsion energy), and Lewis acid-base forces to calculate interaction energy as a function of the separation distance between particles. The formulas for the forces depend upon the interacting particle shapes and relative sizes; and, they measure available potential energy for reactions. Van der Waals potential energy equation for two spherical particles is:

$$\phi_{vdW} = -\frac{A_{131}}{12} \left(\frac{\frac{rp_2}{rp_1}}{h^2+4ah} + \frac{2a^2}{h^2+4ah+4a^2} + \ln \frac{h^2+4ah}{h^2+4ah+4a^2} \right) \quad (1)$$

Where

a = radius of the particle (m)

$A_{colloid-water-colloid/collector}$ = Hamaker constant for shape(s) of particles

h = distance between surfaces of particles (m)

r_p = the radius of the colloid (m)

The van der Waals formula (ϕ_{vdW}) for one spherical and one platy particle is:

$$\phi_{vdW} = -\frac{A_{132}r_p}{6h} \left[1 + \left(\frac{14h}{\lambda} \right) \right] \quad (2)$$

Where

$\lambda = 10^{-7}$ m is wavelength for sphere-sphere or sphere-plate

The electrostatic repulsive potential energy (ϕ_{EDL}) for sphere-sphere particles:

$$\phi_{EDL} = \pi \epsilon_r \epsilon_0 \frac{r_{p1} r_{p2}}{(r_{p1} + r_{p2})} \left[2 \Psi_{p1} \Psi_{p2} \ln \frac{1 + \exp^{-\kappa h}}{1 - \exp^{-\kappa h}} + (\Psi_{p1}^2 \Psi_{p2}^2) \ln(1 - e^{-2\kappa h}) \right] \quad (3)$$

Where

ϵ_r = dielectric constant of the solution (dimensionless)

ϵ_0 = the permittivity of free space (Coulomb²/(Joules-m))

Ψ_{p1} = the surface potential of the colloid 1 (Volts)

Ψ_{p2} = the surface potential of the colloid 2 (Volts)

$$\kappa = \text{Debye-Hückel reciprocal length (m}^{-1}\text{)} = \left[\frac{2I_s N_A 1000 e^2}{\epsilon_r \epsilon_0 k_B T} \right]^{1/2} \quad (4)$$

I_s = solution ionic strength (mol/L)

$N_A = 6.02 \times 10^{23}$ (1/mol)

$e = 1.602 \times 10^{-19}$ Coulombs

$T = 298$ Kelvin

$k_B = 1.38 \times 10^{-23}$ J/K

The electrostatic repulsive potential energy (ϕ_{EDL}) for sphere-plate particles:

$$\phi_{EDL} = \pi \epsilon_r \epsilon_0 r_p \left[2 \Psi_p \Psi_s \ln \frac{1 + \exp^{-\kappa h}}{1 - \exp^{-\kappa h}} + (\Psi_p^2 \Psi_s^2) \ln(1 - e^{-2\kappa h}) \right] \quad (5)$$

Where Ψ_p = the surface potential of the colloid (Volts)

Ψ_s = the surface potential of the larger collector particle (Volts)

The Lewis acid-base force, ϕ_{AB} , prevents the distance between particles from becoming lower than 0.3 nanometer (nm) (Chrysikopoulos & Syngouna, 2012; Gentile, Cruz, Rajal, & Fidalgo de Cortalezzi, 2018). The formula for ϕ_{AB} potential energy between two spheres is as follows:

$$\phi_{AB} = 2\pi \frac{r_1 r_2}{r_1 + r_2} \lambda_{AB} \phi_{AB(h=h_0)} \exp\left(\frac{h_0 - h}{\lambda_{AB}}\right) \quad (6)$$

Where λ_{AB} = decay length of water at h_0 contact (nm)

$\phi_{AB(h=h_0)}$ = Lewis acid-base free energy of interaction at $h = h_0$

$$\phi_{AB(h=h_0)} = -\frac{K}{2\pi h_0 \lambda_{AB}} \quad (7)$$

$$\log K_{132} = -7.0 (\cos \theta_1 + \cos \theta_3) - 18 \quad (8)$$

Where θ = contact angle of surface ($^\circ$)

The formula for (ϕ_{AB}) interaction energy between a sphere and a plate is as follows:

$$\phi_{AB} = 2\pi r_p \lambda_{AB} \phi_{AB(h=h_0)} e^{\frac{h_0 - h}{\lambda_{AB}}} \quad (9)$$

The formula for total potential interaction energy is as follows:

$$\phi_{Total} = \phi_{EDL} + \phi_{VDL} + V_{AB} \quad (10)$$

Using the calculations above, the total interaction energy can be predicted to compare with the observed behavior of MS2 with KAO and FG in a DI water solution.

IV. Results

4.1 MS2 Removal Kinetics

Figure 3 shows the removal of MS2 in the presence of KAO and FG particles for the first experimental trial; the y-axis shows the standardized fluorescence associated with the MS2 viruses present in solution and the x-axis shows time in minutes. The standardized fluorescence is the measured fluorescence at the individual sampling times divided by the initial measured fluorescence. The measured data points shown in the figure are the average of three measurements and first-order model curve regressions are shown in dashed lines. A first-order rate reaction means that the rate is proportional to the concentration of the fluorescence (Chang, 2007). The model curve regression equation used was $(\frac{\partial C}{\partial t} = k(C - C_{sat}))$. The removal rate constant, k , and the saturation concentration of dye, C_{sat} , were obtained using MATLAB. The coefficients of determination for the model curve-fittings for the KAO profiles were 0.99, which means that the model regressions are well-aligned with the measured data points; however, the FG model regressions were not as accurate. This may be due to non-homogeneous mixing, a phenomena that is not included in the first-order adsorption model (Weber Jr. & DiGiano, 1996). Additionally, the FG showed fluctuating adsorption longer than KAO, a phenomena that could be due to silanol functional groups of FG dissociating in water differently than the functional groups of KAO (Behrens & Grier, 2001). By the first sampling time, in the presence of KAO the standardized fluorescence was reduced

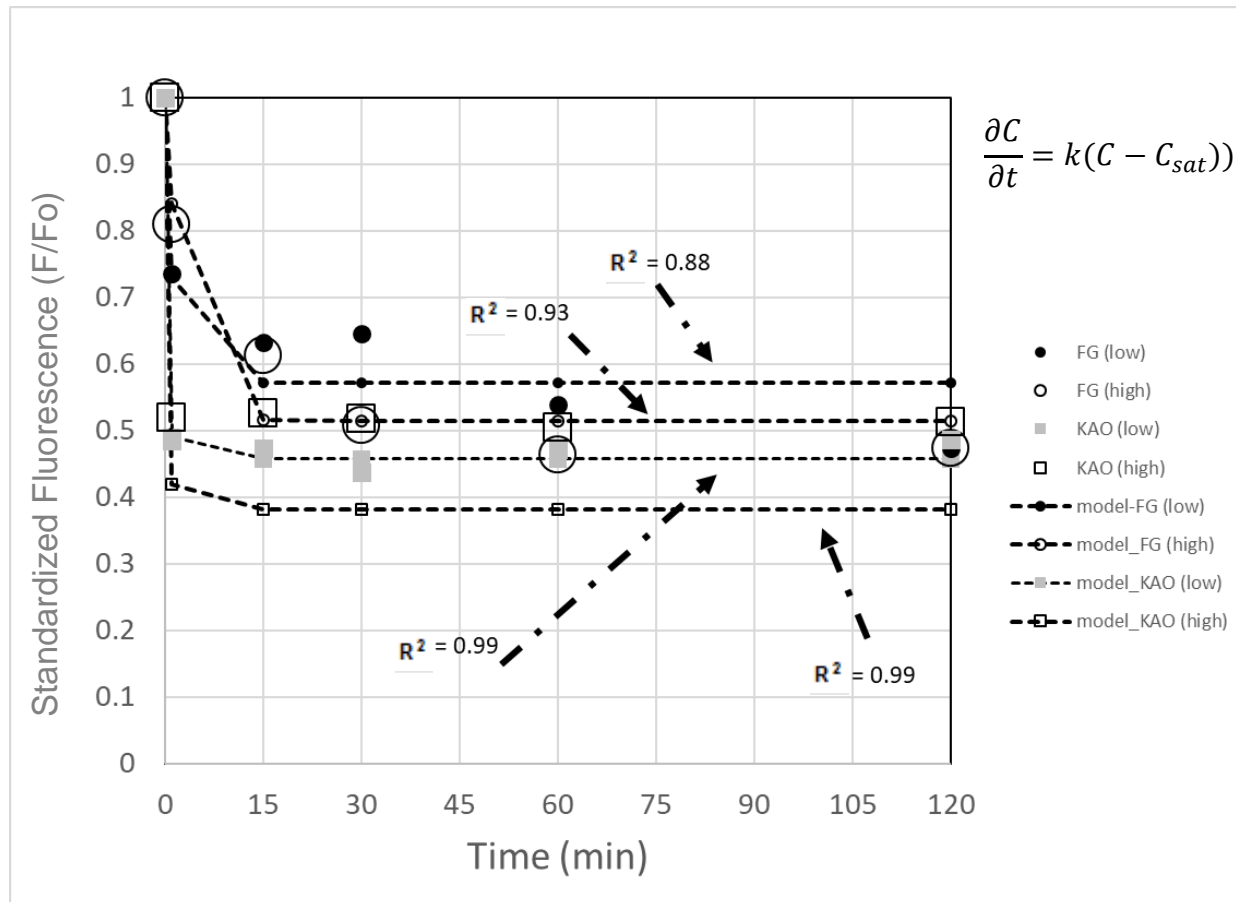


Figure 3. MS2 removal in the presence of colloids: First experiment. The actual data points are displayed as hollow and filled circles and squares. The dashed lines are the regression curves for the two concentrations for each colloid stock, and these were used to find the removal rate constant values.

from 1 to 0.48 and 0.41 (for the low 147 mg/L and high 447 mg/L particle concentrations respectively), and in the presence of FG it was reduced from 1 to 0.73 and 0.83 (for the low 59 mg/L and high 83 mg/L colloid concentrations respectively). Statistically significant removal of MS2 was observed by the first sampling time (Appendix A, Figure 36-Figure 39). In the case of KAO, equilibrium was reached within the first 15 minutes and within the first hour for FG. When equilibrium was reached in the presence of KAO the standardized fluorescence was reduced from 1 to approx. 0.46 and 0.38 (for the low and high stock concentrations respectively), and from 1 to 0.57 and 0.51 (for the low and high stock concentrations respectively) in the presence of FG. The first order rate constants retrieved from curve regressions were approx. 1.0 min^{-1} (FG-low), 0.4 min^{-1} (FG-high), 2.8 min^{-1} (KAO-low), and 2.8 min^{-1} (KAO-high). However, the FG rate constants may be anomalous.

Figure 4 shows the results from the second experimental trial. The model curve regressions were also in good alignment with measured data points. Statistically significant removal of MS2 was observed by the first sampling time (Appendix A, Figure 40-Figure 43). By the first sampling time, the standardized fluorescence was reduced in the presence of KAO from 1 to approx. 0.32 and 0.28 (for the low 147 mg/L and high 447 mg/L stock concentrations respectively) and from 1 to 0.61 and 0.26 (for the low 59 mg/L and high 83 mg/L stock concentrations respectively) in the presence of FG. The standardized fluorescence values at equilibrium were approx. 0.27 and 0.21 of the initial amount of fluorescence added (low and high KAO respectively) and 0.21 and 0.35 of the initial amount of fluorescence added (low and high FG respectively). Equilibrium was reached within the first 15 minutes. The first order rate constants were approx. 0.7 min^{-1}

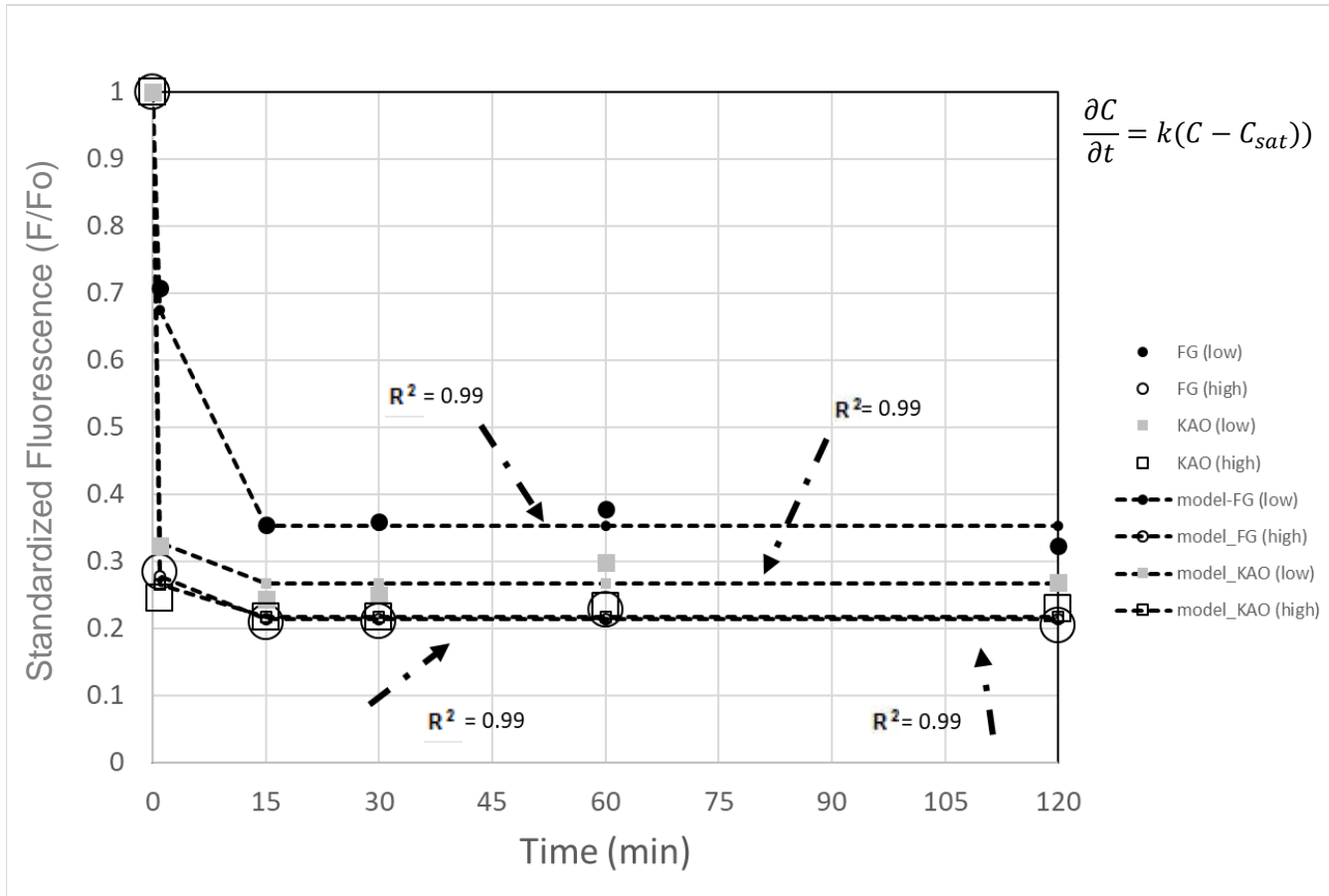


Figure 4. MS2 removal in the presence of colloids: Second experiment

. The actual data points are displayed as hollow and filled circles and squares. The dashed lines are the regression curves for the two concentrations for each colloid stock, and these were used to find the removal rate constant values.

(FG-low), 2.5 min⁻¹ (FG-high), 2.5 min⁻¹ (KAO-low), and 2.8 min⁻¹ (KAO-high) (Table 2); these rate constants are similar to those measured for ion exchange processes used for removal of ions (Blanchard, Maunaye, & Martin, 1984; Papadopoulos et al., 2004).

Results from the third trial showed significant MS2 removal by the first sampling time, good agreement with model curve regressions, and equilibrium after 15 minutes (Figure 5 and Figure 44-Figure 47). The rate constants retrieved from the third trial were approx. 2.8 min⁻¹ (FG-low), 2.8 min⁻¹ (FG-high), 2.8 min⁻¹ (KAO-low), and 2.8 min⁻¹ (KAO-high) (Table 2). Overall, these experimental results showed that significant MS2 reduction occurred by the initial sampling time, the rate constants for the KAO experiments were either greater than or equal to those of the FG experiments, and the range of rate constants retrieved from “high concentration” experiments was wider than the “low concentration” experiments. The FG particle size was more variable compared to the KAO particle, and XDLVO forces are sensitive to particle size (Israelachvili, 2011). Particle size could explain the wider range of rate constants for FG. Raw data for all batch experiments is presented in Appendix B (Table 4-Table 7).

Table 2. First Order Rate Constants from All Three Experiments

First order rate constants				
	FG (low)	FG (high)	KAO (low)	KAO (high)
Trial 1	1.0 min ⁻¹	0.4 min ⁻¹	2.8 min ⁻¹	2.8 min ⁻¹
Trial 2	0.7 min ⁻¹	2.5 min ⁻¹	2.5 min ⁻¹	2.8 min ⁻¹
Trial 3	2.8 min ⁻¹	2.8 min ⁻¹	2.8 min ⁻¹	2.8 min ⁻¹

The kinetics observed in the current study are at least one order-of-magnitude faster than those of Stagg et al. (1977) who mixed 1.9x10⁵ PFU/ml MS2 with 35 mg/L of clay particles in DI water and observed a first order removal rate constant of 0.04 min⁻¹. The current kinetics are several orders of magnitude greater than what was measured by

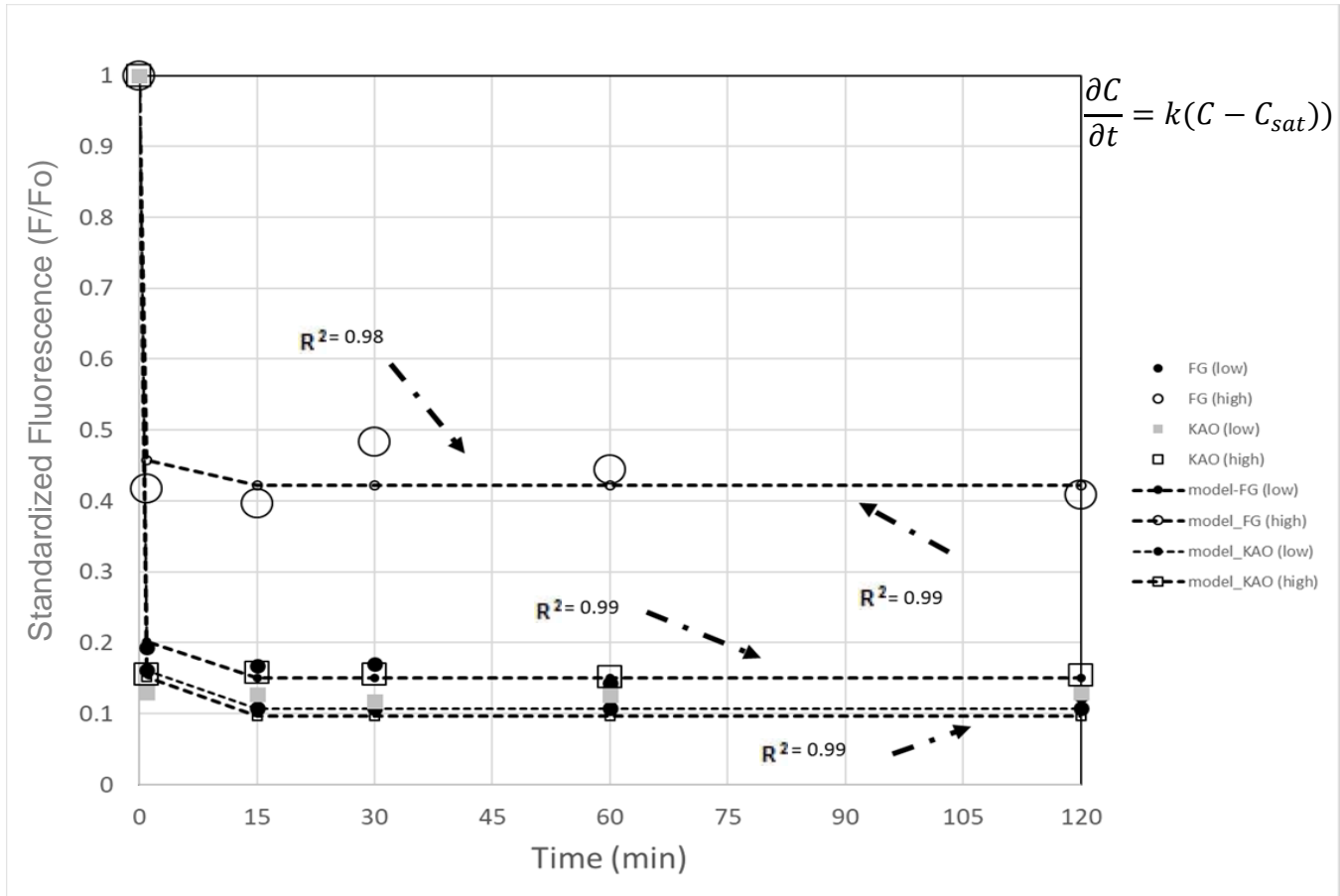


Figure 5. MS2 removal in the presence of colloids: Third experiment. The actual data points are displayed as hollow and filled circles and squares. The dashed lines are the regression curves for the two concentrations for each colloid stock, and these were used to find the removal rate constant values.

Bellou et al. (2015) who mixed MS2 with KAO in tubes mounted to a vertical rotator ($k \sim 0.02 \text{ day}^{-1}$ in the presence of KAO). The current results also stand in sharp contrast with those of Moore et al., 1975, who mixed 60 pfu/ml of bacteriophage f2, a virus that is very similar to MS2, with 16 mg/L of KAO in DI water and found negligible adsorption after 30 minutes; they also reported similar results in the case of adsorption to bentonite. Two possible reasons why the previously observed removal rates could be slower than those reported in this thesis. The first could be that the colloid concentrations were higher than those reported by Moore et al. (1975) and Stagg et al. (1977). Another possible contributor to the difference in removal rates is mixing speed. Stagg et al. (1977) specified that a rotary table was used for agitation during experiments. Moore et al. (1975) shook their solutions every five minutes during a 30 minute adsorption period. In this study, the colloid solutions were mixed with a magnetic stirring bar just fast enough so minimal splashing occurred. The current results showed that MS2 removal in the presence of colloidal particles can be much faster than previously suggested in the peer-reviewed literature.

The adsorption of MS2 to KAO and FG was confirmed with a large panel of XPS spectra (Figure 6-Figure 7) and fluorescent and bright field microscopic images (Figure 8-Figure 13). For example, the XPS graphs show the chemical composition of the surface of the particles and Table 3 lists the elements detected on the surface of the dye, MS2, KAO, FG, KAO with MS2, and FG with MS2, and their percent atomic composition. The goal of the surface characteristics was to show that MS2 attached to the surface of the KAO, as nitrogen, oxygen, and carbon are a signature of biologicals (Baer & Engelhard, 2010). XPS methodology would need improvement to increase the reliability of the data.

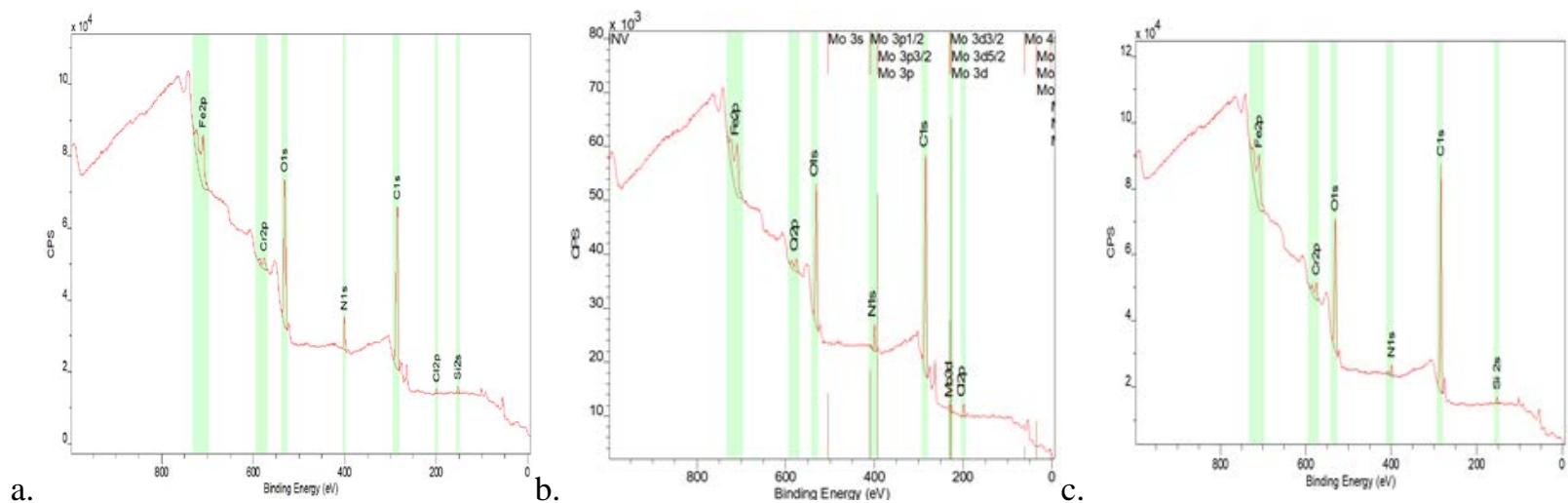


Figure 6. XPS spectra of KAO showing the difference in the chemical composition of the surface of the particles by the chemical's unique binding energies in electronvolts (eV) and the counts per second (CPS) of each chemical. a) is the labelled MS2 without colloids, b) is KAO mixed with MS2 after two hours, and c) is KAO without MS2. The y-axes are different and indicated that labelled-MS2 without KAO (a and c) results in a surface with O1s, N1s, and C1s that are roughly an order-of-magnitude higher than the labelled-MS2 with KAO (b). This would mean that after two hours the surface of the KAO could be covered with MS2.

These XPS-images were courtesy of Dr. Yun Xing.

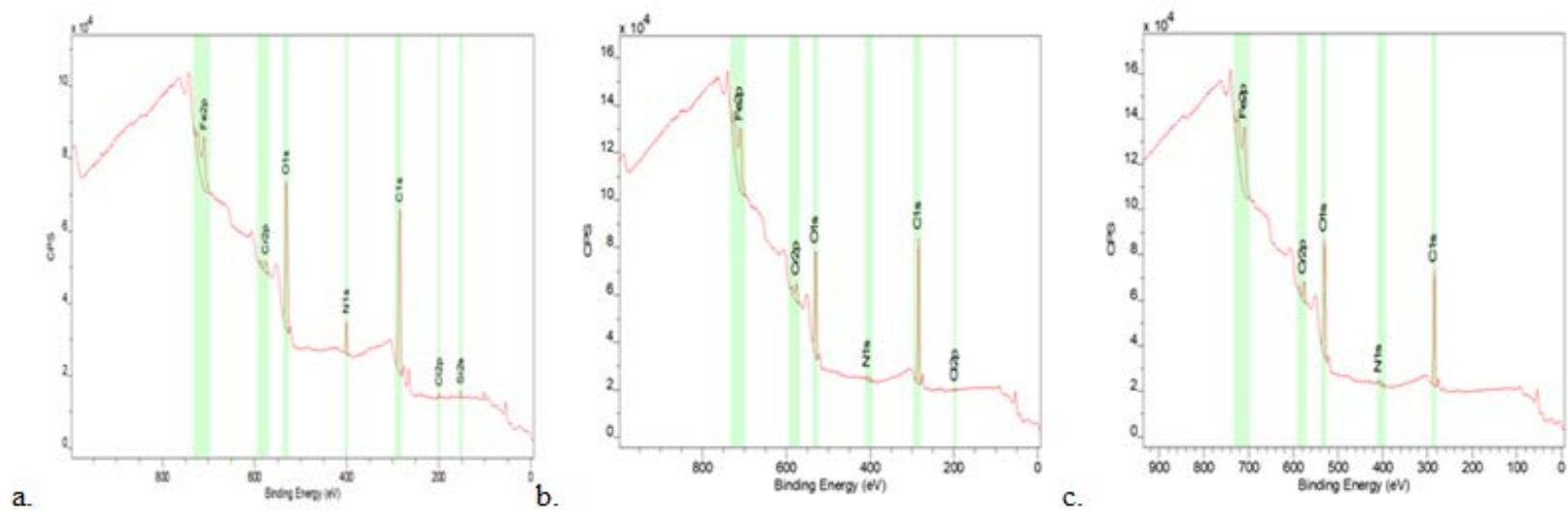


Figure 7. XPS spectra of FG showing the difference in the chemical composition of the surface of the particles by the chemical's unique binding energies in electronvolts (eV) and the counts per second (CPS) of each chemical. a) is the labelled MS2 without colloids, b) is FG mixed with MS2 after two hours, and c) is FG without MS2. The CPS levels shown in b and c match more closely than a and b, therefore the surface of the FG is likely to have less MS2 adsorbed. These XPS-images were courtesy of Dr.

Yun Xing.

Table 3. XPS Surface Data (courtesy of Dr. Xing)

Element Orbital	% Atomic Composition						
	SYTO™ 9 green fluorescent dye	MS2	Dye with MS2	Low Concentration KAO		Low Concentration FG	
				Before Labelled MS2	After Labelled MS2	Before Labelled MS2	After Labelled MS2
O 1s	26.58	36.55	29.87	27.17	26.16	26.52	24.74
N 1s	---	1.82	3.84	2.08	3.71	1.7	1.95
C 1s	23.08	24.14	34.64	33.98	36.02	19.71	23.94
Fe 2p	42.52	32.24	26.38	29.95	26.15	45.18	41.39
Cr 2p	7.82	5.26	3.84	5.65	4.47	6.89	7.85
Si 2s	---	---	0.91	1.14	---	---	---
Cl 2p	---	---	0.51	---	1.68	---	0.13
Mo 3d	---	---	---	---	1.82	---	---

Fluorescent and bright field images were overlaid (Figure 8-Figure 13) and are presented as examples to show unadsorbed, adsorbed, and MS2 in the bulk liquid at different sample times. Green fluorescence observed in the images was MS2. If green fluorescence occurred in the same location as a colloid, that was adsorption. If the green fluorescence occurred and no colloid was present, that was unadsorbed MS2. In the case of FG, a photo of a sample taken immediately after inoculating the colloids showed MS2 to be collocated with FG (Figure 8). A photograph of a sample taken at 30 minutes showed MS2 clustered around where fibers crossed (collocation) and floating in the bulk liquid (Figure 9). After 120 minutes of mixing, a photo of a sample showed the MS2 adsorbed along the fibers and where they crossed, as well (Figure 10).

Similar qualitative support was obtained for MS2 adsorption to KAO (Figure 11-Figure 13). Figure 11 is a photo of a sample taken immediately following the inoculation with MS2 and showed MS2 adsorption to KAO. After 30 minutes of mixing, a photo of a sample showed MS2 clustered around the KAO, KAO without MS2 adsorbed, and in the

bulk liquid (Figure 12). A photo of a sample taken 120 minutes after mixing showed adsorption on the surface of the KAO, and in the bulk liquid (Figure 13). These images provide qualitative evidence showing MS2 aggregates in the bulk liquid and adsorption onto the colloids.

There is reason to suspect that the observed kinetics of MS2 adsorption may be influenced by the presence of divalent cations and functional groups of the colloids and MS2. The MS2 outer surface has a slightly negative overall charge at neutral pH (Floyd & Sharp, 1979; Gerba, 1984; Wienczek et al., 1990), which can form electrostatic interactions with charged functional groups present on the surface of the colloids. However, the quantitative evidence for this is not yet conclusive. Some limited quantitative support shown by Moore et al. (1975) was based on two trials showing that calcium ion with KAO had less f2 phage remaining in solution than without calcium. They also showed that without divalent cations no viruses adsorbed to organic particulates. Stagg et al. (1977) showed that magnesium ions increased the amount of MS2 that adsorbed to bentonite particles. Tong et al. (2012) observed increased MS2 adsorption with increased ionic strength of the divalent cations. Finally, Shen, Kim, Tong, & Li (2011) used divalent calcium cations with viral RNA and silica, and observed a greater deposition efficiency than with monovalent sodium. Further research is needed to investigate the removal rates in the presence of divalent cations and organic substances to see how the rate is impacted by divalent cations and other dissolved constituents.



Figure 8. First experiment low concentration FG after introducing MS2. Particle F1 is FG without MS2, and particles A1 and A2 are FG particles with MS2 collocated.

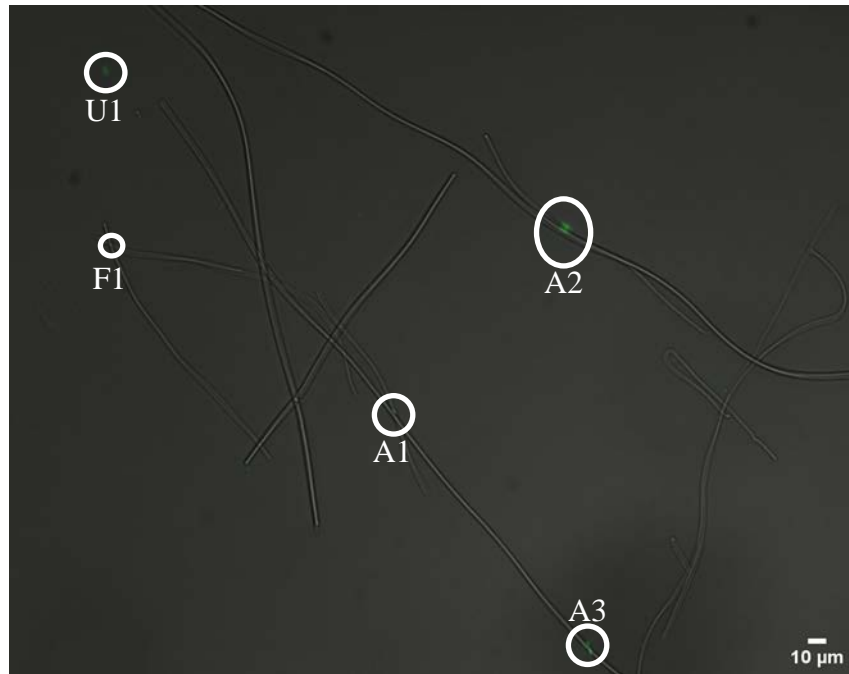


Figure 9. First experiment low concentration FG after 30 minutes of mixing with MS2 with identical fluorescent image overlay. Particles A1-A3 denote FG colloids with labeled MS2 in the same location. FG colloids are shown without MS2 adsorbed, and an example is denoted by F1. Particle U1 was MS2 occurring in a location without visually observable FG colloids in the same location.

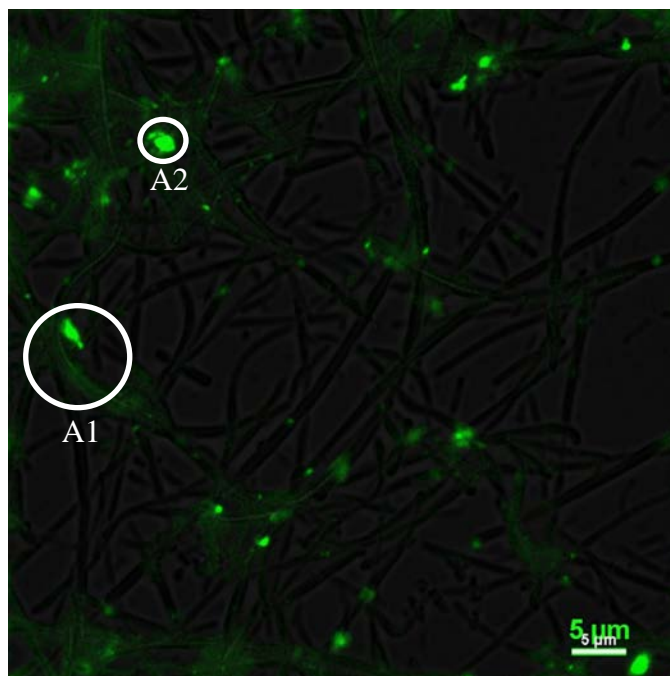


Figure 10. Second experiment high concentration FG colloids after 120 minutes of mixing labeled MS2 photographed with the help of Air Force Research Laboratory and Dr. Irina Drachuk. Particles A1 and A2 show MS2 at the locations of along the surface of FG and where FG colloids cross, respectively. Unadsorbed MS2 aggregates were not observed in this FG image.

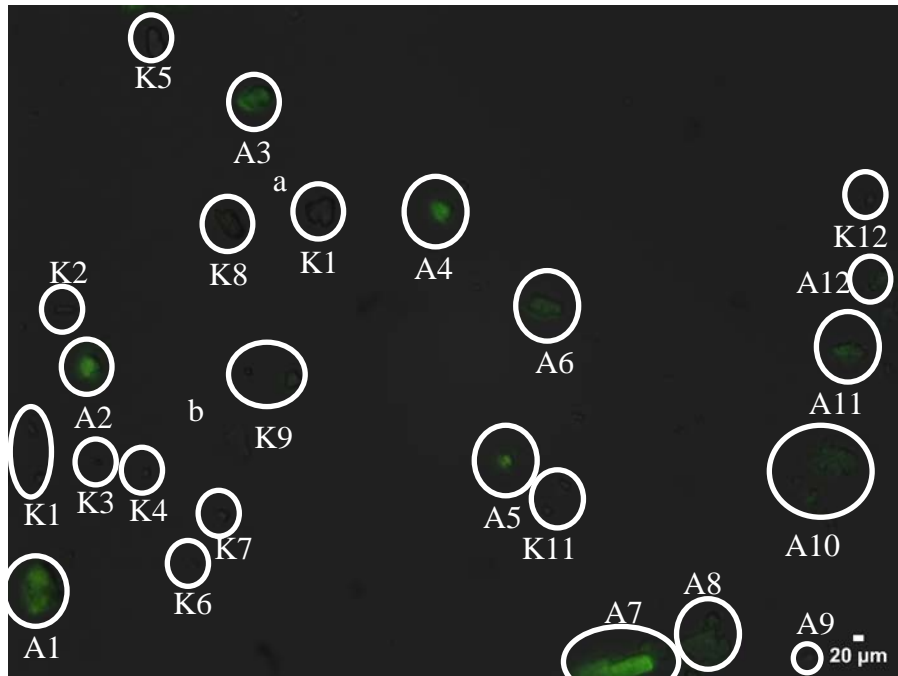


Figure 11. First experiment low concentration KAO after introducing MS2, which adsorbed to some KAO, but not all. Colloidal particles K1-K12 are KAO without MS2 and A1 – A12 are KAO colloids with MS2.

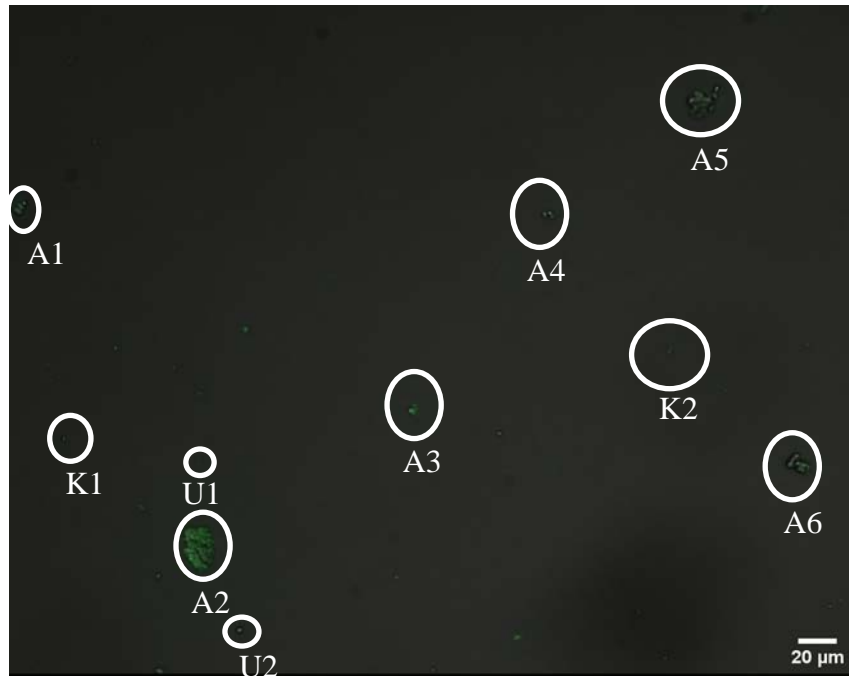


Figure 12. Second experiment low concentration KAO after 30 minutes of mixing with labeled MS2 with identical fluorescent image overlay. Colloidal particles A1-A6 denote KAO colloids with labeled MS2 in the same location. Colloidal particles K1-K2 are KAO colloids without MS2 adsorbed. Colloidal particles U1-U2 are MS2 occurring in locations without visually observable KAO colloids in the same location.

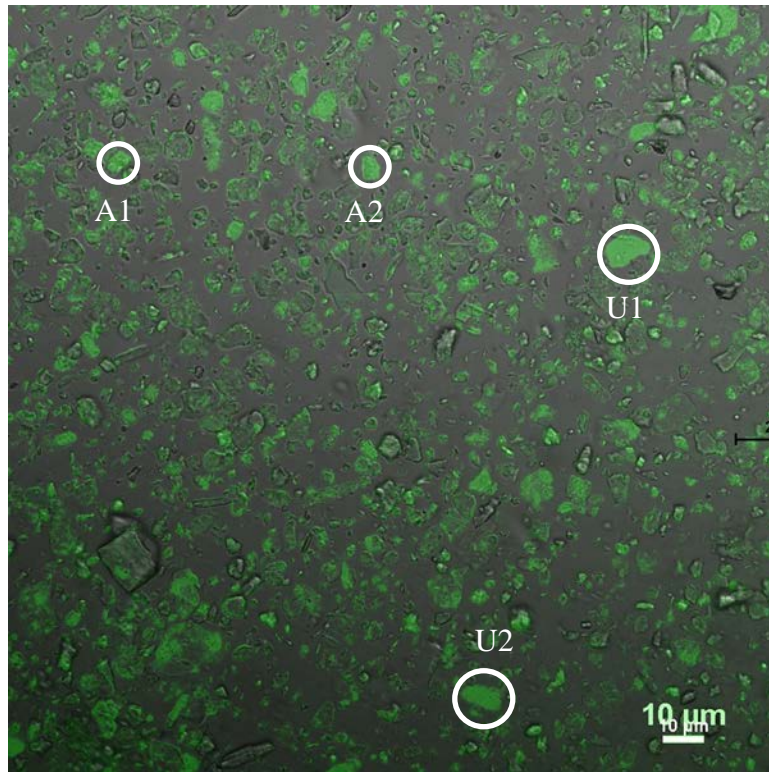


Figure 13. Second experiment high concentration KAO colloids after 120 minutes of mixing labeled MS2 photographed with the help of Air Force Research Laboratory and Dr. Irina Drachuk. Colloidal particles A1-A6 denote KAO with labeled MS2 in the same location. Colloidal particles U1-U2 are MS2 occurring in locations without visually observable KAO in the same location.

4.2 Bond Strength

Bond strength was assessed by collecting and washing the pellets and measuring the resulting fluorescence in the supernatants. The washing procedure allowed MS2 aggregates and colloid particles to be separated from weakly bound viruses in the wash-supernatant. MS2 viruses that were washed off of the pellet were characterized as weakly bound. The strongly bound fraction was calculated by mass balance and may have included MS2 viruses trapped within MS2 aggregates. Figure 14 shows the bond strength profile for MS2 in the presence of FG (low concentration, experiment 1). The y-axis is the percentage of MS2 that is associated with each bond characteristic shown on the x-axis. The percentages of the unbound MS2 were calculated by finding the ratio of the difference between the initial measured amount of fluorescence in the supernatant (before adding colloids) and the measured amount of fluorescence in the supernatant at the sample time, dividing the difference by the initial amount of fluorescence, and then multiplying by 100%. The percentages of the weakly bound MS2 were calculated by finding the ratio of the difference between the initial measured amount of fluorescence in the supernatant (before adding colloids) and the measured amount of fluorescence in the supernatant of the washed pellet at the sample time, dividing the difference by the initial amount of fluorescence, and then multiplying by 100%. For experiments 1 and 2, twelve measurements of the fluorescence of the MS2 stock were averaged and used as the initial amount of fluorescence. For the third experiment, three measurements of the MS2 stock were averaged and used as the initial fluorescence. The amount of the strongly bound MS2 was found by subtracting the unadsorbed and weakly adsorbed fluorescence from

the initial fluorescence. Then, the percentage was found by multiplying the ratio of the strongly bound fluorescence to the initial amount of fluorescence. Figure 14 also shows p-values associated with the statistical significance of the differences that were observed. In the FG (low) experiment, the percentage of strongly bound MS2 increased from 26.7% at 1.48 min to 55.2% at 120 minutes; the percentage of weakly bound MS2 was between 6.7% and 8.4% throughout the experiment (Figure 14). The differences between the strongly and weakly bound MS2 were significant at all time points using a two-tailed t-test. In the FG (high) experiment, the percentage of strongly bound MS2 increased from 31.7% at 2.04 min to 54.6% at 120 minutes; the percentage of weakly bound MS2 was between 5% and 11% throughout the experiment (Figure 15). The differences between the strongly and weakly bound MS2 were significant at all time points. In the KAO (low) experiments, the percentage of strongly bound MS2 did not increase with time, and was between 51.3% and 60%; the percentage of weakly bound MS2 was between 3.2% and 10.8% throughout the experiment (Figure 16). Similar results were observed in the KAO (high) experiments (Figure 17). The percentage of strongly bound MS2 did not increase with time, and was between 60.9% and 63.2%; the percentage of weakly bound MS2 was between 4.4% and 6.8% throughout the experiment. The differences between the strongly and weakly bound MS2 were significant at all time points.

During the second FG (low) experiments, the percentage of strongly bound MS2 increased from 28.6% at 1.48 min to 65.2% at 120 minutes; the percentage of weakly bound MS2 was between 1.6% and 9% throughout the experiment (Figure 18). In the second FG (high) experiments, the percentage of strongly bound MS2 increased from 69.2% at 1.48 min to 80.8% at 120 minutes; the percentage of weakly bound MS2 was

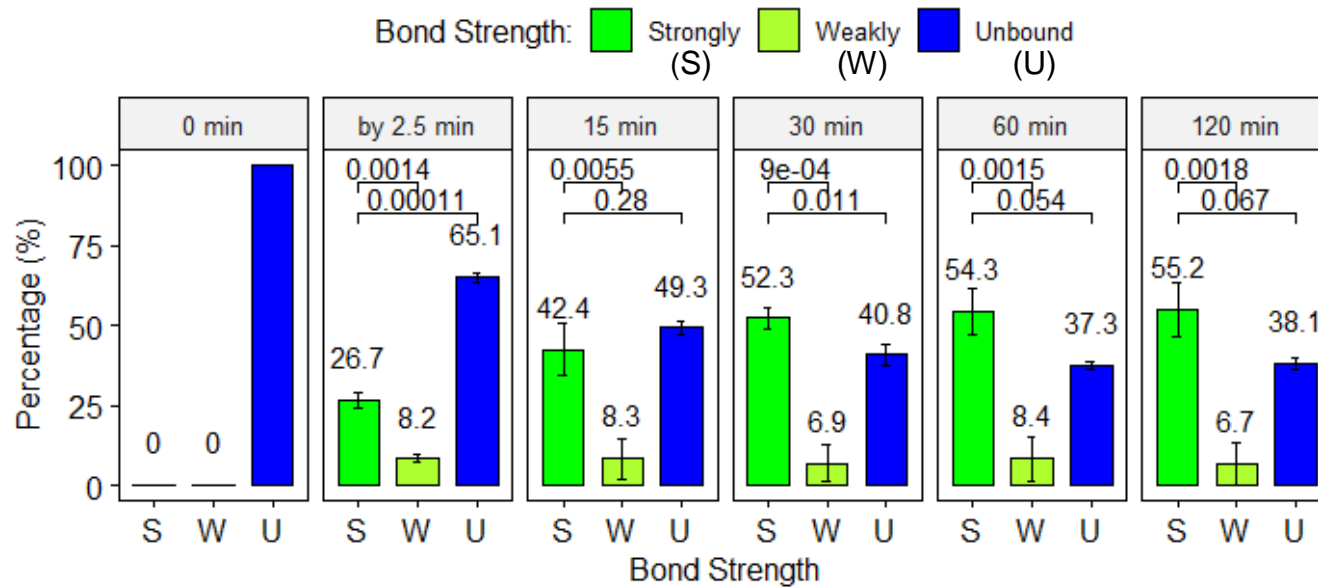


Figure 14. Bond strength profile: Experiment one low concentration FG. The percentages of each bond characteristic are shown at each sample time. MS2 viruses that were measured in the removal kinetics were considered to be unadsorbed (U). Viruses that washed off the colloids in the pellet were characterized as weakly bound (W). The difference between the U and W viruses were characterized as strongly bound (S). At the zero minute time point, all MS2 was unadsorbed, until the colloids were added. Then, the initial sampling occurred at the next time interval, and at 15, 30, 60, and 120 minutes after adding the labelled MS2 to the colloids. The p-values of significance (two-tailed t-test) are shown above the colored bond characteristic percentage bars.

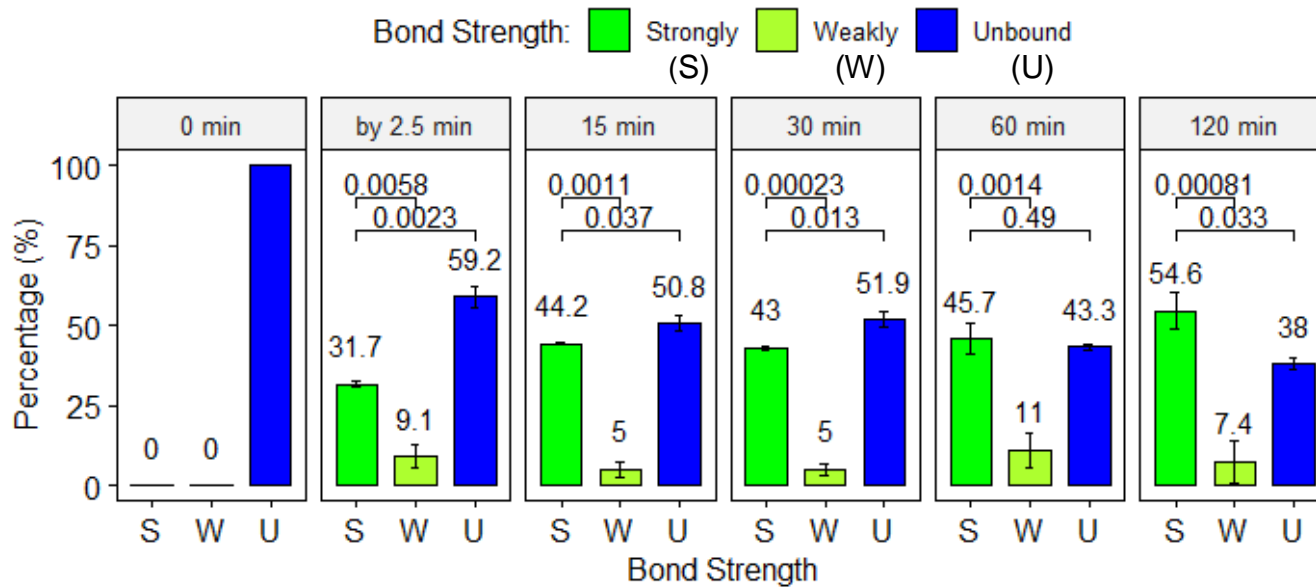


Figure 15. Bond strength profile: Experiment one high concentration FG. The percentages of each bond characteristic are shown at each sample time. MS2 viruses that were measured in the removal kinetics were considered to be unadsorbed (U). Viruses that washed off the colloids in the pellet were characterized as weakly bound (W). The difference between the U and W viruses were characterized as strongly bound (S). At the zero minute time point, all MS2 was unadsorbed, until the colloids were added. Then, the initial sampling occurred at the next time interval, and at 15, 30, 60, and 120 minutes after adding the labelled MS2 to the colloids. The p-values of significance (two-tailed t-test) are shown above the colored bond characteristic percentage bars.

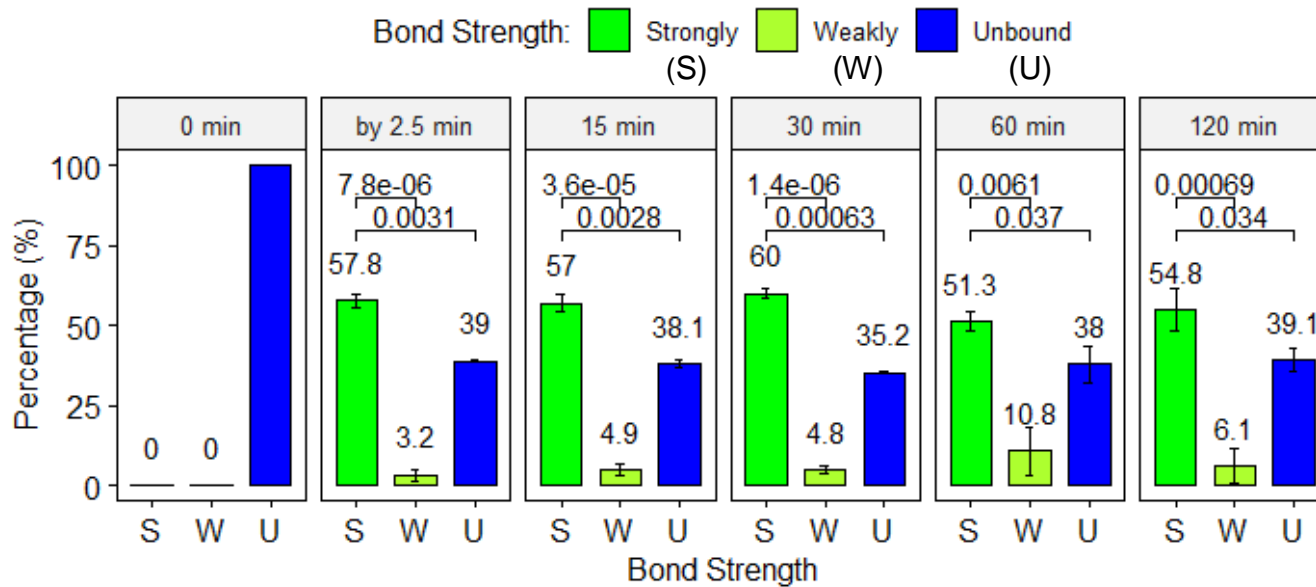


Figure 16. Bond strength profile: Experiment one low concentration KAO. The percentages of each bond characteristic are shown at each sample time. MS2 viruses that were measured in the removal kinetics were considered to be unadsorbed (U). Viruses that washed off the colloids in the pellet were characterized as weakly bound (W). The difference between the U and W viruses were characterized as strongly bound (S). At the zero minute time point, all MS2 was unadsorbed, until the colloids were added. Then, the initial sampling occurred at the next time interval, and at 15, 30, 60, and 120 minutes after adding the labelled MS2 to the colloids. The p-values of significance (two-tailed t-test) are shown above the colored bond characteristic percentage bars.

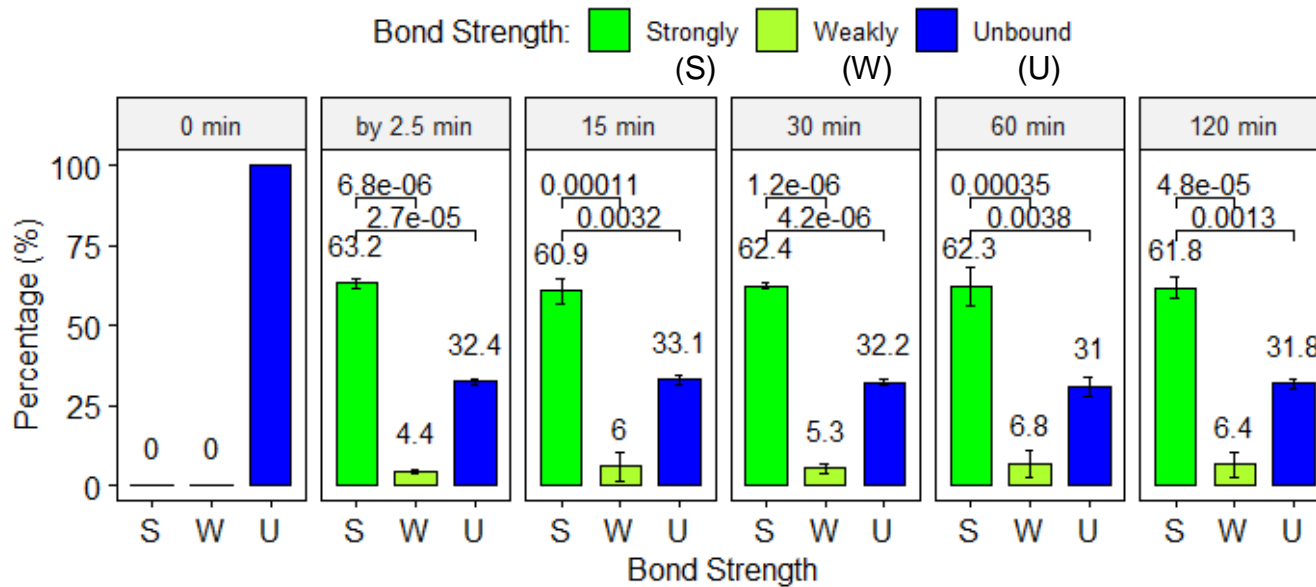


Figure 17. Bond strength profile: Experiment one high concentration KAO. The percentages of each bond characteristic are shown at each sample time. MS2 viruses that were measured in the removal kinetics were considered to be unadsorbed (U). Viruses that washed off the colloids in the pellet were characterized as weakly bound (W). The difference between the U and W viruses were characterized as strongly bound (S). At the zero minute time point, all MS2 was unadsorbed, until the colloids were added. Then, the initial sampling occurred at the next time interval, and at 15, 30, 60, and 120 minutes after adding the labelled MS2 to the colloids. The p-values of significance (two-tailed t-test) are shown above the colored bond characteristic percentage bars.

between 3% and 6.5% throughout the experiment (Figure 19). In the second KAO (low) experiments, the percentage of strongly bound MS2 did not increase with time, and was between 79.2% and 81.7%; the percentage of weakly bound MS2 was between 2% and 5.1% throughout the experiment (Figure 20). In the second KAO (high) experiments, the percentage of strongly bound MS2 did not increase with time, and was between 81.8% and 83.3%; the percentage of weakly bound MS2 was between 3.1% and 4% throughout the experiment (Figure 21). The differences between the strongly and weakly bound MS2 were significant at all time points, materials, and concentrations.

During the third FG (low) experiments, the percentage of strongly bound MS2 did not increase with time and was between 49.4% and 56.7%; the percentage of weakly bound MS2 was between 4.8% and 8% throughout the experiment (Figure 22). In the third FG (high) experiments, the percentage of strongly bound MS2 increased slightly from 72.9% at 2.04 min to 80.3% at 120 minutes; the percentage of weakly bound MS2 was between 4.7% and 8.8% throughout the experiment (Figure 23). In the third KAO (low) experiments, the percentage of strongly bound MS2 did not increase with time, and was between 82.4% and 85%; the percentage of weakly bound MS2 was between 2.7% and 6.2% throughout the experiment (Figure 24). In the third KAO (high) experiments, the percentage of strongly bound MS2 did not increase with time, and was between 85.9% and 87.9%; the percentage of weakly bound MS2 was between 1.3% and 3.8% throughout the experiment (Figure 25). The differences between the strongly and weakly bound MS2 were significant at all time points, materials, and concentrations. Most of the adsorbed MS2 was strongly bound. These results are in agreement with research by Stagg et al. (1977) in which they found that less than 1% of the virus could be recovered.

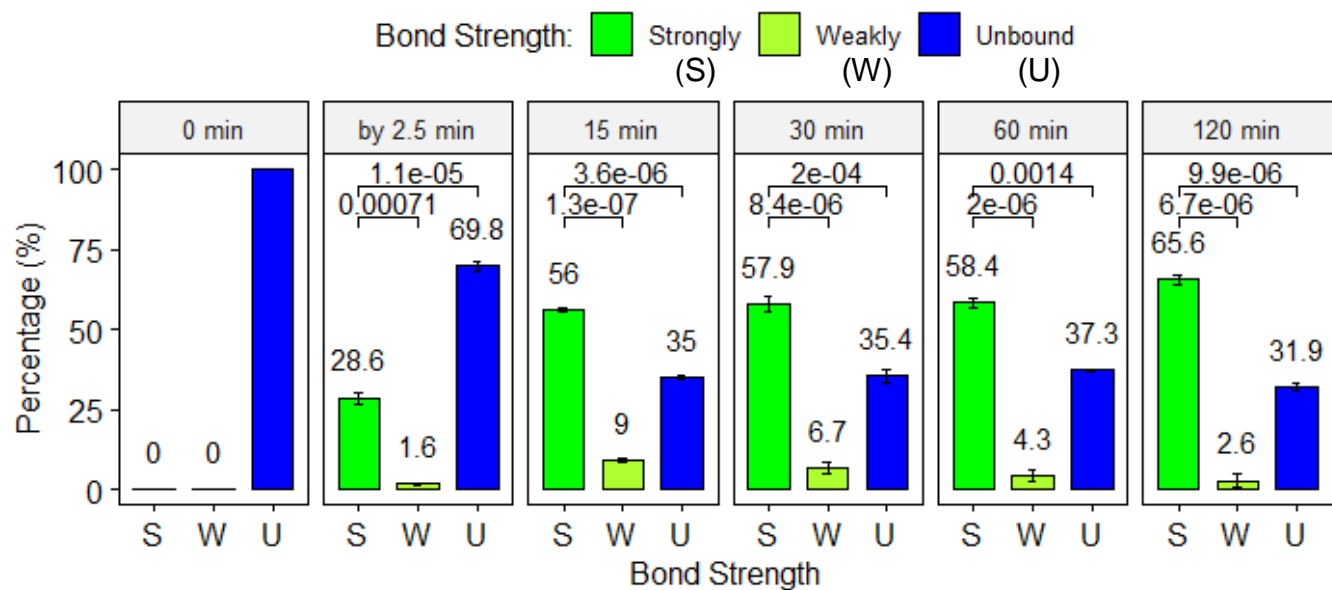


Figure 18. Bond strength profile: Experiment two low concentration FG. The percentages of each bond characteristic are shown at each sample time. MS2 viruses that were measured in the removal kinetics were considered to be unadsorbed (U). Viruses that washed off the colloids in the pellet were characterized as weakly bound (W). The difference between the U and W viruses were characterized as strongly bound (S). At the zero minute time point, all MS2 was unadsorbed, until the colloids were added. Then, the initial sampling occurred at the next time interval, and at 15, 30, 60, and 120 minutes after adding the labelled MS2 to the colloids. The p-values of significance (two-tailed t-test) are shown above the colored bond characteristic percentage bars.

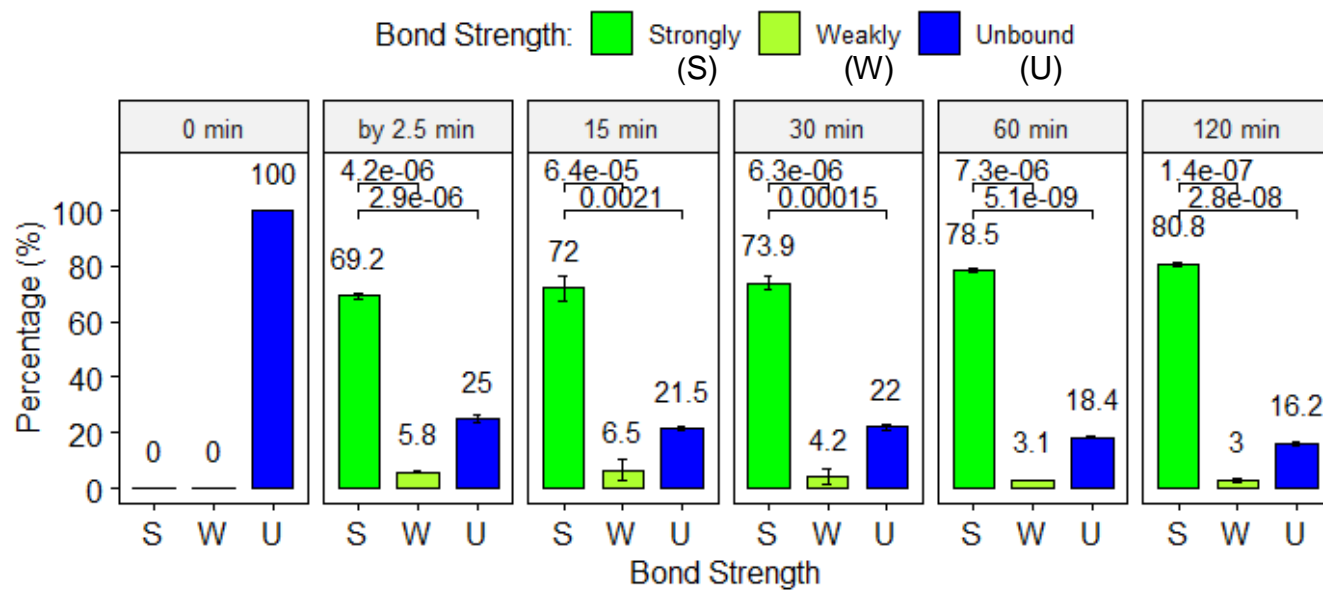


Figure 19. Bond strength profile: Experiment two high concentration FG. The percentages of each bond characteristic are shown at each sample time. MS2 viruses that were measured in the removal kinetics were considered to be unadsorbed (U). Viruses that washed off the colloids in the pellet were characterized as weakly bound (W). The difference between the U and W viruses were characterized as strongly bound (S). At the zero minute time point, all MS2 was unadsorbed, until the colloids were added. Then, the initial sampling occurred at the next time interval, and at 15, 30, 60, and 120 minutes after adding the labelled MS2 to the colloids. The p-values of significance (two-tailed t-test) are shown above the colored bond characteristic percentage bars.

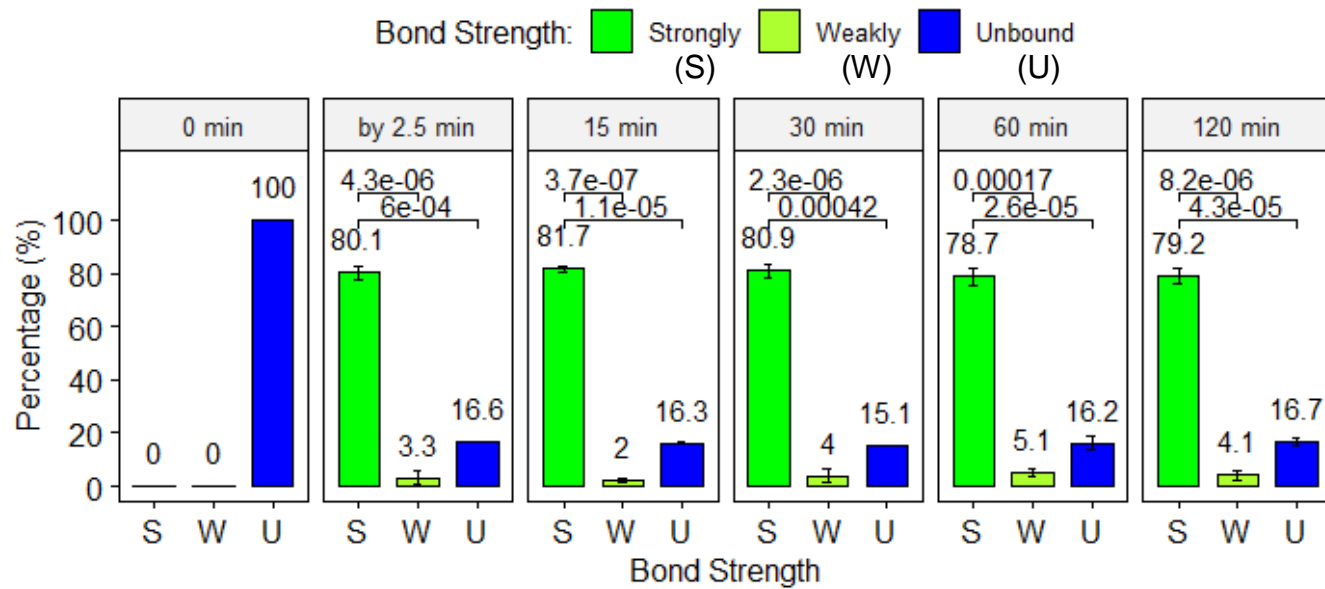


Figure 20. Bond strength profile: Experiment two low concentration KAO. The percentages of each bond characteristic are shown at each sample time. MS2 viruses that were measured in the removal kinetics were considered to be unadsorbed (U). Viruses that washed off the colloids in the pellet were characterized as weakly bound (W). The difference between the U and W viruses were characterized as strongly bound (S). At the zero minute time point, all MS2 was unadsorbed, until the colloids were added. Then, the initial sampling occurred at the next time interval, and at 15, 30, 60, and 120 minutes after adding the labelled MS2 to the colloids. The p-values of significance (two-tailed t-test) are shown above the colored bond characteristic percentage bars.

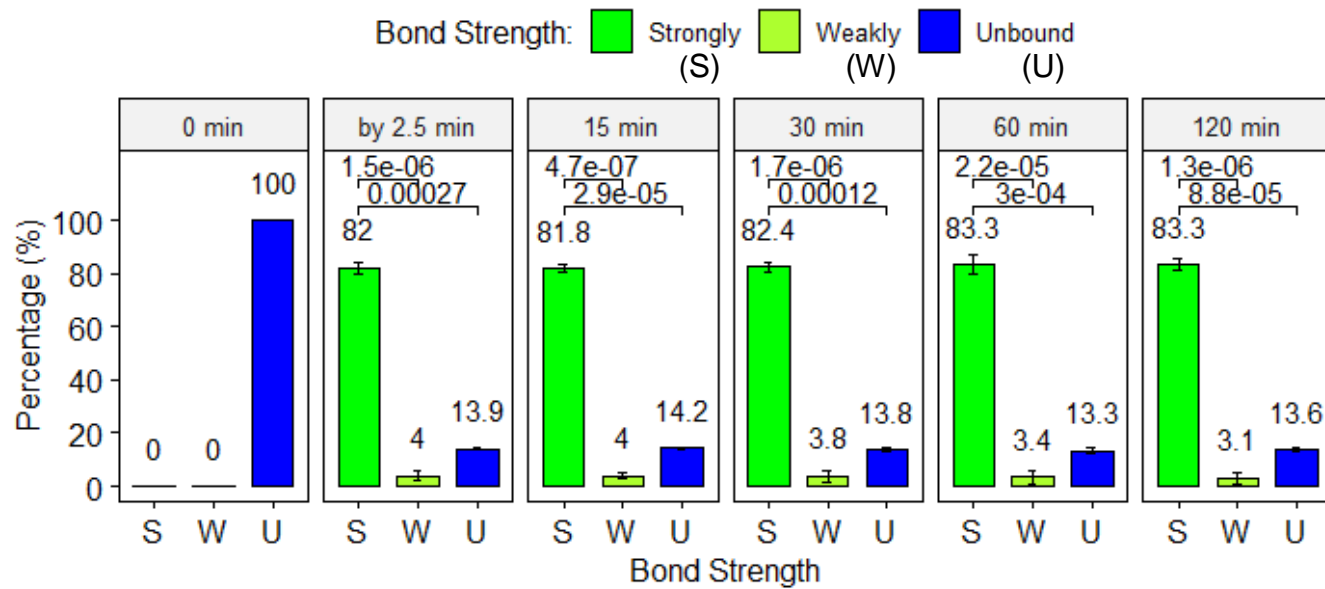


Figure 21. Bond strength profile: Experiment two high concentration KAO. The percentages of each bond characteristic are shown at each sample time. MS2 viruses that were measured in the removal kinetics were considered to be unadsorbed (U). Viruses that washed off the colloids in the pellet were characterized as weakly bound (W). The difference between the U and W viruses were characterized as strongly bound (S). At the zero minute time point, all MS2 was unadsorbed, until the colloids were added. Then, the initial sampling occurred at the next time interval, and at 15, 30, 60, and 120 minutes after adding the labelled MS2 to the colloids. The p-values of significance (two-tailed t-test) are shown above the colored bond characteristic percentage bars.

This bond strength distinction has important operational implications. Weakly bound MS2 viruses may readily de-attach from colloidal particles in water and be vulnerable to inactivation due to shading from ultraviolet radiation disinfection or the colloid absorbing the chemical used for disinfection (Stagg et al., 1977; Wu et al., 2018). However, MS2 aggregates may remain in the bulk liquid or re-attach to colloidal particles in a dynamic water treatment system. Strongly bound MS2 viruses will be transported by colloidal particles, and likely end up either in the sludge or in the effluent as a viable pathogen. Our data showed that most of the MS2 was either strongly bound to the colloids or enmeshed in aggregates that co-settled with colloids. To the author's knowledge, this study appears to be the first to present evidence for adsorption strength characteristics for MS2 in the presence of colloidal materials. In a full-scale water treatment facility, the fate of strongly bound viruses will likely be different than unbound MS2 viruses or weakly bound MS2 viruses, which may detach. Tightly bound MS2 viruses will likely end up in sludge or effluent, associated with colloids and likely be viable.

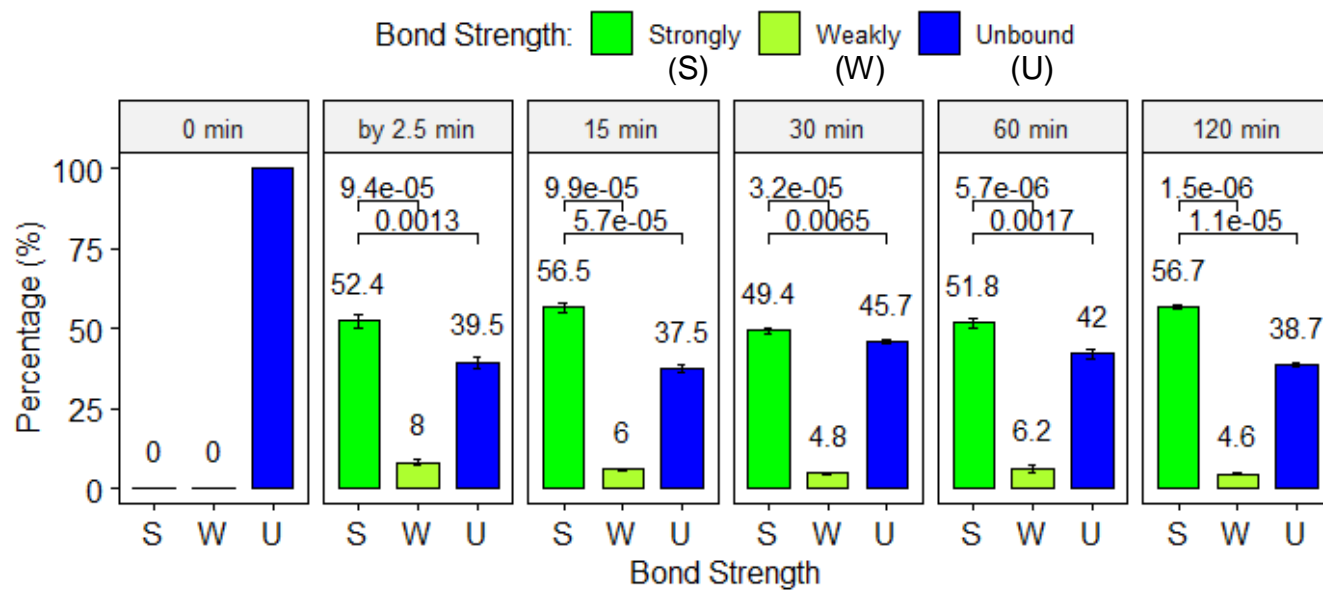


Figure 22. Bond strength profile: Experiment three low concentration FG. The percentages of each bond characteristic are shown at each sample time. MS2 viruses that were measured in the removal kinetics were considered to be unadsorbed (U). Viruses that washed off the colloids in the pellet were characterized as weakly bound (W). The difference between the U and W viruses were characterized as strongly bound (S). At the zero minute time point, all MS2 was unadsorbed, until the colloids were added. Then, the initial sampling occurred at the next time interval, and at 15, 30, 60, and 120 minutes after adding the labelled MS2 to the colloids. The p-values of significance (two-tailed t-test) are shown above the colored bond characteristic percentage bars.

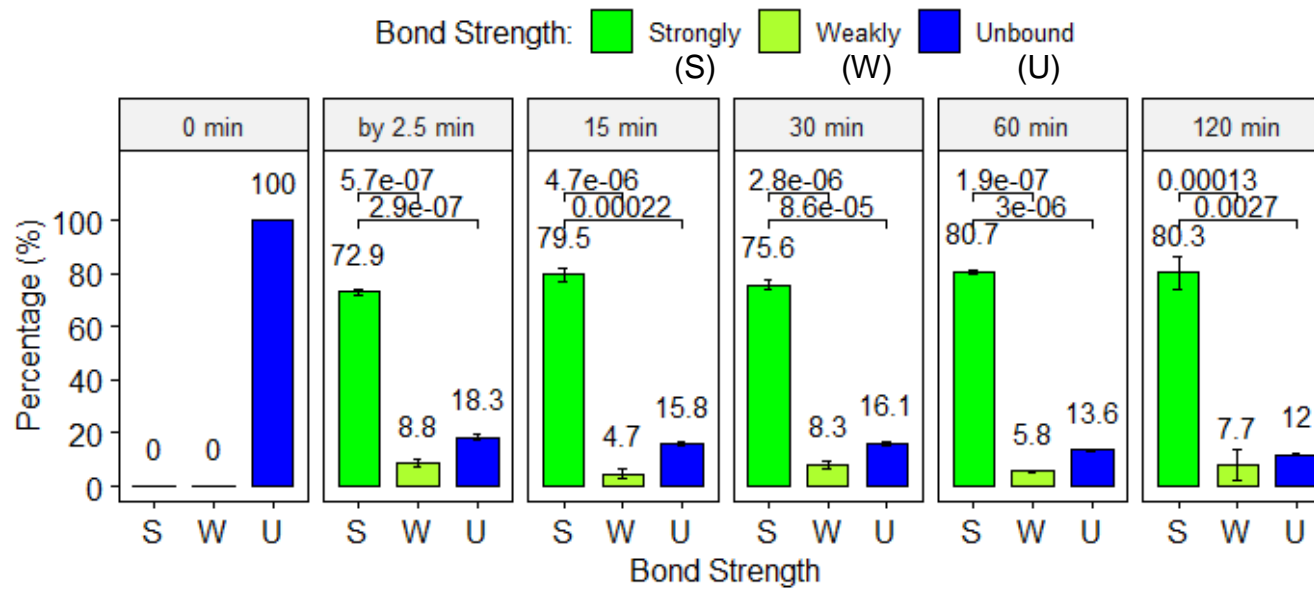


Figure 23. Bond strength profile: Experiment three high concentration FG. The percentages of each bond characteristic are shown at each sample time. MS2 viruses that were measured in the removal kinetics were considered to be unadsorbed (U). Viruses that washed off the colloids in the pellet were characterized as weakly bound (W). The difference between the U and W viruses were characterized as strongly bound (S). At the zero minute time point, all MS2 was unadsorbed, until the colloids were added. Then, the initial sampling occurred at the next time interval, and at 15, 30, 60, and 120 minutes after adding the labelled MS2 to the colloids. The p-values of significance (two-tailed t-test) are shown above the colored bond characteristic percentage bars.

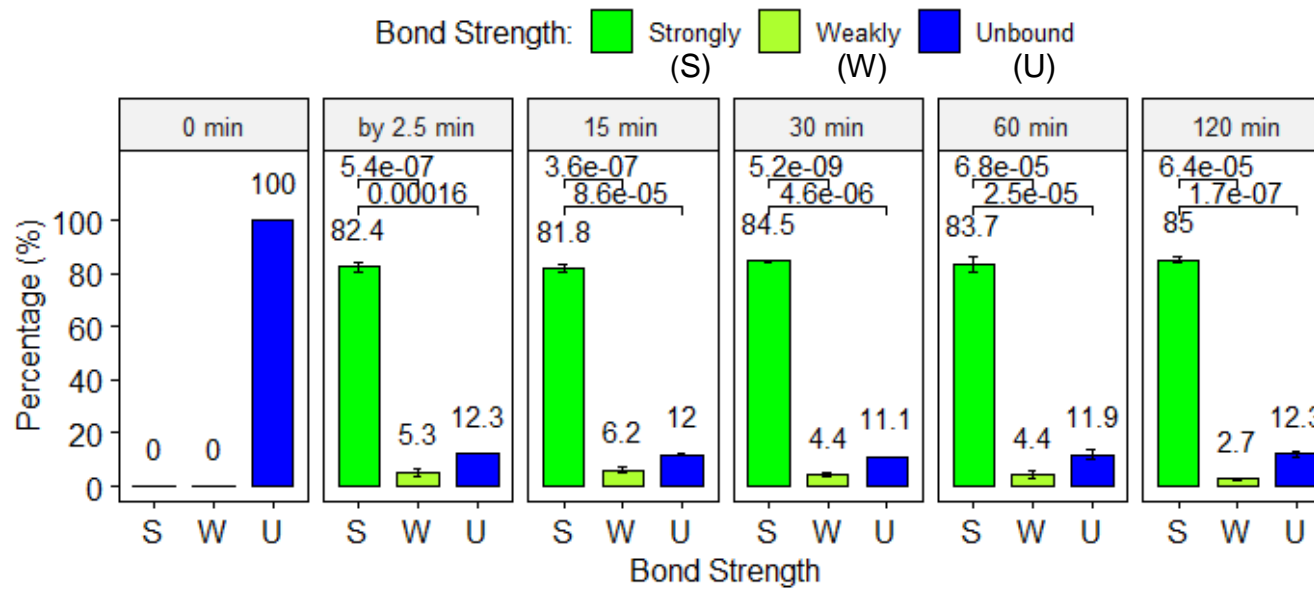


Figure 24. Bond strength profile: Experiment three low concentration KAO. The percentages of each bond characteristic are shown at each sample time. MS2 viruses that were measured in the removal kinetics were considered to be unadsorbed (U). Viruses that washed off the colloids in the pellet were characterized as weakly bound (W). The difference between the U and W viruses were characterized as strongly bound (S). At the zero minute time point, all MS2 was unadsorbed, until the colloids were added. Then, the initial sampling occurred at the next time interval, and at 15, 30, 60, and 120 minutes after adding the labelled MS2 to the colloids. The p-values of significance (two-tailed t-test) are shown above the colored bond characteristic percentage bars.

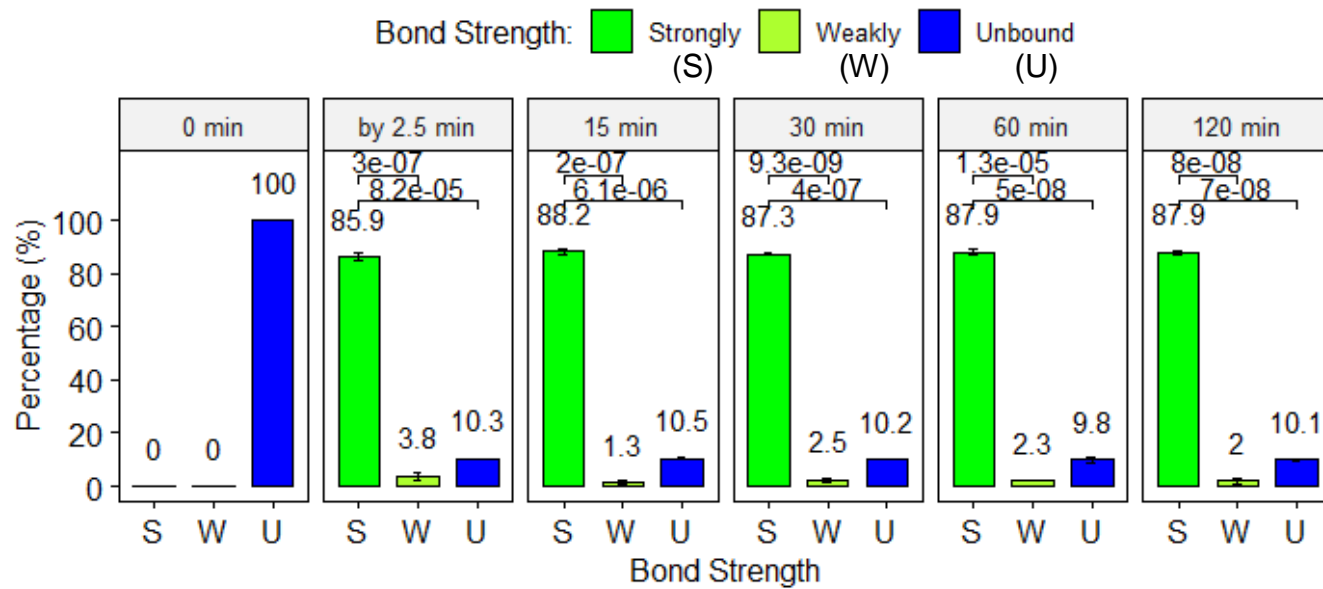


Figure 25. Bond strength profile: Experiment three high concentration KAO. The percentages of each bond characteristic are shown at each sample time. MS2 viruses that were measured in the removal kinetics were considered to be unadsorbed (U). Viruses that washed off the colloids in the pellet were characterized as weakly bound (W). The difference between the U and W viruses were characterized as strongly bound (S). At the zero minute time point, all MS2 was unadsorbed, until the colloids were added. Then, the initial sampling occurred at the next time interval, and at 15, 30, 60, and 120 minutes after adding the labelled MS2 to the colloids. The p-values of significance (two-tailed t-test) are shown above the colored bond characteristic percentage bars.

4.3 Surface Attachment and Aggregation

XDLVO modeling was carried out to investigate the relative importance of the forces affecting MS2 and the KAO or FG colloids, and applied to the initial interactions with individual MS2 phages (Figure 26-Figure 29). Along the y-axis was plotted the dimensionless potential interaction energy as the separation distance between particles varies along the x-axis. The parameters used for these figures are provided in Appendix D Table 11. The XDLVO profiles showed an energy barrier at a separation distance of approximately 2.5 nm, but as the separation distance approaches zero there is a deep primary energy minimum. Figure 26 shows three curves. The green curve is MS2 aggregation. The red curve shows FG-MS2 adsorption, and the blue curve shows KAO-MS2 adsorption. The green MS2 aggregation curve shows the lowest energy barrier. This suggests that MS2 aggregation would be favored over KAO-MS2 and FG-MS2 adsorption. The results also show that the energy barrier was a function of the surface potentials of MS2 (Figure 27), FG (Figure 28), and KAO (Figure 29). For MS2-MS2, FG-MS2, and KAO-MS2 interactions, as the surface potential of MS2 would become more negative adsorption would become less favorable and the particles would become more stable. The surface potentials for MS2 and the colloidal particles are expected to be negative in DI water at neutral pH (Chrysikopoulos & Syngouna, 2012; Meissner et al., 2015). These

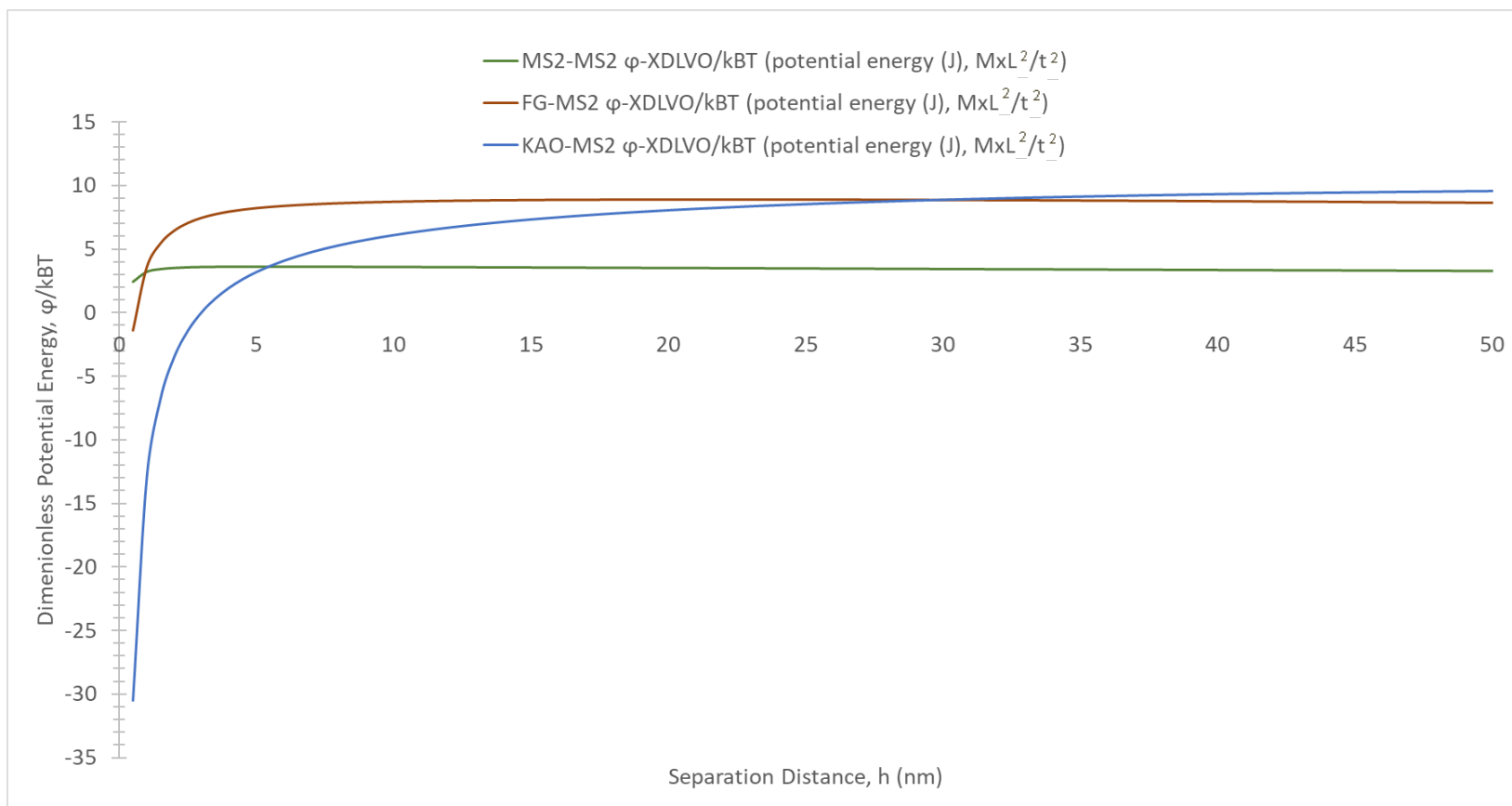


Figure 26. XDLVO interaction energy profiles: MS2-MS2, FG-MS2, and KAO-MS2 interactions in DI water. (MS2 Ψ -potential = -0.02V, KAO Ψ -potential = -0.04V, FG Ψ -potential = -0.02V, ionic strength = 8.8×10^{-7} M, sphere-sphere for MS2-MS2 XDLVO calculations and sphere-plate formulas for the FG- and KAO-MS2 XDLVO calculations)

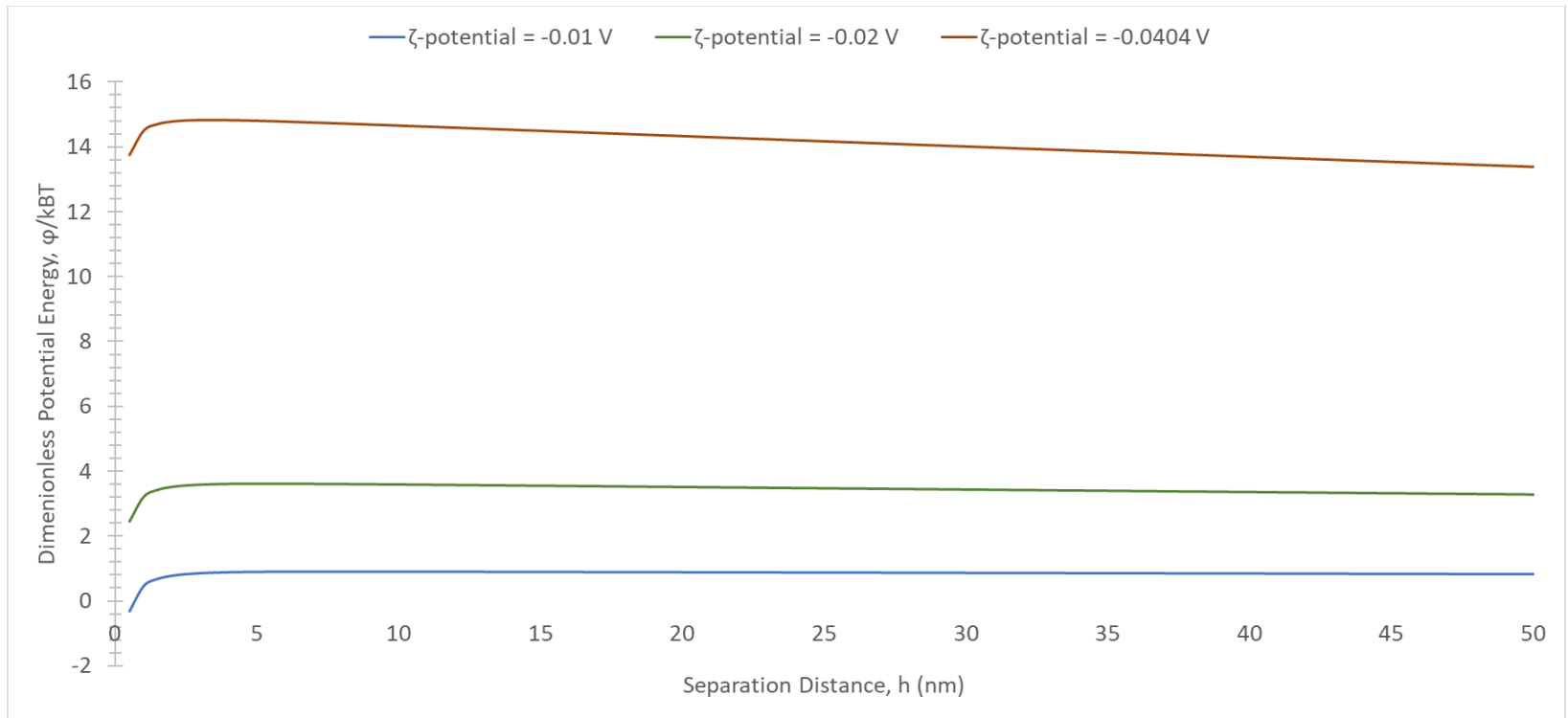


Figure 27. XDLVO interaction energy profiles: MS2-MS2 varying surface-potentials in DI water. (MS2 surface-potential varies, ionic strength = 8.8×10^{-7} M, sphere-sphere for MS2-MS2 XDLVO calculations).

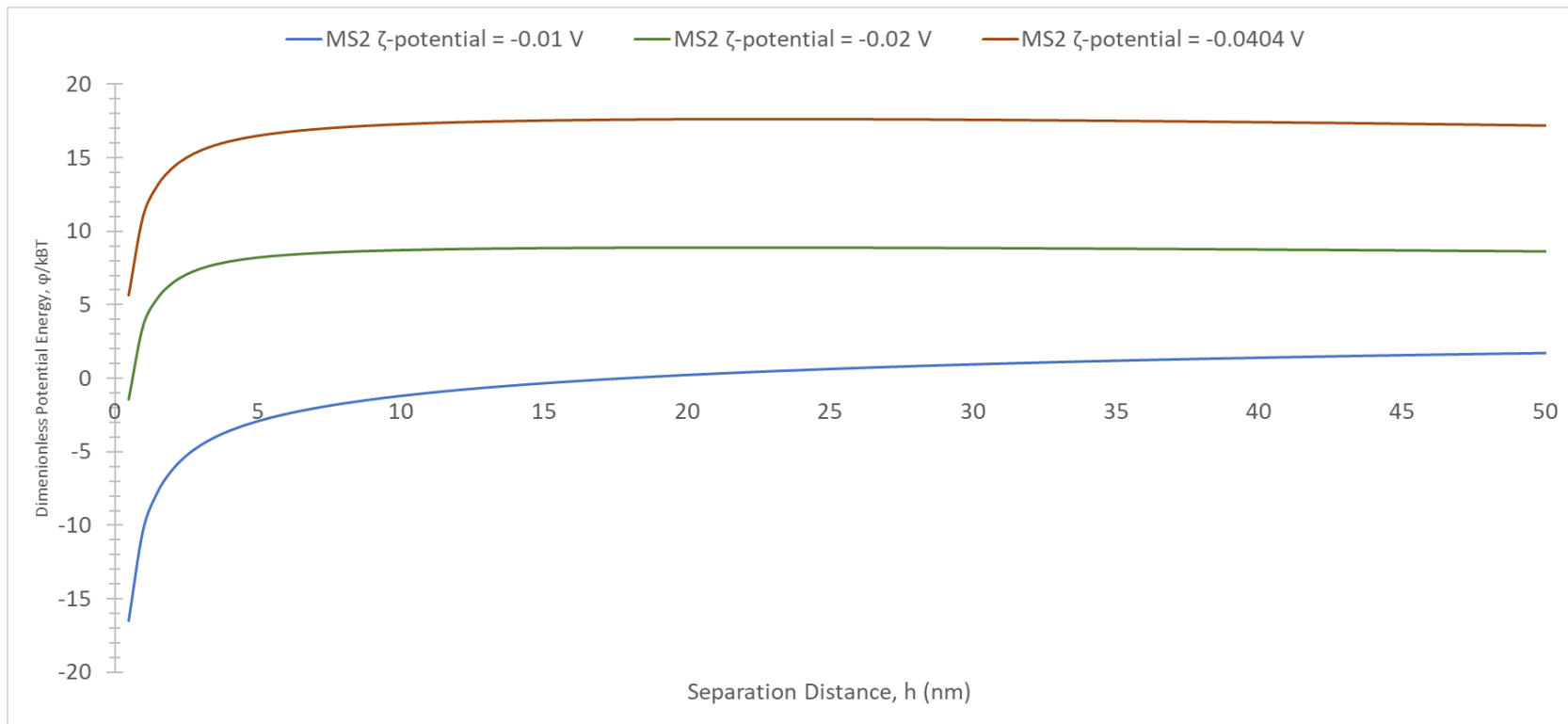


Figure 28. XDLVO energy profile: FG-MS2, holding constant FG surface-potential at -0.028V and varying the MS2 surface-potential. (MS2 Ψ -potential varies, ionic strength = 8.8×10^{-7} M, sphere-plate formulas)

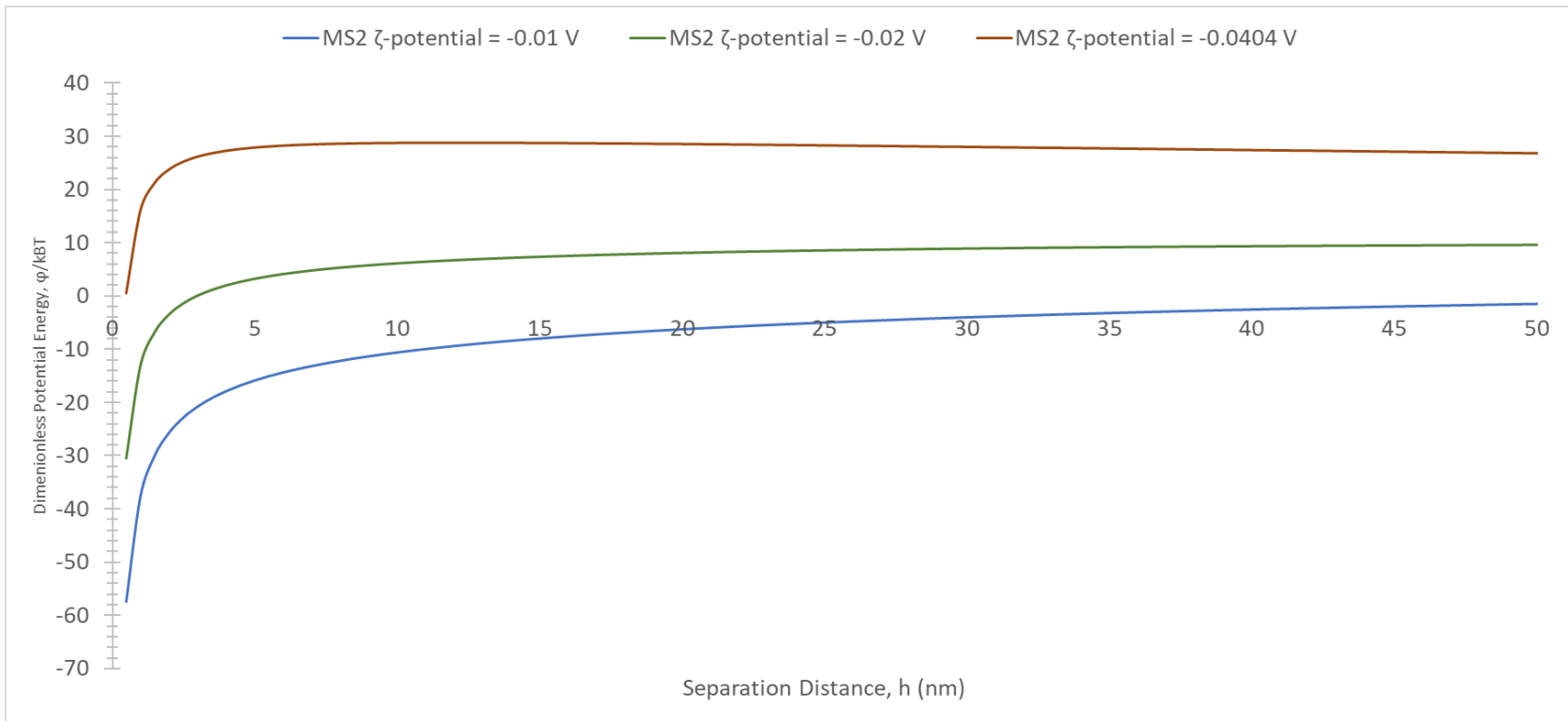


Figure 29. XDLVO energy profile: KAO-MS2, KAO surface potential constant at -0.0404V and varying the MS2 surface potential. (MS2 Ψ -potential varies, ionic strength = 8.8×10^{-7} M, sphere-plate formulas)

findings suggest that MS2 may initially aggregate before attaching to the colloidal surface.

AFM images provided qualitative evidence of MS2 aggregation (Figure 30-Figure 32). AFM images were provided courtesy of Dr. Yun Xing of the AFIT Engineering Department. MS2 adsorption to KAO colloids was shown in Figure 30. MS2 adsorption to FG colloids were shown in Figure 31 and Figure 32, and, similar to the KAO images, evidence of MS2 aggregates were shown. MS2 aggregates in the FG solution not near FG reflect the qualitative results of the lower adsorbed percentage, weaker bonds, and longer amount of time for equilibrium to be reached between FG and MS2 as compared with KAO and MS2. Additionally, particle size and topography were determined. MS2 aggregates ranged from 20 to 30nm in diameter. KAO particles were found to be flat, platy, 2 μm in thickness, and 120-600 μm in lateral size with 120-200 μm being the most observed size. These findings are in agreement with those of Bellou et al. (2015), and Chrysikopoulos & Syngouna (2012). FG particles were found to have a diameter of 0.5 μm -1.7 μm .

XDLVO theory is concerned with single particles contacting each other, however images (section 4.1) showed unadsorbed MS2. A control experiment was done to further investigate MS2 aggregation. These experiments were carried out with the same protocols explained in the methods section, except that no colloidal particles were added into the batch test. Figure 33 shows that the fluorescence decreased from approx. 1069 arbitrary units (a.u.) to 766 a.u. in 2 hours. The concentration of MS2 present in the supernatant decreased. These data were fitted to an exponential decay trend ($R^2 = 0.78$)

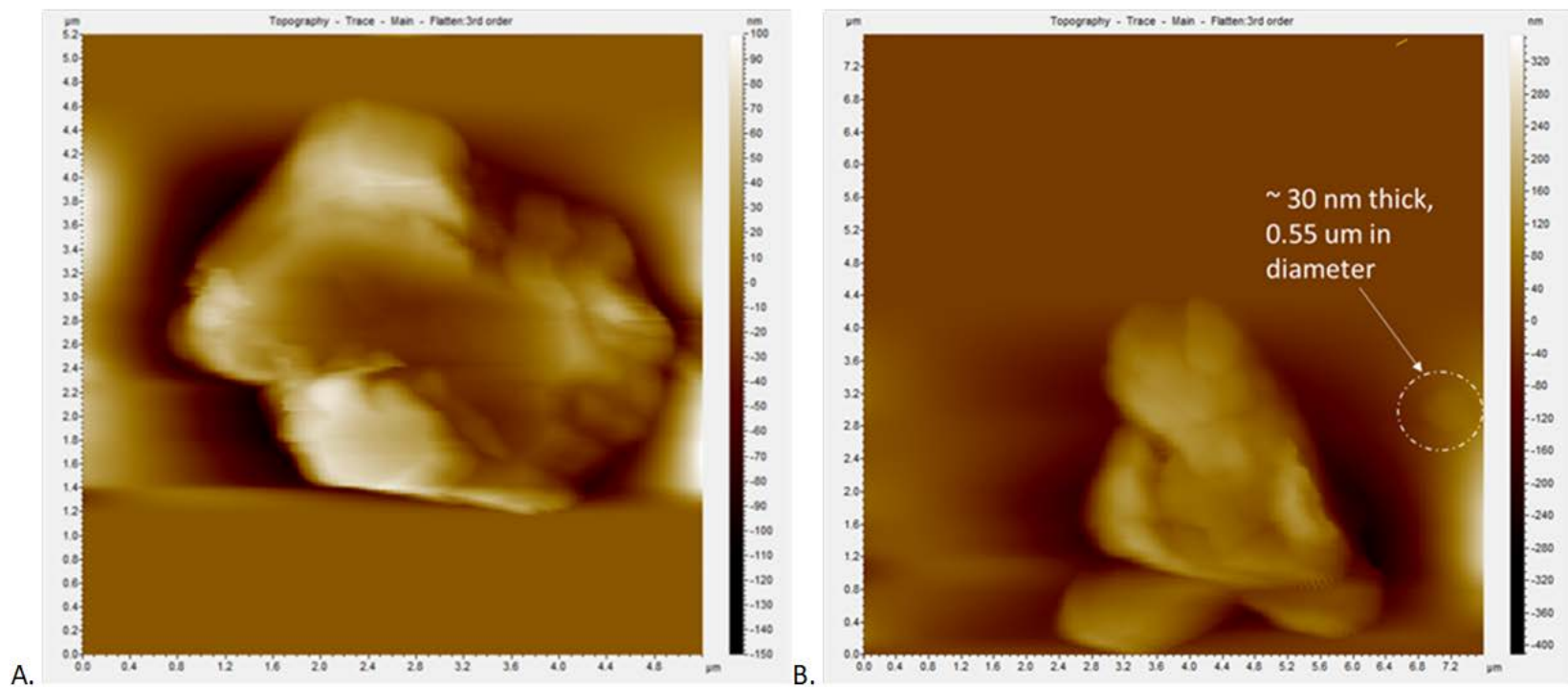


Figure 30. AFM images: KAO without MS2 and with MS2 show adsorption. A) KAO without MS2, and B) KAO with MS2 clusters adsorbed to its surface. Image B also shows evidence of MS2 aggregates unbound to KAO. AFM images also provided particle size information, thickness (120-600 nm) and lateral length (2 μm), and topography (angular edges and smooth surface).

AFM images were courtesy of Dr. Yun Xing.

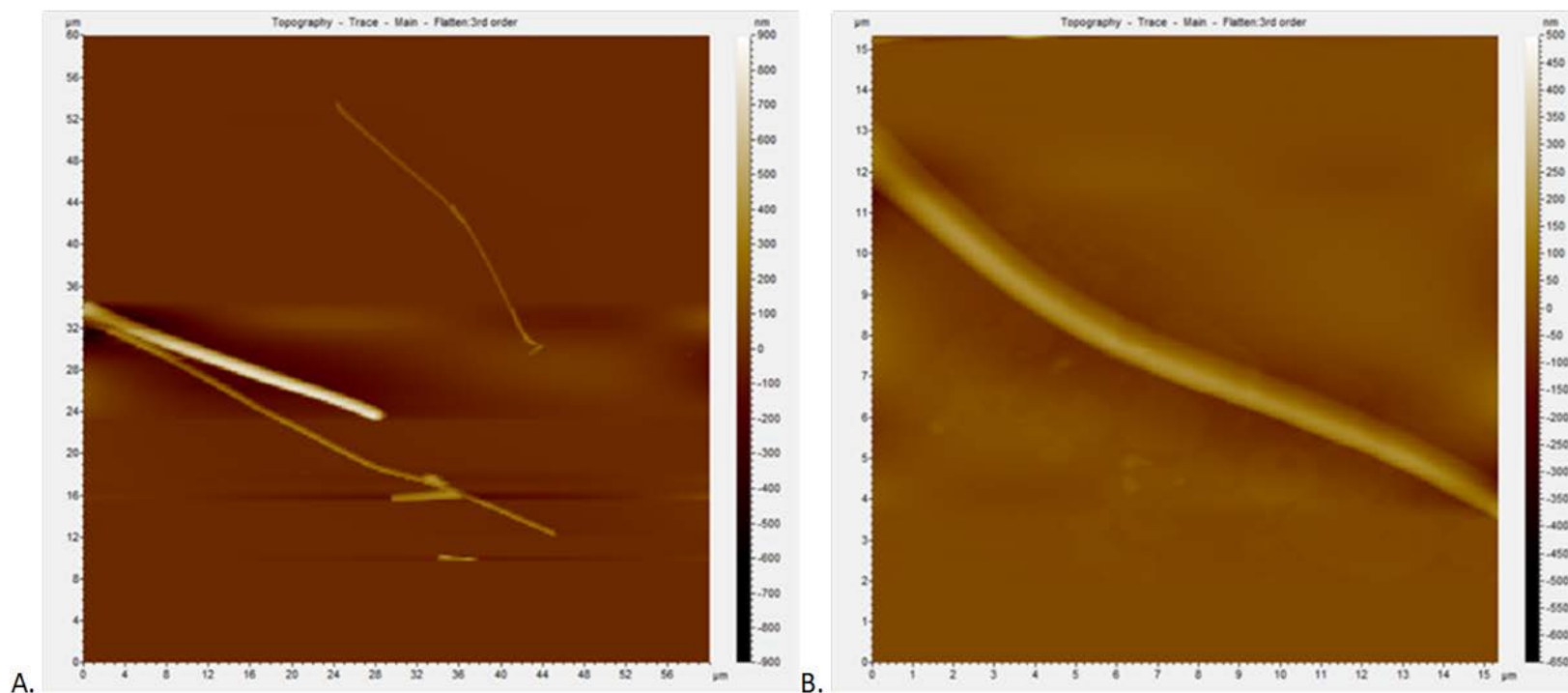


Figure 31. AFM images: FG without MS2 and with MS2 show adsorption. A) FG without MS2, and B) FG with MS2 clusters adsorbed to its surface. Image B also shows evidence of MS2 aggregates unbound to FG. AFM images also provided particle size information, diameter ($0.5\mu\text{m}$ - $1.7\mu\text{m}$) but fiber length was too long to measure with AFM, and topography (smooth surface).

AFM images were courtesy of Dr. Yun Xing.

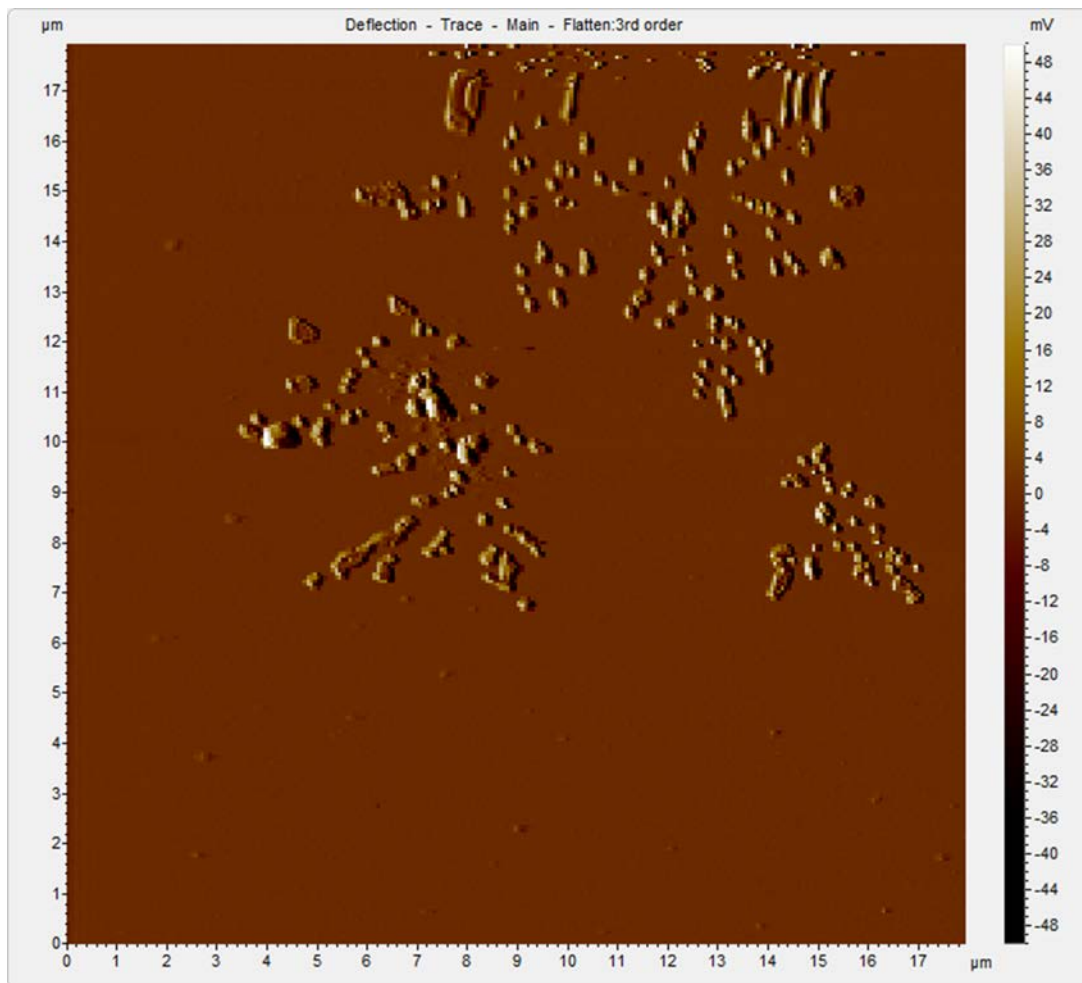


Figure 32. AFM image: FG with MS2 showing MS2 aggregation without FG . AFM images also provided particle size information, diameter (20-30nm). AFM images were courtesy of Dr. Yun Xing.

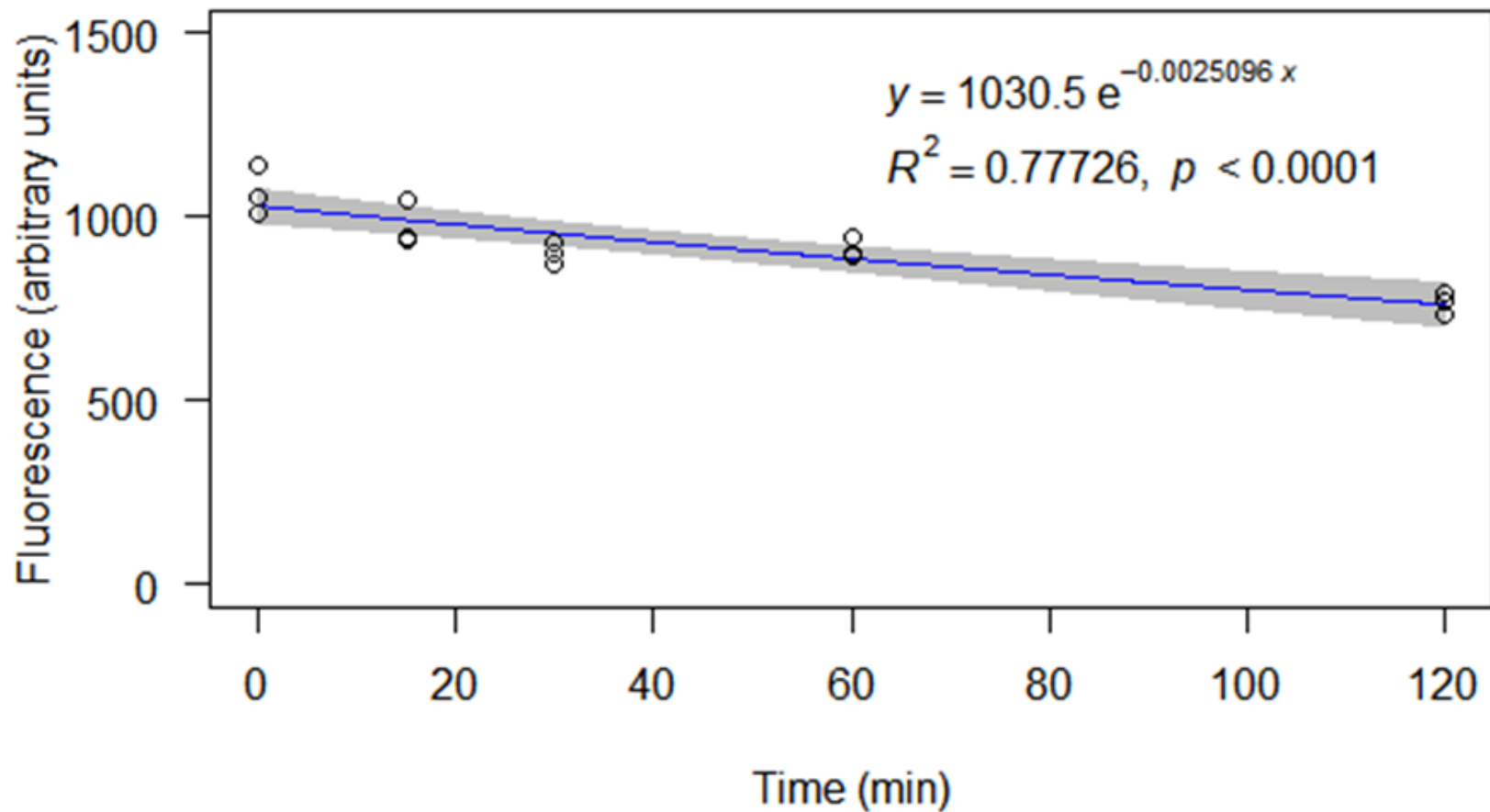


Figure 33. MS2 control experiment: declining slope supported qualitative data showing aggregation. A blue exponential decay rate trendline was fitted to the data. The R^2 of 0.78, p-value, and the confidence interval (gray shading) were obtained with R software.

consistent with the well-established kinetics of particle flocculation, including: IEP of virus and the pH of the medium, ionic strength of the medium, and the surface charge of the colloid and collector particles (Armanious et al., 2016; Dika, Gantzer, Perrin, & Duval, 2013; Floyd & Sharp, 1979; Israelachvili, 2011; Timchak & Gitis, 2012). The decrease in the fluorescence appears to be caused by the formation of MS2 clusters. These results are consistent with the results of XDLVO modeling, and they suggest that the interactions discussed in section 4.1 may have occurred between colloids and MS2 clusters, not just individual MS2 for which XDLVO theory has been used. Also, the results of section 4.2 suggest that these clusters strongly bind to the colloids; they do not simply co-settle and associate with colloids.

XLDVO modeling also showed that adsorption/aggregation behavior could be sensitive to ionic strength as shown in Figure 34. The green curves for MS2 aggregation, FG-MS2 and KAO-MS2 adsorption interaction energy have the lowest energy barrier to overcome and have the highest ionic strength. Furthermore, the MS2-KAO and MS2-FG interaction energies approach those of MS2-MS2 when the ionic strength is higher (Figure 34), and when the MS2 surface potential is positive (Figure 35). This is due to the ion screening effect, which causes the suppression of the electrostatic repulsive forces (Bharti, Meissner, Klapp, & Findenegg, 2014; Israelachvili, 2011). The ion screening effect partially explains previous results that show more favorable MS2 adsorption in the presence of divalent cations (Armanious et al., 2016; Floyd & Sharp, 1979; Israelachvili, 2011; Timchak & Gitis, 2012). These findings may impact wastewater treatment facilities that receive wastes with higher dissolved solids content.

It is also important to note that the XDVLO model does not account for functional group interactions between MS2 and KAO or FG. The model also does not simulate the interactions between MS2 aggregates and colloidal surfaces, or surfaces covered with MS2 viruses. These model limitations should be investigated in future research because such interactions may possibly change the relative favorability of surface adsorption and MS2 aggregation. The speed and strength of MS2 adsorption observed in the current study imply energetically-favorable interactions involving aggregates. Thus, there appears to be an opportunity to improve the underlying theory.

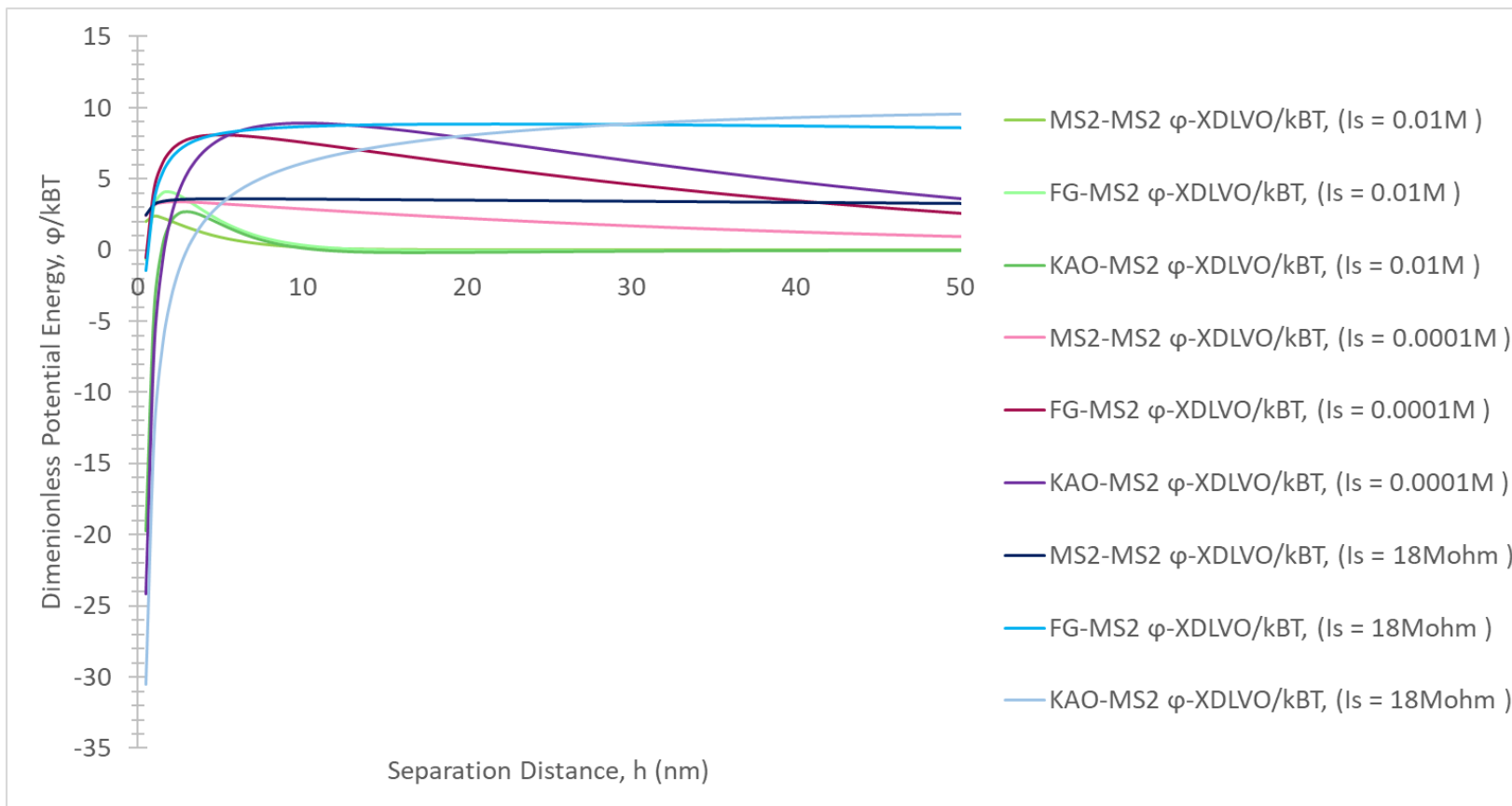


Figure 34. XDLVO energy profile: Different ionic strengths to show that ionic strength increases the interaction energies of FG-MS2, KAO-MS2, and MS2-MS2. The vertical lines emphasize the decreasing differences between MS2-MS2, FG-MS2, and KAO-MS2 as the ionic strength varies between 18Mohm (blues), 0.0001M (purples), and 0.01M (greens).

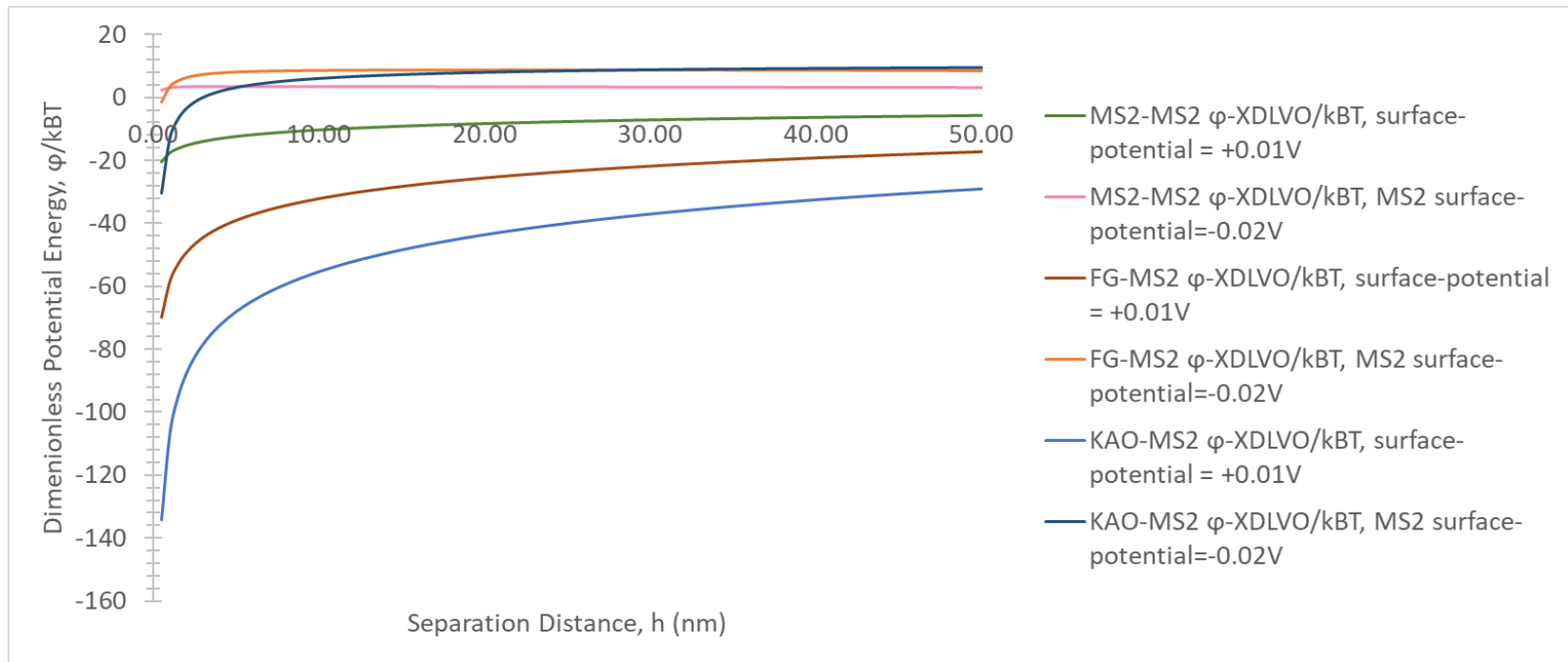


Figure 35. XDLVO energy profiles: Positive MS2 surface-potential compared to negative MS2 surface-potential (FG and KAO surface potentials held constant, ionic strength = 18 ohms) to show that when MS2 has a positive surface-potential FG-MS2 and KAO-MS2 adsorption interaction energies (with positive MS2 surface potential) approach interaction energies of MS2 aggregation.

V. Conclusions

5.1 Conclusions

To the best of the author's knowledge, this study observed kinetics that were faster than any other study that has previously investigated the adsorption of bacteriophage MS2 to colloidal particle suspensions of KAO and FG in water. The adsorption profiles fit a first order kinetic model with coefficients of determination that were generally equal to 0.99, and the first order rate constants were between 0.4 and 2.8 min^{-1} , at least an order of magnitude greater than those reported in previous studies carried out under comparable experimental conditions. This study also reported, for the first time, significant adsorptive MS2 removal by the first sampling time of each experiment and equilibrium within 15 minutes. Qualitative evidence for MS2 adsorption was collected with fluorescent and bright field microscopic images, which showed MS2 clustered on and around the KAO and FG colloids. XDLVO modeling confirmed the presence of favorable adsorption interactions at separation distances of approx. 2 nm or less, and it also confirmed that MS2 aggregation was energetically favored over adsorption to KAO. MS2 aggregation was confirmed experimentally. The experimental and computational results, taken together, imply that MS2 clusters adsorb quickly and strongly to colloidal particles.

These results have both practical and theoretical impacts. Treatment plants receiving bio-contaminated water need to pay attention to colloidal particles in water because individual and clusters of viruses can quickly and strongly bind to them and receive transport and protection from them. As for theoretical implications, XDLVO theory needs to be extended to account for MS2 aggregates interacting with surfaces.

This would involve the accounting for the particle size and surface potential of the MS2 cluster. The approximate shape of the cluster and its relative size compared to the colloid could influence the employed shape-specific van der Waals, electrostatic double layer, and Lewis acid-base formulas.

Appendix A Statistically Significant Removal of MS2

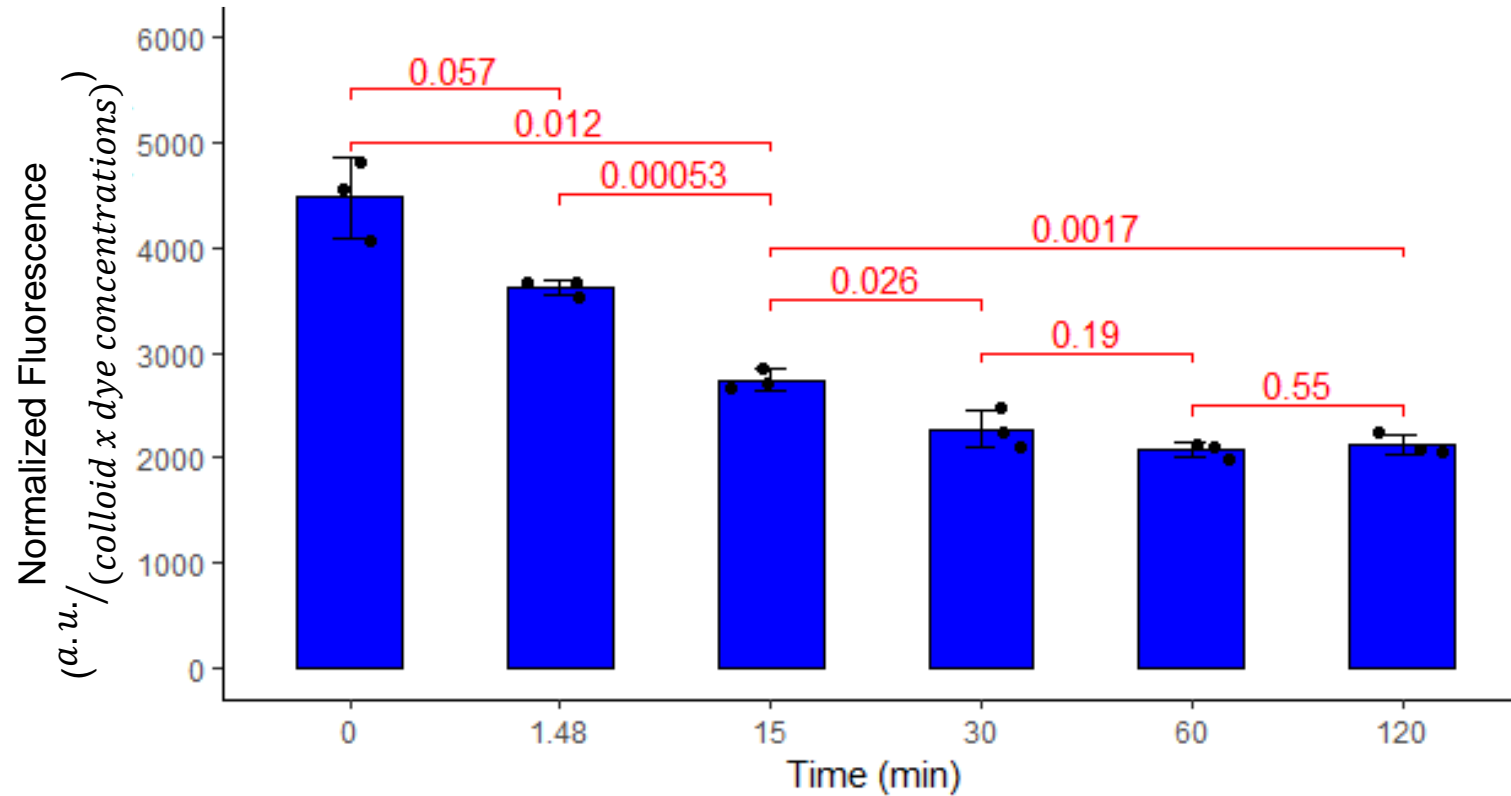


Figure 36. Significant MS2 removal: Experiment one low concentration FG. Normalized fluorescence taken at sample times and significance of the change between specific times is shown in red. The three sample measurements are shown with error bars.

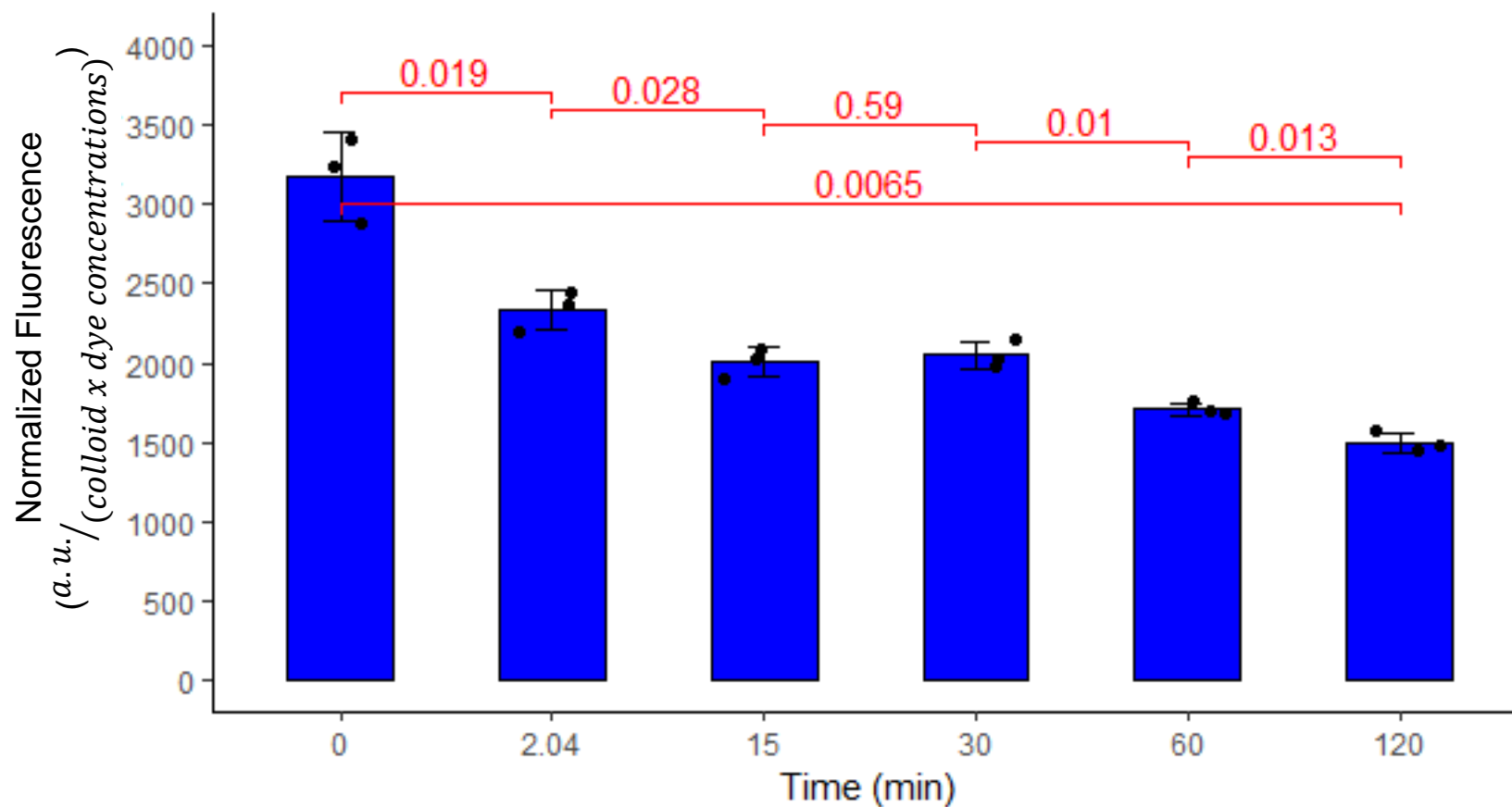


Figure 37. Significant MS2 removal: Experiment one high concentration FG. Normalized fluorescence taken at sample times and significance of the change between specific times is shown in red. The three sample measurements are shown with error bars.

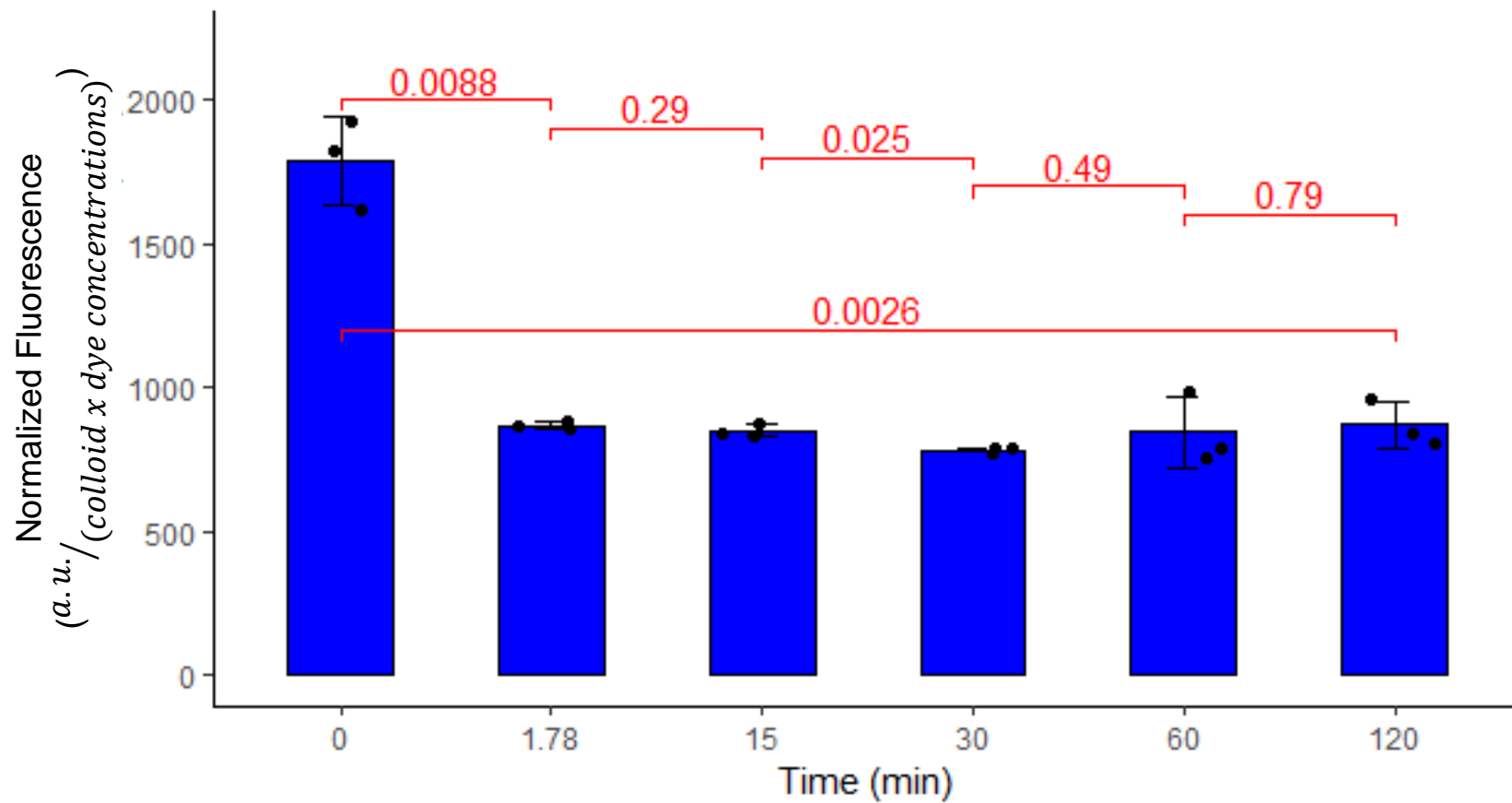


Figure 38. Significant MS2 removal: Experiment one low concentration KAO. Normalized fluorescence taken at sample times and significance of the change between specific times is shown in red. The three sample measurements are shown with error bars.

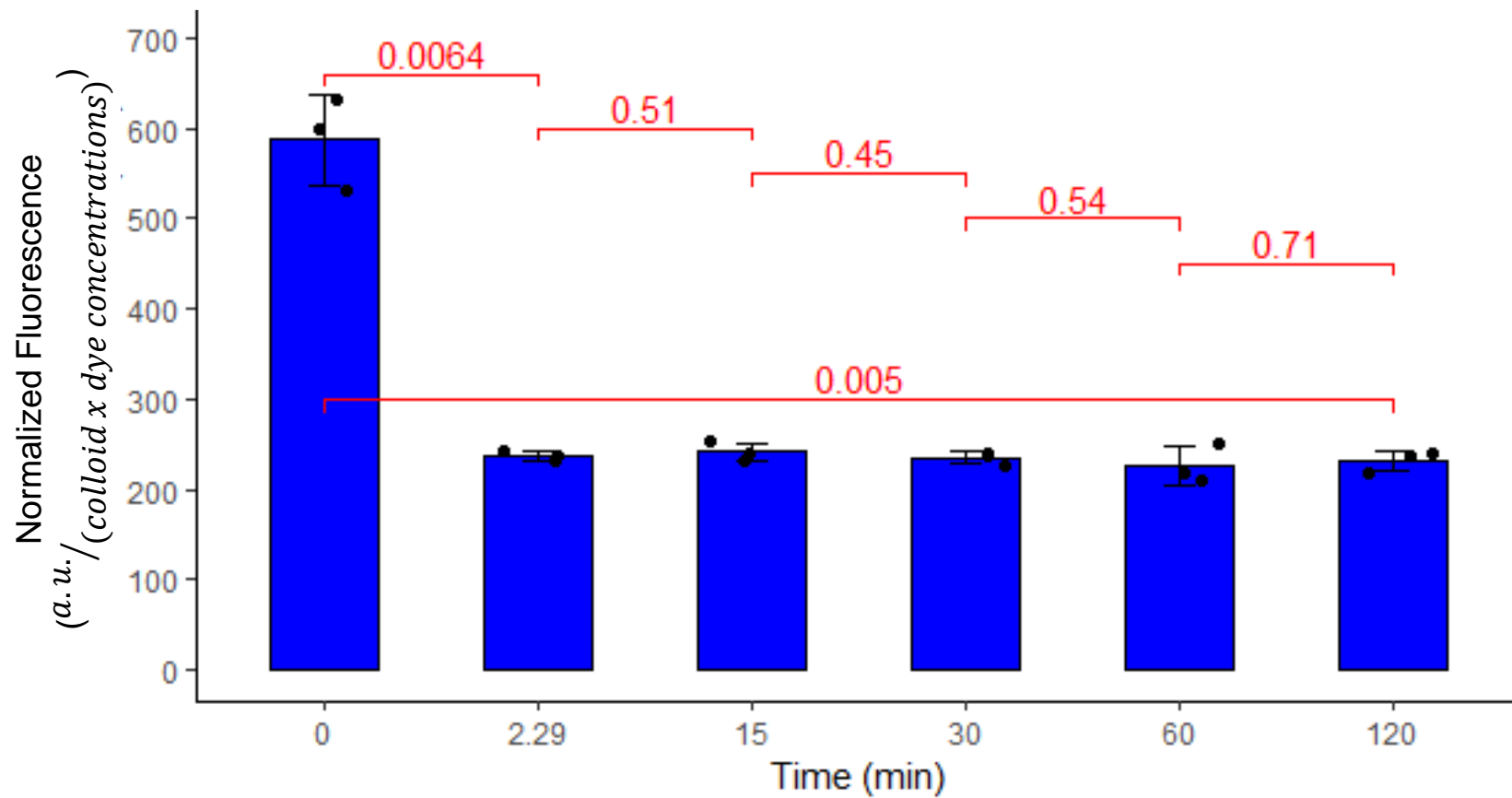


Figure 39. Significant MS2 removal: Experiment one high concentration KAO. Normalized fluorescence taken at sample times and significance of the change between specific times is shown in red. The three sample measurements are shown with error bars.

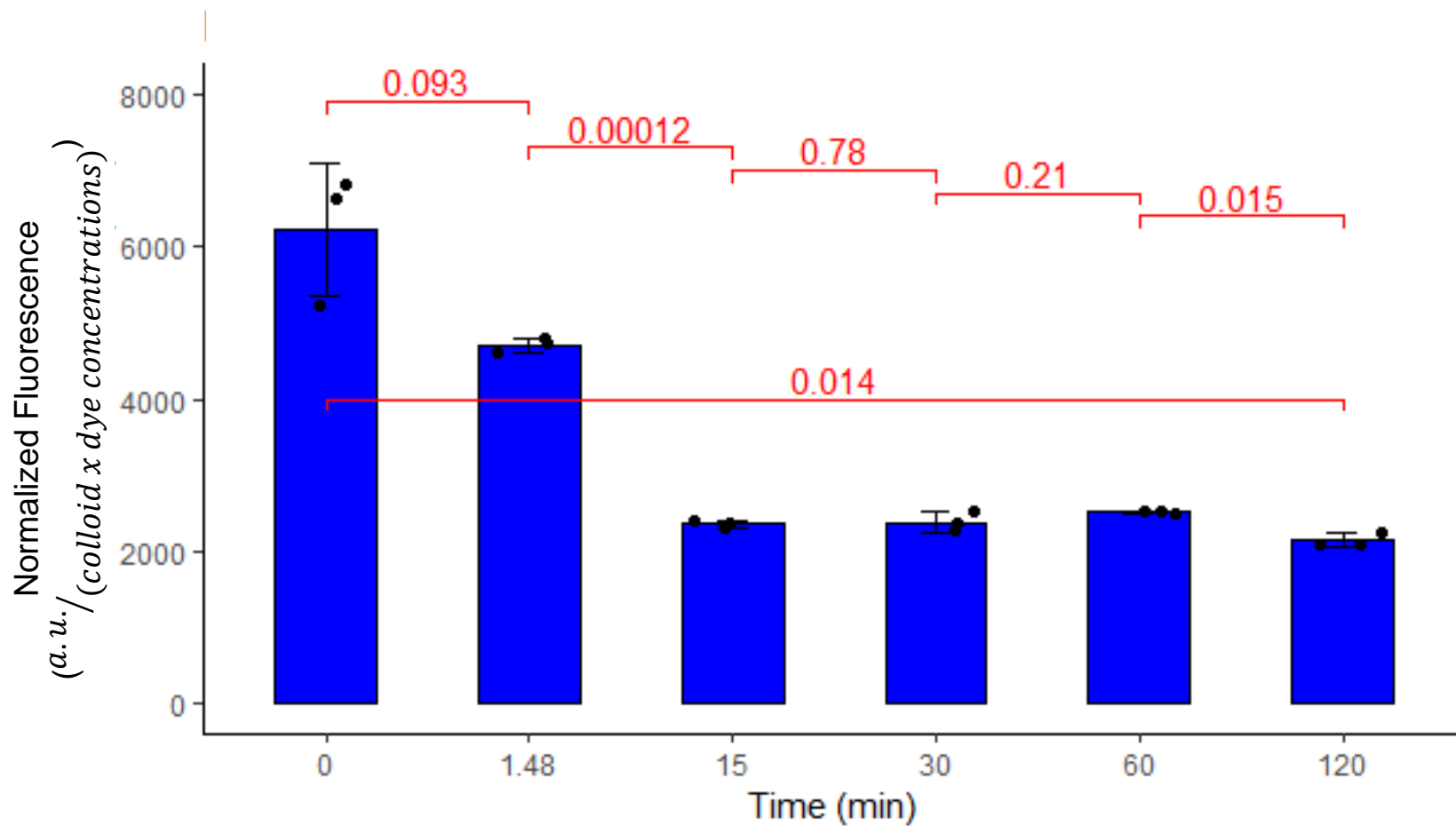


Figure 40. Significant MS2 removal: Experiment two low concentration FG. Normalized fluorescence taken at sample times and significance of the change between specific times is shown in red. The three sample measurements are shown with error bars.

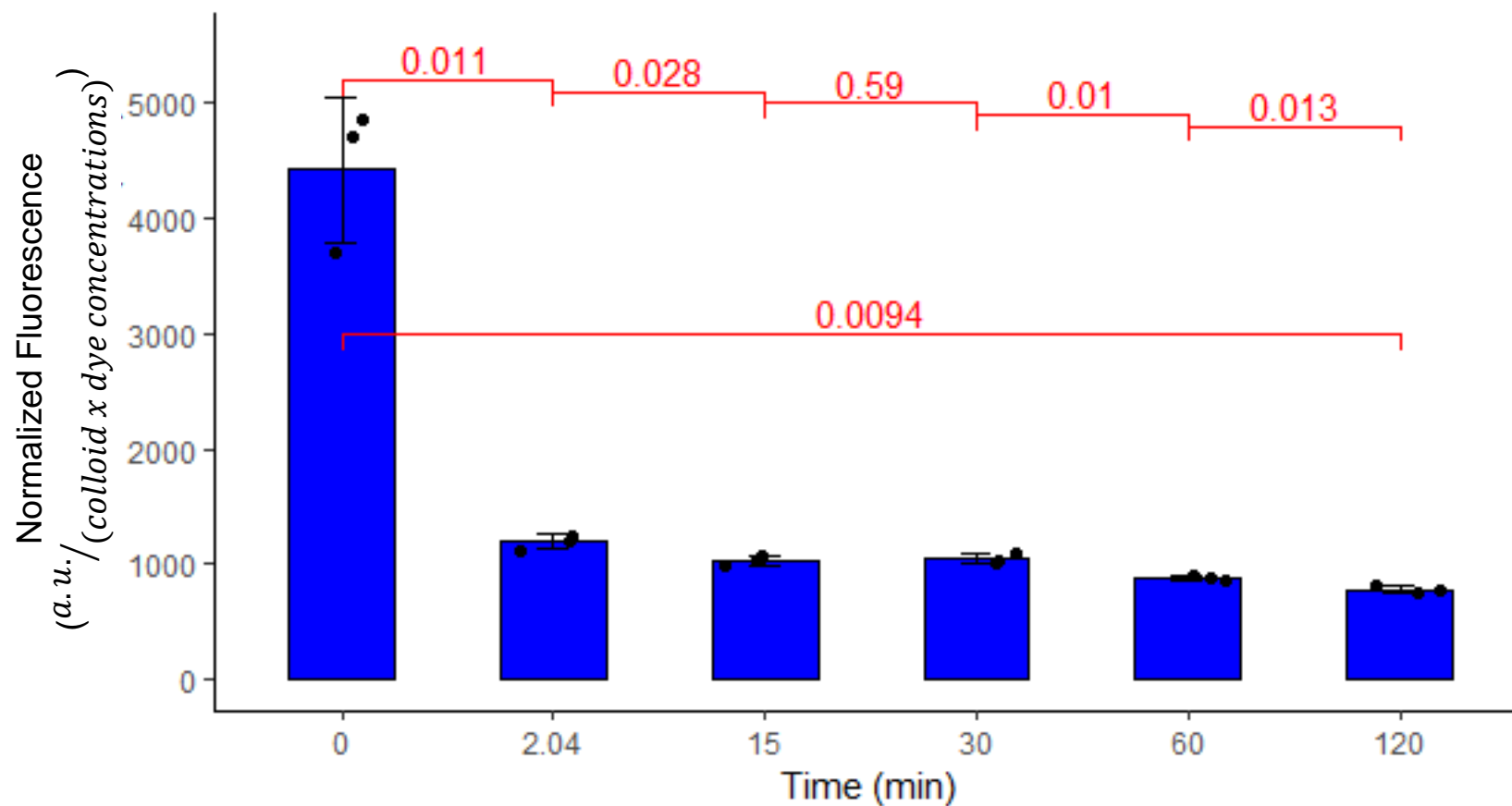


Figure 41. Significant MS2 removal: Experiment two high concentration FG. Normalized fluorescence taken at sample times and significance of the change between specific times is shown in red. The three sample measurements are shown with error bars.

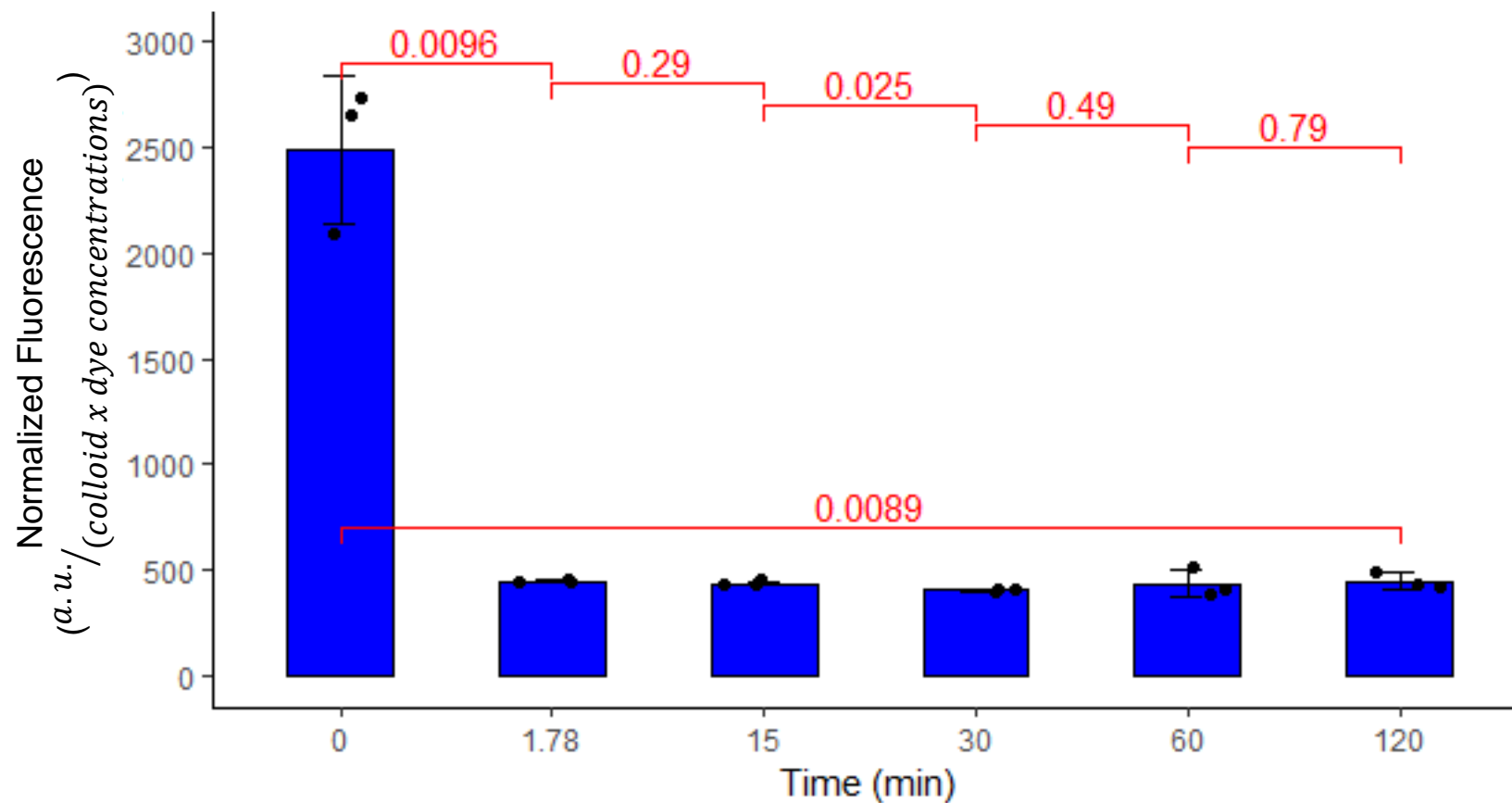


Figure 42. Significant MS2 removal: Experiment two low concentration KAO. Normalized fluorescence taken at sample times and significance of the change between specific times is shown in red. The three sample measurements are shown with error bars.

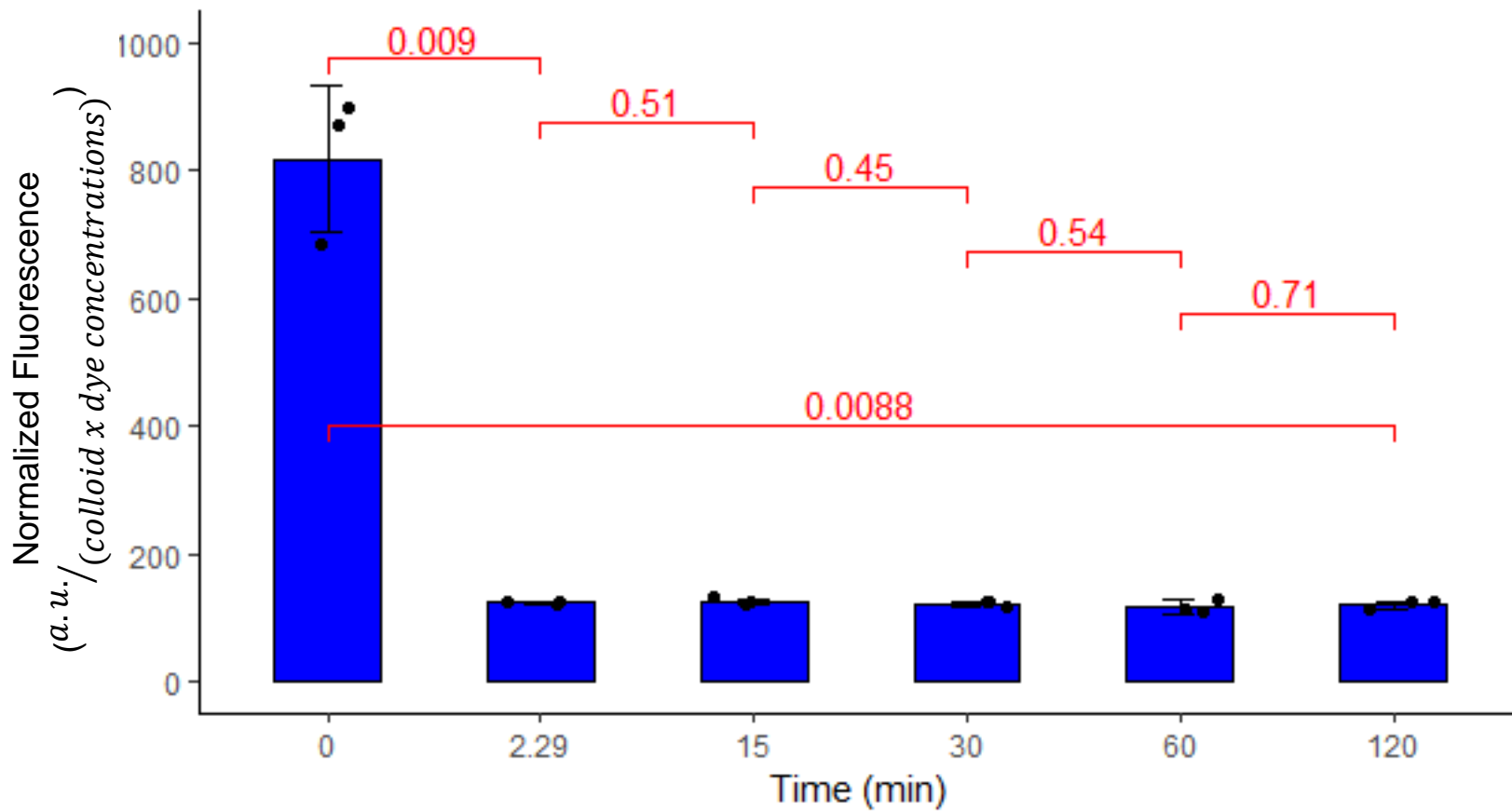


Figure 43. Significant MS2 removal: Experiment two high concentration KAO. Normalized fluorescence taken at sample times and significance of the change between specific times is shown in red. The three sample measurements are shown with error bars.

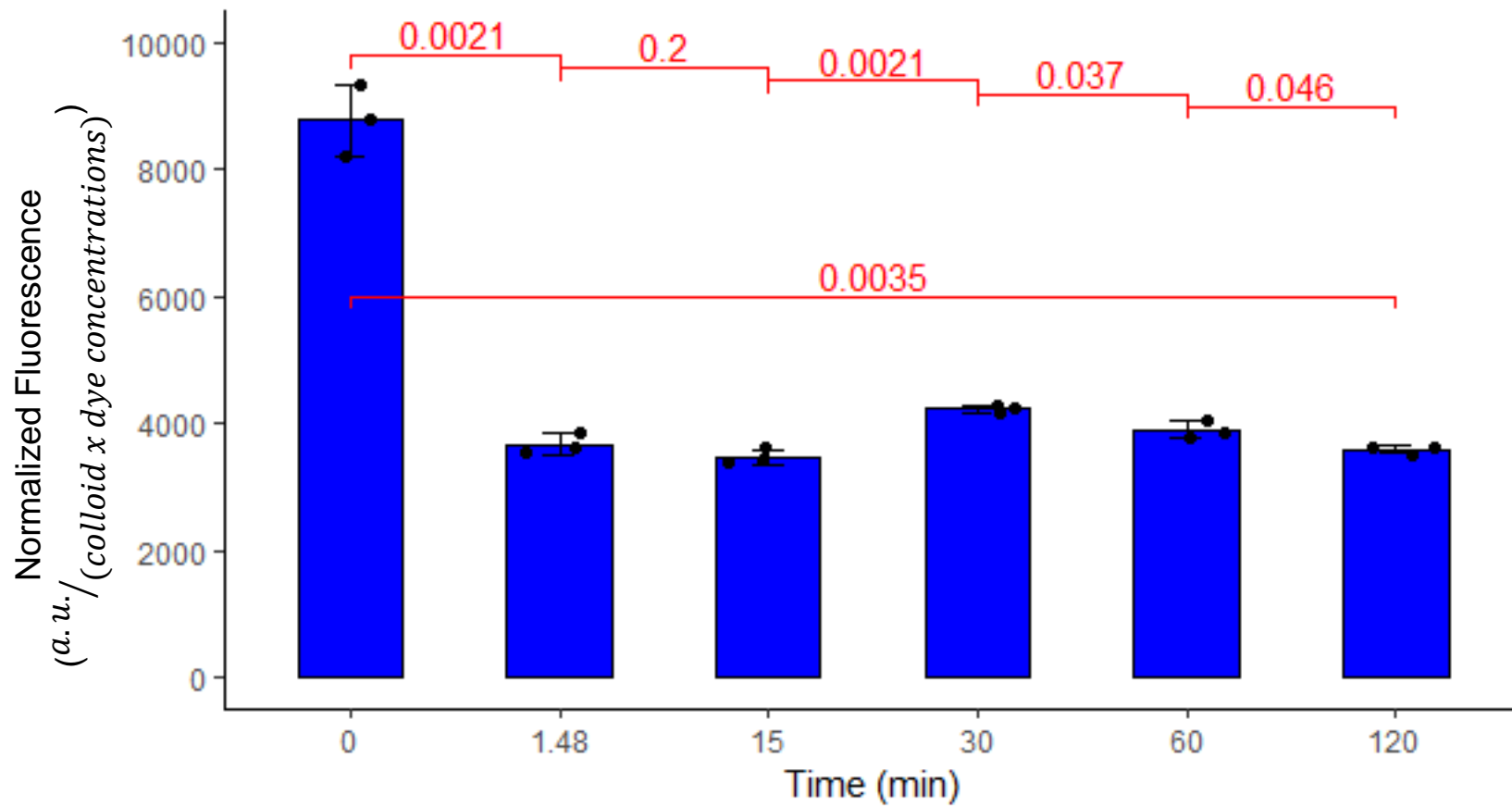


Figure 44. Significant MS2 removal: Experiment three low concentration FG. Normalized fluorescence taken at sample times and significance of the change between specific times is shown in red. The three sample measurements are shown with error bars.

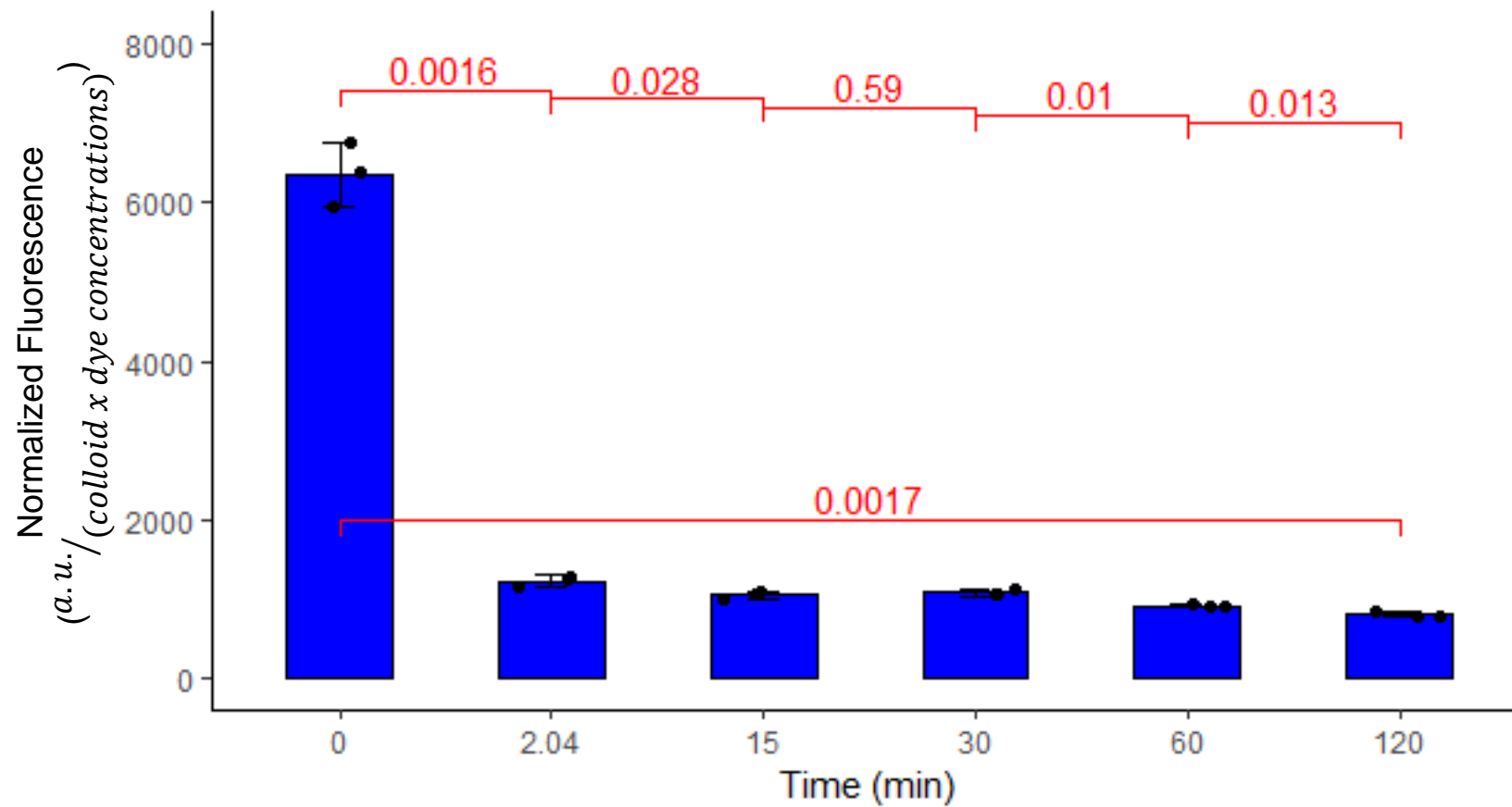


Figure 45. Significant MS2 removal: Experiment three high concentration FG. Normalized fluorescence taken at sample times and significance of the change between specific times is shown in red. The three sample measurements are shown with error bars.

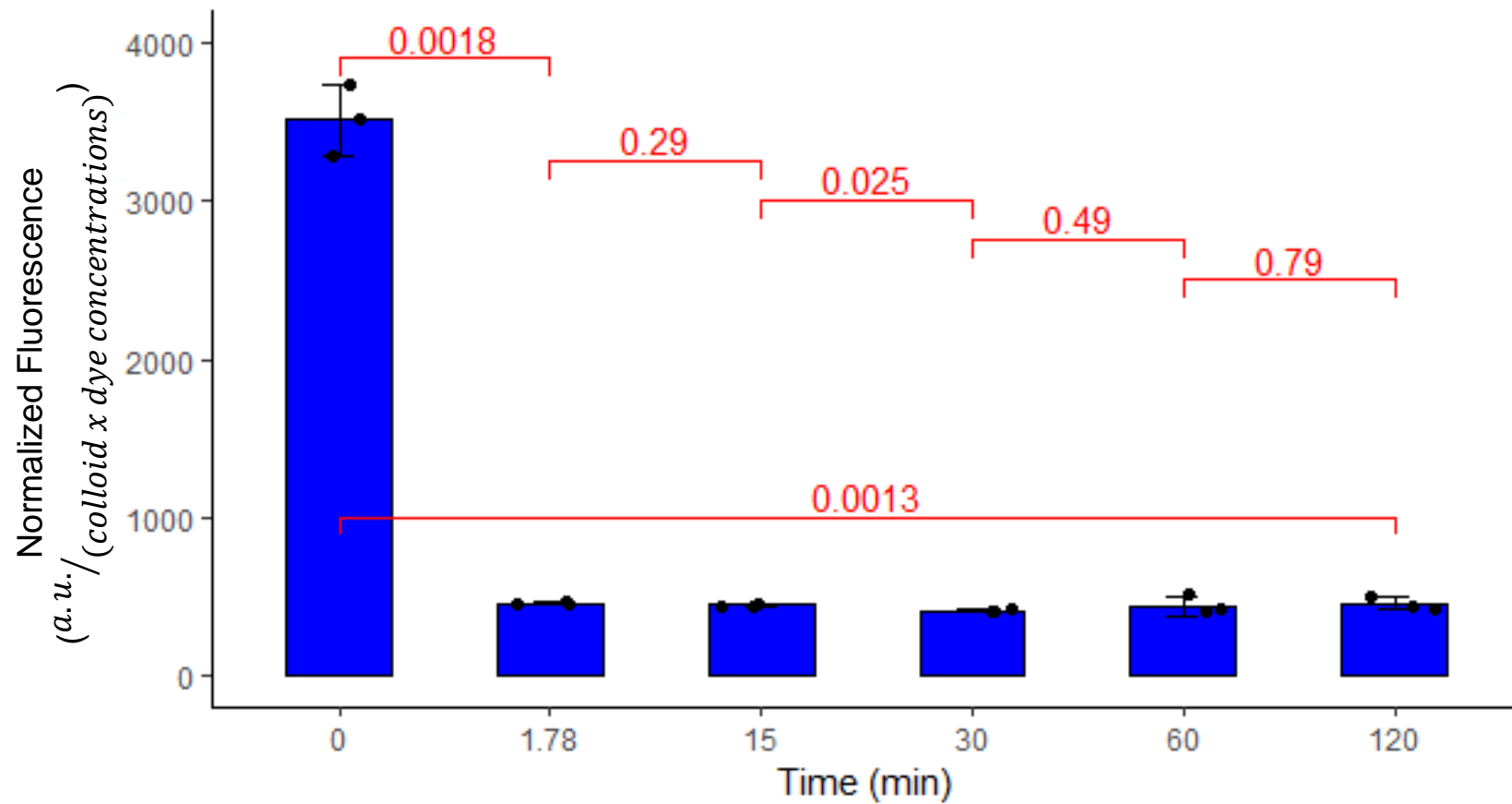


Figure 46. Significant MS2 removal: Experiment three low concentration KAO. Normalized fluorescence taken at sample times and significance of the change between specific times is shown in red. The three sample measurements are shown with error bars.

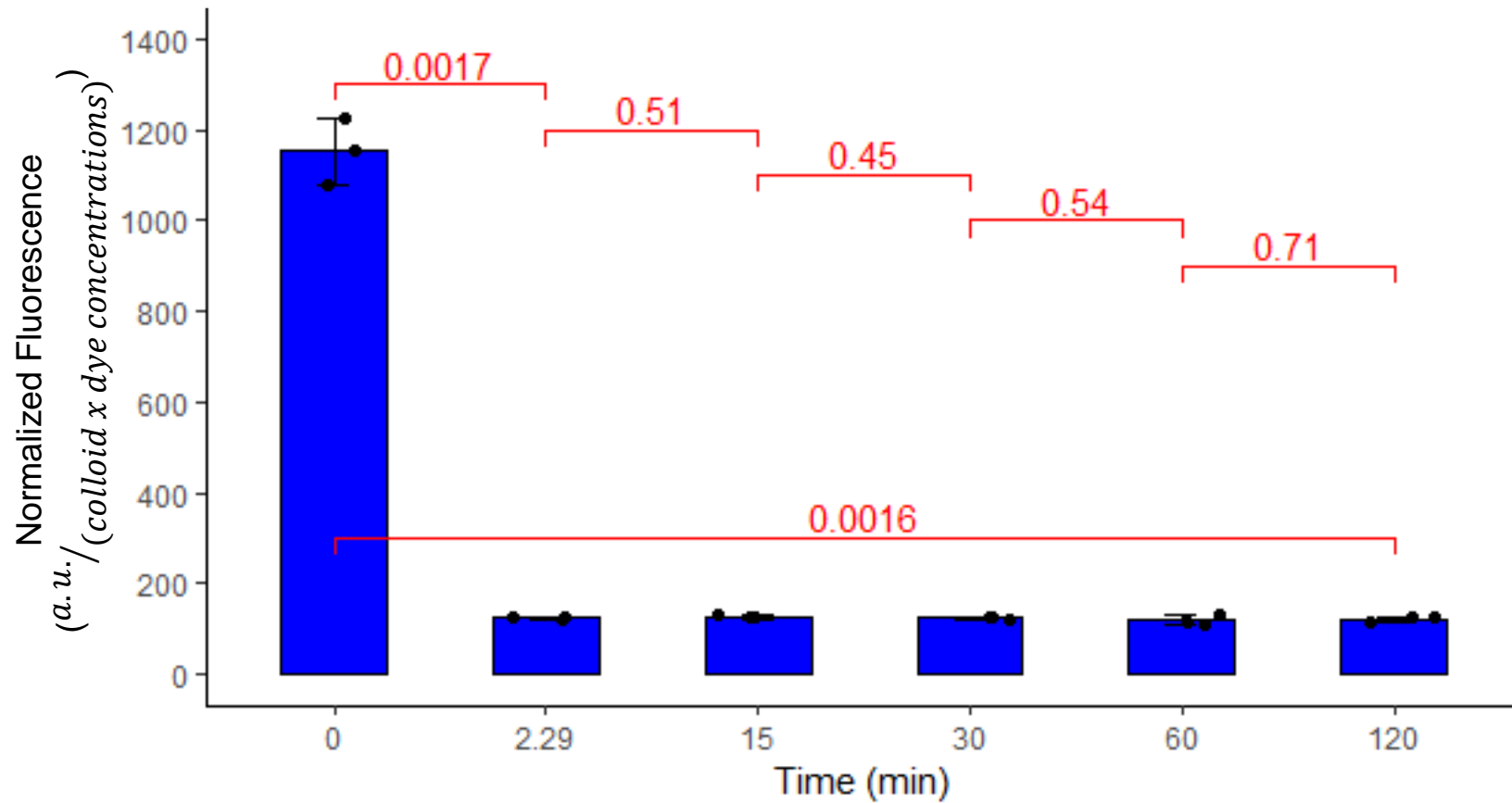


Figure 47. Significant MS2 removal: Experiment three high concentration KAO. Normalized fluorescence taken at sample times and significance of the change between specific times is shown in red. The three sample measurements are shown with error bars.

Appendix B Supernatant Raw Data

Table 4. Experiment One Supernatant Raw Data*

	A	B	C	D	E	F
1	Experiment	Colloid	Concentration	Time	Replicate	Fluorescence
2	1	F	Low	0.00	1	691.95
3	1	F	Low	0.00	2	603.1675
4	1	F	Low	0.00	3	662.9975
5	1	F	Low	1.40	1	542.01
6	1	F	Low	1.48	2	556.88
7	1	F	Low	1.55	3	558.13
8	1	F	Low	15.00	1	438.68
9	1	F	Low	15.00	2	463.03
10	1	F	Low	15.00	3	446.34
11	1	F	Low	30.00	1	375.27
12	1	F	Low	30.00	2	390.38
13	1	F	Low	30.00	3	416.79
14	1	F	Low	60.00	1	375.16
15	1	F	Low	60.00	2	361.79
16	1	F	Low	60.00	3	375.61
17	1	F	Low	120.00	1	370.23
18	1	F	Low	120.00	2	369
19	1	F	Low	120.00	3	389.35
20	1	K	Low	0.00	1	691.95
21	1	K	Low	0.00	2	603.1675
22	1	K	Low	0.00	3	662.9975
23	1	K	Low	1.72	1	378.29
24	1	K	Low	1.78	2	385.68
25	1	K	Low	1.83	3	381.74
26	1	K	Low	15.00	1	373.66
27	1	K	Low	15.00	2	371.96
28	1	K	Low	15.00	3	383.79
29	1	K	Low	30.00	1	359.09
30	1	K	Low	30.00	2	357.62
31	1	K	Low	30.00	3	354.9
32	1	K	Low	60.00	1	349.04
33	1	K	Low	60.00	2	359.11
34	1	K	Low	60.00	3	417.66
35	1	K	Low	120.00	1	373.3

* Blank water reading average = 127.53 arbitrary units of fluorescence

Table 4. Experiment One Supernatant Raw Data* (continued)

	A	B	C	D	E	F
36	1	K	Low	120.00	2	364.73
37	1	K	Low	120.00	3	409.83
38	1	F	High	0.00	1	691.95
39	1	F	High	0.00	2	603.1675
40	1	F	High	0.00	3	662.9975
41	1	F	High	1.98	1	532.88
42	1	F	High	2.02	2	517.96
43	1	F	High	2.12	3	490.25
44	1	F	High	15.00	1	442.91
45	1	F	High	15.00	2	462.57
46	1	F	High	15.00	3	472.7
47	1	F	High	30.00	1	482.41
48	1	F	High	30.00	2	461.22
49	1	F	High	30.00	3	455.48
50	1	F	High	60.00	1	409.29
51	1	F	High	60.00	2	404.74
52	1	F	High	60.00	3	417.29
53	1	F	High	120.00	1	367.72
54	1	F	High	120.00	2	371.72
55	1	F	High	120.00	3	387.55
56	1	K	High	0.00	1	691.95
57	1	K	High	0.00	2	603.1675
58	1	K	High	0.00	3	662.9975
59	1	K	High	2.23	1	340.06
60	1	K	High	2.28	2	333.73
61	1	K	High	2.37	3	343.34
62	1	K	High	15.00	1	353.14
63	1	K	High	15.00	2	335.4
64	1	K	High	15.00	3	341.61
65	1	K	High	30.00	1	330.86
66	1	K	High	30.00	2	342.82
67	1	K	High	30.00	3	340.29
68	1	K	High	60.00	1	314.65
69	1	K	High	60.00	2	351.63
70	1	K	High	60.00	3	322.39
71	1	K	High	120.00	1	340.08
72	1	K	High	120.00	2	340.9
73	1	K	High	120.00	3	323.35

* Blank water reading average = 127.53 arbitrary units of fluorescence

Table 5. Experiment Two Supernatant Raw Data*

	A	B	C	D	E	F
	Experiment	Colloid	Concentration	Time	Replicate	Fluorescence
74	2	F	Low	0.00	1	1674.2475
75	2	F	Low	0.00	2	1722.095
76	2	F	Low	0.00	3	1344.995
77	2	F	Low	1.40	1	1229.61
78	2	F	Low	1.48	2	1242.2
79	2	F	Low	1.55	3	1197.32
80	2	F	Low	15.00	1	681.72
81	2	F	Low	15.00	2	663.73
82	2	F	Low	15.00	3	672.51
83	2	F	Low	30.00	1	710.48
84	2	F	Low	30.00	2	672.37
85	2	F	Low	30.00	3	652.22
86	2	F	Low	60.00	1	712
87	2	F	Low	60.00	2	703.25
88	2	F	Low	60.00	3	711.43
89	2	F	Low	120.00	1	609.03
90	2	F	Low	120.00	2	646.75
91	2	F	Low	120.00	3	612.22
92	2	K	Low	0.00	1	1674.2475
93	2	K	Low	0.00	2	1722.095
94	2	K	Low	0.00	3	1344.995
95	2	K	Low	1.72	1	625.3
96	2	K	Low	1.78	2	581.23
97	2	K	Low	1.83	3	598.95
98	2	K	Low	15.00	1	474.02
99	2	K	Low	15.00	2	512.31
100	2	K	Low	15.00	3	461.38
101	2	K	Low	30.00	1	488.99
102	2	K	Low	30.00	2	492.57
103	2	K	Low	30.00	3	494.85
104	2	K	Low	60.00	1	586.36
105	2	K	Low	60.00	2	571.6
106	2	K	Low	60.00	3	537.46
107	2	K	Low	120.00	1	538.19
108	2	K	Low	120.00	2	500.62
109	2	K	Low	120.00	2	500.62

* Blank water reading average = 119.15 arbitrary units of fluorescence

Table 5. Experiment Two Supernatant Raw Data* (continued)

	A	B	C	D	E	F
110	2	K	Low	120.00	3	526.09
111	2	F	High	0.00	1	1674.2475
112	2	F	High	0.00	2	1722.095
113	2	F	High	0.00	3	1344.995
114	2	F	High	1.98	1	536.47
115	2	F	High	2.02	2	605.37
116	2	F	High	2.12	3	574.29
117	2	F	High	15.00	1	425.3
118	2	F	High	15.00	2	461.63
119	2	F	High	15.00	3	469.3
120	2	F	High	30.00	1	450.49
121	2	F	High	30.00	2	478.09
122	2	F	High	30.00	3	432.83
123	2	F	High	60.00	1	478.23
124	2	F	High	60.00	2	494.06
125	2	F	High	60.00	3	470.54
126	2	F	High	120.00	1	425.27
127	2	F	High	120.00	2	453.32
128	2	F	High	120.00	3	451.62
129	2	K	High	0.00	1	1674.2475
130	2	K	High	0.00	2	1722.095
131	2	K	High	0.00	3	1344.995
132	2	K	High	2.23	1	415.61
133	2	K	High	2.28	2	417.47
134	2	K	High	2.37	3	400.86
135	2	K	High	15.00	1	364.95
136	2	K	High	15.00	2	381.95
137	2	K	High	15.00	3	388.27
138	2	K	High	30.00	1	367.69
139	2	K	High	30.00	2	381.23
140	2	K	High	30.00	3	384.57
141	2	K	High	60.00	1	412.12
142	2	K	High	60.00	2	388.12
143	2	K	High	60.00	3	391.37
144	2	K	High	120.00	1	385.38
145	2	K	High	120.00	2	398.32
146	2	K	High	120.00	3	395.89

* Blank water reading average = 119.15 arbitrary units of fluorescence

Table 6. Experiment Three Supernatant Raw Data*

	A	B	C	D	E	F
147	Experiment	Colloid	Concentration	Time	Replicate	Fluorescence
148	3	F	Low	0.00	1	2304.32
149	3	F	Low	0.00	2	2182.4
150	3	F	Low	0.00	3	2041.86
151	3	F	Low	1.40	1	1020.51
152	3	F	Low	1.48	2	960.61
153	3	F	Low	1.55	3	944.33
154	3	F	Low	15.00	1	911.92
155	3	F	Low	15.00	2	918.53
156	3	F	Low	15.00	3	961.95
157	3	F	Low	30.00	1	1113.64
158	3	F	Low	30.00	2	1095.17
159	3	F	Low	30.00	3	1122.19
160	3	F	Low	60.00	1	1067.14
161	3	F	Low	60.00	2	1019.52
162	3	F	Low	60.00	3	1003.78
163	3	F	Low	120.00	1	940.91
164	3	F	Low	120.00	2	964.41
165	3	F	Low	120.00	3	966.83
166	3	K	Low	0.00	1	2304.32
167	3	K	Low	0.00	2	2182.4
168	3	K	Low	0.00	3	2041.86
169	3	K	Low	1.72	1	719.01
170	3	K	Low	1.78	2	668.19
171	3	K	Low	1.83	3	668.26
172	3	K	Low	15.00	1	589.99
173	3	K	Low	15.00	2	633.09
174	3	K	Low	15.00	3	623.91
175	3	K	Low	30.00	1	739.76
176	3	K	Low	30.00	2	710.34
177	3	K	Low	30.00	3	685.55
178	3	K	Low	60.00	1	672.98
179	3	K	Low	60.00	2	698.26
180	3	K	Low	60.00	3	659.96
181	3	K	Low	120.00	1	625.54
182	3	K	Low	120.00	2	633.45

* Blank water reading average = 115.26 arbitrary units of fluorescence

Table 6. Experiment Three Supernatant Raw Data* (continued)

	A	B	C	D	E	F
183	3	K	Low	120.00	3	643.43
184	3	F	High	0.00	1	2304.32
185	3	F	High	0.00	2	2182.4
186	3	F	High	0.00	3	2041.86
187	3	F	High	1.98	1	985.61
188	3	F	High	2.02	2	1013.46
189	3	F	High	2.12	3	969.16
190	3	F	High	15.00	1	923.47
191	3	F	High	15.00	2	877.33
192	3	F	High	15.00	3	896.06
193	3	F	High	30.00	1	1035.26
194	3	F	High	30.00	2	1042.44
195	3	F	High	30.00	3	1040.18
196	3	F	High	60.00	1	988.1
197	3	F	High	60.00	2	1031.69
198	3	F	High	60.00	3	1006.65
199	3	F	High	120.00	1	881.86
200	3	F	High	120.00	2	946.36
201	3	F	High	120.00	3	891.21
202	3	K	High	0.00	1	2304.32
203	3	K	High	0.00	2	2182.4
204	3	K	High	0.00	3	2041.86
205	3	K	High	2.23	1	481.92
206	3	K	High	2.28	2	394.76
207	3	K	High	2.37	3	378.57
208	3	K	High	15.00	1	394.67
209	3	K	High	15.00	2	383.47
210	3	K	High	15.00	3	380.23
211	3	K	High	30.00	1	410.3
212	3	K	High	30.00	2	441.32
213	3	K	High	30.00	3	443.78
214	3	K	High	60.00	1	388.23
215	3	K	High	60.00	2	384.36
216	3	K	High	60.00	3	376.98
217	3	K	High	120.00	1	362.13
218	3	K	High	120.00	2	358.35
219	3	K	High	120.00	3	366.63

* Blank water reading average = 115.26 arbitrary units of fluorescence

Table 7. Experiment Control Supernatant Raw Data*

	A	B	C	D	E	F
	Experiment	Colloid	Concentration	Time	Replicate	Fluorescence
220	Control	F	Low	0.00	1	154.32
221	Control	F	Low	0.00	2	184.4
222	Control	F	Low	0.00	3	129.52
223	Control	F	Low	1.40	1	109.07
224	Control	F	Low	1.48	2	160.97
225	Control	F	Low	1.55	3	108.97
226	Control	F	Low	15.00	1	114.14
227	Control	F	Low	15.00	2	160.44
228	Control	F	Low	15.00	3	148.59
229	Control	F	Low	30.00	1	155.87
230	Control	F	Low	30.00	2	128.3
231	Control	F	Low	30.00	3	128.96
232	Control	F	Low	60.00	1	124.15
233	Control	F	Low	60.00	2	128.44
234	Control	F	Low	60.00	3	184.55
235	Control	F	Low	120.00	1	167.98
236	Control	F	Low	120.00	2	109.64
237	Control	F	Low	120.00	3	129.05
238	Control	K	Low	0.00	1	154.32
239	Control	K	Low	0.00	2	184.4
240	Control	K	Low	0.00	3	129.52
241	Control	K	Low	1.72	1	180.62
242	Control	K	Low	1.78	2	114.93
243	Control	K	Low	1.83	3	107.04
244	Control	K	Low	15.00	1	141.27
245	Control	K	Low	15.00	2	182.09
246	Control	K	Low	15.00	3	160.07
247	Control	K	Low	30.00	1	150.47
248	Control	K	Low	30.00	2	151.89
249	Control	K	Low	30.00	3	151.93
250	Control	K	Low	60.00	1	165.94
251	Control	K	Low	60.00	2	110.64
252	Control	K	Low	60.00	3	153.26
253	Control	K	Low	120.00	1	157.21
254	Control	K	Low	120.00	2	159.17
255	Control	K	Low	120.00	3	125.71
256	Control	F	High	0.00	1	154.32
257	Control	F	High	0.00	2	184.4
258	Control	F	High	0.00	3	129.52
259	Control	F	High	1.98	1	125.61
260	Control	F	High	2.02	2	133.12
261	Control	F	High	2.12	3	159.51
262	Control	F	High	15.00	1	157.7
263	Control	F	High	15.00	2	176.74
264	Control	F	High	15.00	3	153.51
265	Control	F	High	15.00	3	153.51

* Blank water reading average = 156.08 arbitrary units of fluorescence

Table 7. Experimental Control Supernatant Raw Data* (continued)

	A	B	C	D	E	F
266	Control	F	High	30.00	1	125.31
267	Control	F	High	30.00	2	189.31
268	Control	F	High	30.00	3	116.7
269	Control	F	High	60.00	1	173.95
270	Control	F	High	60.00	2	174.4
271	Control	F	High	60.00	3	191.17
272	Control	F	High	120.00	1	115.85
273	Control	F	High	120.00	2	143.63
274	Control	F	High	120.00	3	151.89
275	Control	K	High	0.00	1	154.32
276	Control	K	High	0.00	2	184.4
277	Control	K	High	0.00	3	129.52
278	Control	K	High	2.23	1	160.19
279	Control	K	High	2.28	2	111.51
280	Control	K	High	2.37	3	112.02
281	Control	K	High	15.00	1	148.68
282	Control	K	High	15.00	2	172.28
283	Control	K	High	15.00	3	116.44
284	Control	K	High	30.00	1	132.42
285	Control	K	High	30.00	2	133.26
286	Control	K	High	30.00	3	137.16
287	Control	K	High	60.00	1	172.03
288	Control	K	High	60.00	2	133.63
289	Control	K	High	60.00	3	123.19
290	Control	K	High	120.00	1	181.42
291	Control	K	High	120.00	2	139.52
292	Control	K	High	120.00	3	110.36
293	Control	MS2	4	0	1	2304.32
294	Control	MS2	4	0	2	2182.4
295	Control	MS2	4	0	3	2041.86
296	Control	MS2	4	1.40	1	1300.09
297	Control	MS2	4	1.48	2	1209.69
298	Control	MS2	4	1.55	3	1167.49
299	Control	MS2	4	15.00	1	1202.61
300	Control	MS2	4	15.00	2	1094.64
301	Control	MS2	4	15.00	3	1100.92
302	Control	MS2	4	30.00	1	1027.88
303	Control	MS2	4	30.00	2	1088.61
304	Control	MS2	4	30.00	3	1057.55
305	Control	MS2	4	60.00	1	1103.88
306	Control	MS2	4	60.00	2	1055.44
307	Control	MS2	4	60.00	3	1049.89
308	Control	MS2	4	120.00	1	893.54
309	Control	MS2	4	120.00	2	945.93
310	Control	MS2	4	120.00	3	927.47

* Blank water reading average = 156.08 arbitrary units of fluorescence

Appendix C Washed Pellet Raw Data

Table 8. Washed Pellet Raw Data Experiment One*

	A	B	C	D	E	F
1	Experiment	Colloid	Concentration	Time	Replicate	Fluorescence
2	1	F	Low	0.00	1	0
3	1	F	Low	0.00	2	0
4	1	F	Low	0.00	3	0
5	1	F	Low	1.40	1	174.07
6	1	F	Low	1.48	2	189.48
7	1	F	Low	1.55	3	180.3
8	1	F	Low	15.00	1	165.38
9	1	F	Low	15.00	2	229.13
10	1	F	Low	15.00	3	150.46
11	1	F	Low	30.00	1	213.45
12	1	F	Low	30.00	2	158.62
13	1	F	Low	30.00	3	145.11
14	1	F	Low	60.00	1	142.2
15	1	F	Low	60.00	2	172.23
16	1	F	Low	60.00	3	232.3
17	1	F	Low	120.00	1	153.05
18	1	F	Low	120.00	2	139.19
19	1	F	Low	120.00	3	220.97
20	1	K	Low	0.00	1	0
21	1	K	Low	0.00	2	0
22	1	K	Low	0.00	3	0
23	1	K	Low	1.72	1	135.38
24	1	K	Low	1.78	2	152.06
25	1	K	Low	1.83	3	158.55
26	1	K	Low	15.00	1	157.01
27	1	K	Low	15.00	2	150.1
28	1	K	Low	15.00	3	171.3
29	1	K	Low	30.00	1	163.59
30	1	K	Low	30.00	2	162.04
31	1	K	Low	30.00	3	150.55
32	1	K	Low	60.00	1	217.64
33	1	K	Low	60.00	2	234.62
34	1	K	Low	60.00	3	141.15
35	1	K	Low	120.00	1	207.49
36	1	K	Low	120.00	2	136.04

* Blank water reading average = 127.53 arbitrary units of fluorescence

Table 8. Washed Pellet Raw Data Experiment One* (continued)

	A	B	C	D	E	F
37	1	K	Low	120.00	3	157.97
38	1	F	High	0.00	1	0
39	1	F	High	0.00	2	0
40	1	F	High	0.00	3	0
41	1	F	High	1.98	1	171.2
42	1	F	High	2.02	2	174.69
43	1	F	High	2.12	3	215.62
44	1	F	High	15.00	1	177.59
45	1	F	High	15.00	2	154.83
46	1	F	High	15.00	3	147.25
47	1	F	High	30.00	1	146.33
48	1	F	High	30.00	2	168.72
49	1	F	High	30.00	3	166.34
50	1	F	High	60.00	1	183.73
51	1	F	High	60.00	2	241.09
52	1	F	High	60.00	3	172.89
53	1	F	High	120.00	1	224.72
54	1	F	High	120.00	2	143.95
55	1	F	High	120.00	3	159.01
56	1	K	High	0.00	1	0
57	1	K	High	0.00	2	0
58	1	K	High	0.00	3	0
59	1	K	High	2.23	1	160.46
60	1	K	High	2.28	2	151.87
61	1	K	High	2.37	3	156.44
62	1	K	High	15.00	1	157.97
63	1	K	High	15.00	2	199.62
64	1	K	High	15.00	3	142.12
65	1	K	High	30.00	1	167.19
66	1	K	High	30.00	2	151.9
67	1	K	High	30.00	3	168.1
68	1	K	High	60.00	1	185.38
69	1	K	High	60.00	2	188.21
70	1	K	High	60.00	3	141.34
71	1	K	High	120.00	1	188.09
72	1	K	High	120.00	2	142.22
73	1	K	High	120.00	3	178.54

* Blank water reading average = 127.53 arbitrary units of fluorescence

Table 9. Washed Pellet Raw Data Experiment Two*

	A	B	C	D	E	F
74	Experiment	Colloid	Concentration	Time	Replicate	Fluorescence
75	2	F	Low	0.00	1	0
76	2	F	Low	0.00	2	0
77	2	F	Low	0.00	3	0
78	2	F	Low	1.40	1	138.2
79	2	F	Low	1.48	2	154.33
80	2	F	Low	1.55	3	140.83
81	2	F	Low	15.00	1	251.47
82	2	F	Low	15.00	2	259.04
83	2	F	Low	15.00	3	272.55
84	2	F	Low	30.00	1	226.2
85	2	F	Low	30.00	2	195.34
86	2	F	Low	30.00	3	253.27
87	2	F	Low	60.00	1	165.79
88	2	F	Low	60.00	2	181.44
89	2	F	Low	60.00	3	213.8
90	2	F	Low	120.00	1	153.46
91	2	F	Low	120.00	2	128.36
92	2	F	Low	120.00	3	196.68
93	2	K	Low	0.00	1	0
94	2	K	Low	0.00	2	0
95	2	K	Low	0.00	3	0
96	2	K	Low	1.72	1	154.04
97	2	K	Low	1.78	2	217.45
98	2	K	Low	1.83	3	140.06
99	2	K	Low	15.00	1	141.69
100	2	K	Low	15.00	2	147.97
101	2	K	Low	15.00	3	162.57
102	2	K	Low	30.00	1	219.19
103	2	K	Low	30.00	2	145.76
104	2	K	Low	30.00	3	184.18
105	2	K	Low	60.00	1	178.23
106	2	K	Low	60.00	2	208.27
107	2	K	Low	60.00	3	212.25
108	2	K	Low	120.00	1	212.64
109	2	K	Low	120.00	2	151.58
110	2	K	Low	120.00	3	187.55

* Blank water reading average = 143.20 arbitrary units of fluorescence

Table 9. Washed Pellet Raw Data Experiment Two* (continued)

	A	B	C	D	E	F
111	2	F	High	0.00	1	0
112	2	F	High	0.00	2	0
113	2	F	High	0.00	3	0
114	2	F	High	1.98	1	201.86
115	2	F	High	2.02	2	216.43
116	2	F	High	2.12	3	215.23
117	2	F	High	15.00	1	187.11
118	2	F	High	15.00	2	183.47
119	2	F	High	15.00	3	294.05
120	2	F	High	30.00	1	163.35
121	2	F	High	30.00	2	156.25
122	2	F	High	30.00	3	235.42
123	2	F	High	60.00	1	167.94
124	2	F	High	60.00	2	167.92
125	2	F	High	60.00	3	167.14
126	2	F	High	120.00	1	181.88
127	2	F	High	120.00	2	159.11
128	2	F	High	120.00	3	156.36
129	2	K	High	0.00	1	0
130	2	K	High	0.00	2	0
131	2	K	High	0.00	3	0
132	2	K	High	2.23	1	172.99
133	2	K	High	2.28	2	159.42
134	2	K	High	2.37	3	216.8
135	2	K	High	15.00	1	197.01
136	2	K	High	15.00	2	190.06
137	2	K	High	15.00	3	159.96
138	2	K	High	30.00	1	215.62
139	2	K	High	30.00	2	146.58
140	2	K	High	30.00	3	174.5
141	2	K	High	60.00	1	139.42
142	2	K	High	60.00	2	214.95
143	2	K	High	60.00	3	162.4
144	2	K	High	120.00	1	128.29
145	2	K	High	120.00	2	191.15
146	2	K	High	120.00	3	183.51

* Blank water reading average = 143.20 arbitrary units of fluorescence

Table 10. Washed Pellet Raw Data Experiment Three*

	A	B	C	D	E	F
147	Experiment	Colloid	Concentration	Time	Replicate	Fluorescence
148	3	F	Low	0.00	1	0
149	3	F	Low	0.00	2	0
150	3	F	Low	0.00	3	0
151	3	F	Low	1.40	1	285.11
152	3	F	Low	1.48	2	312.9
153	3	F	Low	1.55	3	273.29
154	3	F	Low	15.00	1	251.84
155	3	F	Low	15.00	2	237.26
156	3	F	Low	15.00	3	247.63
157	3	F	Low	30.00	1	218.74
158	3	F	Low	30.00	2	215.14
159	3	F	Low	30.00	3	228.06
160	3	F	Low	60.00	1	233.74
161	3	F	Low	60.00	2	280.44
162	3	F	Low	60.00	3	235.22
163	3	F	Low	120.00	1	213.29
164	3	F	Low	120.00	2	225.11
165	3	F	Low	120.00	3	205.57
166	3	K	Low	0.00	1	0
167	3	K	Low	0.00	2	0
168	3	K	Low	0.00	3	0
169	3	K	Low	1.72	1	213.08
170	3	K	Low	1.78	2	268.81
171	3	K	Low	1.83	3	210.06
172	3	K	Low	15.00	1	276.21
173	3	K	Low	15.00	2	217.65
174	3	K	Low	15.00	3	255.44
175	3	K	Low	30.00	1	198.58
176	3	K	Low	30.00	2	216.57
177	3	K	Low	30.00	3	219.1
178	3	K	Low	60.00	1	189.33
179	3	K	Low	60.00	2	201.67
180	3	K	Low	60.00	3	240.71
181	3	K	Low	120.00	1	172.31
182	3	K	Low	120.00	2	172.37
183	3	K	Low	120.00	3	175.44

* Blank water reading average = 178.78 arbitrary units of fluorescence

Table 10. Washed Pellet Raw Data Experiment Three* (continued)

	A	B	C	D	E	F
184	3	F	High	0.00	1	0
185	3	F	High	0.00	2	0
186	3	F	High	0.00	3	0
187	3	F	High	1.98	1	277.77
188	3	F	High	2.02	2	324.98
189	3	F	High	2.12	3	319.68
190	3	F	High	15.00	1	183.94
191	3	F	High	15.00	2	205.41
192	3	F	High	15.00	3	262.73
193	3	F	High	30.00	1	324.73
194	3	F	High	30.00	2	265.55
195	3	F	High	30.00	3	294.37
196	3	F	High	60.00	1	241.5
197	3	F	High	60.00	2	230.54
198	3	F	High	60.00	3	249.48
199	3	F	High	120.00	1	213.48
200	3	F	High	120.00	2	207.67
201	3	F	High	120.00	3	429.3
202	3	K	High	0.00	1	0
203	3	K	High	0.00	2	0
204	3	K	High	0.00	3	0
205	3	K	High	2.23	1	161.74
206	3	K	High	2.28	2	227.55
207	3	K	High	2.37	3	202.8
208	3	K	High	15.00	1	160.18
209	3	K	High	15.00	2	140.71
210	3	K	High	15.00	3	130.11
211	3	K	High	30.00	1	173.36
212	3	K	High	30.00	2	153.55
213	3	K	High	30.00	3	181.26
214	3	K	High	60.00	1	160
215	3	K	High	60.00	2	163.06
216	3	K	High	60.00	3	170.15
217	3	K	High	120.00	1	136.89
218	3	K	High	120.00	2	163.86
219	3	K	High	120.00	3	176.9

* Blank water reading average = 178.78 arbitrary units of fluorescence

Appendix D XDLVO Parameters

Table 11. XDLVO Parameters and References

Parameter		Quantity for MS2-MS2 Interaction	Quantity for KAO - MS2 Interaction	Quantity for FG - MS2 Interaction	Unit	Reference(s)
A_{ijk}	combined Hamaker constant, $M_i * L^2 / t^2$	7.50E-21	3.10E-20	8E-21	J	(Chrysikopoulos & Syngouna, 2012) ^{1,2} , (Yoon, Flinn, & Rabinovich, 1997)
r_p	average colloidal particle radius, L	1.25E-08	1.25E-08	1.25E-08	m	(Chrysikopoulos & Syngouna, 2012)
λ	characteristic wavelength of interaction between two approaching surfaces, L	0.0000001	0.0000001	0.0000001	m	(Chrysikopoulos & Syngouna, 2012)
ϵ_0	permittivity of free space (C ² /(J m))	8.85E-12	8.85E-12	8.85E-12	C ² /(Jm)	(Chrysikopoulos & Syngouna, 2012)
ϵ_r	relative dielectric constant of the suspending liquid (-)	7.84E+01	7.84E+01	7.84E+01	-	(Chrysikopoulos & Syngouna, 2012)
Ψ_p	surface potential of the colloid particle (V)	-2.00E-02	-2.00E-02	-2.00E-02	V	(Chrysikopoulos & Syngouna, 2012)
Ψ_s	surface potential of the collector surface (V)	-2.00E-02	-4.04E-02	-2.80E-02	V	(Chrysikopoulos & Syngouna, 2012) ^{1,2} , (Gutierrez et al., 2009) ³
K	Debye-Huckel parameter, 1/L	3.09E+06	3.09E+06	3.09E+06	1/m	Calculated
I_s	Ionic Strength	0.00000088	0.00000088	0.00000088	mol/L	Measured

$\Phi_{AB(h=h_0)}$	Lewis acid-base free energy of interaction at $h=h_0$ (J/m ²), M/t ²	-8.57E-25	-2.76E-24	-1.12E-22	J/nm ²	Calculated
H_0	minimum separation distance between two approaching surfaces, L	2.50E-01	2.50E-01	2.50E-01	nm	(Chrysikopoulos & Syngouna, 2012)
K_{123}	hydrophobic force constant (J), MjxL ² /t ²	1.35E-24	4.34E-24	1.76E-22	J	Calculated
$\theta_{MS2/KAO/FG}$	contact angle of MS2 (degree)	33.00	46.10	76.46	°	(Chrysikopoulos & Syngouna, 2012) ^{1,2} , (Van De Velde & Kiekens, 2000) ³

¹ Used for MS2, ² Used for KAO, ³ Used for FG

Bibliography

- American Society of Civil Engineers. (2017). 2017 Infrastructure Report Card: Wastewater Overview. Retrieved from <https://www.infrastructurereportcard.org/cat-item/wastewater/>
- Arduino, M., Finley, C., Ginsberg, M., Hilton, C., Lynch, M., Magnuson, M., ... Spiesman, A. (2015). *Progress on Water Sector Decontamination Recommendations & Proposed Strategic Plan*.
- Armanious, A., Aeppli, M., Jacak, R., Refardt, D., Sigstam, T., Kohn, T., & Sander, M. (2016). Viruses at Solid-Water Interfaces: A Systematic Assessment of Interactions Driving Adsorption. *Environmental Science and Technology*, 50(2), 732–743. <https://doi.org/10.1021/acs.est.5b04644>
- Attinti, R., Wei, J., Kniel, K., Sims, J., & Jin, Y. (2010). Virus' (MS2, phiX174, and Aichi) Attachment on Sand Measured by Atomic Force Microscopy and Their Transport through Sand Columns. *Environmental Science & Technology*, 44(7), 2426–2432.
- Baalousha, M., Lead, J., von der Kammer, F., & Hofmann, T. (2009). Environmental and Human Health Impacts of Nanotechnology. In J. R. Lead & E. Smith (Eds.), *Environmental and Human Health Impacts of Nanotechnology* (pp. 110–148). Blackwell Publishing Ltd. <https://doi.org/10.1002/9781444307504>
- Baer, D. R., & Engelhard, M. H. (2010). XPS analysis of nanostructured materials and biological surfaces. *Journal of Electron Spectroscopy and Related Phenomena*, 178–179(C), 415–432. <https://doi.org/10.1016/j.elspec.2009.09.003>
- Behrens, S. H., & Grier, D. G. (2001). The charge of glass and silica surfaces. *Journal of Chemical Physics*, 115(14), 6716–6721. <https://doi.org/10.1063/1.1404988>
- Bellou, M. I., Syngouna, V. I., Tselepi, M. A., Kokkinos, P. A., Paparrodopoulos, S. C., Vantarakis, A., & Chrysikopoulos, C. V. (2015). Interaction of human adenoviruses and coliphages with kaolinite and bentonite. *Science of the Total Environment*, 517, 86–95. <https://doi.org/10.1016/j.scitotenv.2015.02.036>
- Benbear, L. S., & Olmstead, S. M. (2008). The Impacts of the “ Right to Know ”: Information Disclosure and the Violation of Drinking Water Standards. *Journal of Environmental Economics and Management*, 56(2), 117–130.
- Berg, J. C. . (2010). *An Introduction to Interfaces & Colloids The Bridge to Nanoscience*

(1st ed.). Singapore: World Scientific Publishing Co. Pte. Ltd.

- Bharti, B., Meissner, J., Klapp, S. H. L., & Findenegg, G. H. (2014). Bridging interactions of proteins with silica nanoparticles: The influence of pH, ionic strength and protein concentration. *Soft Matter*, *10*(5), 718–728.
<https://doi.org/10.1039/c3sm52401a>
- Blanchard, G., Maunay, M., & Martin, G. (1984). Removal of heavy metals from waters by means of natural zeolites. *Water Research*, *18*(12), 1501–1507.
[https://doi.org/10.1016/0043-1354\(84\)90124-6](https://doi.org/10.1016/0043-1354(84)90124-6)
- Buffle, J., Wilkinson, K. J., Stoll, S., Filella, M., & Zhang, J. (1998). A generalized description of aquatic colloidal interactions: The three- colloidal component approach. *Environmental Science and Technology*, *32*(19), 2887–2899.
<https://doi.org/10.1021/es980217h>
- Burakov, A. E., Galunin, E. V., Burakova, I. V., Kucherova, A. E., Agarwal, S., Tkachev, A. G., & Gupta, V. K. (2018). Adsorption of heavy metals on conventional and nanostructured materials for wastewater treatment purposes: A review. *Ecotoxicology and Environmental Safety*, *148*, 702–712.
<https://doi.org/10.1016/j.ecoenv.2017.11.034>
- Chang, R. (2007). *Chemistry* (9th ed.). New York: McGraw-Hill Companies, Inc.
- Chattopadhyay, S., & Puls, R. W. (2000). Forces dictating colloidal interactions between viruses and soil. *Chemosphere*, *41*(8), 1279–1286. [https://doi.org/10.1016/S0045-6535\(99\)00519-6](https://doi.org/10.1016/S0045-6535(99)00519-6)
- Chattopadhyay, S., & Taft, S. (2018). *Exposure Pathways to High-Consequence Pathogens in the Wastewater Collection and Treatment Systems Exposure Pathways to High-Consequence Pathogens in the Wastewater Collection and Treatment Systems*.
- Chaudhry, R. M., Holloway, R. W., Cath, T. Y., & Nelson, K. L. (2015). Impact of virus surface characteristics on removal mechanisms within membrane bioreactors. *Water Research*, *84*, 144–152. <https://doi.org/10.1016/j.watres.2015.07.020>
- Chrysikopoulos, C. V., & Syngouna, V. I. (2012). Attachment of bacteriophages MS2 and ΦX174 onto kaolinite and montmorillonite: Extended-DLVO interactions. *Colloids and Surfaces B: Biointerfaces*, *92*, 74–83.
<https://doi.org/10.1016/j.colsurfb.2011.11.028>

- Cunha, A. G., & Gandini, A. (2010). Turning polysaccharides into hydrophobic materials: A critical review. Part 2. Hemicelluloses, chitin/chitosan, starch, pectin and alginates. *Cellulose*, *17*(6), 1045–1065. <https://doi.org/10.1007/s10570-010-9435-5>
- Dika, C., Gantzer, C., Perrin, A., & Duval, J. F. L. (2013). Impact of the virus purification protocol on aggregation and electrokinetics of MS2 phages and corresponding virus-like particles. *Physical Chemistry Chemical Physics*, *15*(15), 5691–5700. <https://doi.org/10.1039/c3cp44128h>
- EPA. (n.d.). Learn about Small Drinking Water Systems. Retrieved from www.epa.gov
- EPA. (2016). *Drinking Water: EPA Needs to Take Additional Steps to Ensure Small Community Water Systems Designated as Serious Violators Achieve Compliance, Report Number 16-P-0108*. Washington D.C.
- Fanun, M. (Ed.). (2014). *The role of colloidal systems in environmental protection*. Amsterdam: Elsevier.
- Floyd, R., & Sharp, D. G. (1979). Viral aggregation: Buffer effects in the aggregation of poliovirus and reovirus at low and high pH. *Applied and Environmental Microbiology*, *38*(3), 395–401.
- Fu, Y., & Li, J. (2016). A novel delivery platform based on Bacteriophage MS2 virus-like particles. *Virus Research*, *211*, 9–16. <https://doi.org/10.1016/j.virusres.2015.08.022>
- Gentile, G. J., Cruz, M. C., Rajal, V. B., & Fidalgo de Cortalezzi, M. M. (2018). Electrostatic interactions in virus removal by ultrafiltration membranes. *Journal of Environmental Chemical Engineering*, *6*(1), 1314–1321. <https://doi.org/10.1016/j.jece.2017.11.041>
- Gerba, C. P. (1984). Applied and Theoretical Aspects of Virus Adsorption to Surfaces. *Advances in Applied Microbiology*, *30*, 133–168. [https://doi.org/10.1016/S0065-2164\(08\)70054-6](https://doi.org/10.1016/S0065-2164(08)70054-6)
- Gustafsson, Ö., & Gschwend, P. M. (1997). Aquatic colloids: Concepts, definitions, and current challenges. *Limnology and Oceanography*, *42*(3), 519–528.
- Gutierrez, L., Li, X., Wang, J., Nangmenyi, G., Economy, J., Kuhlenschmidt, T. B., ... Nguyen, T. H. (2009). Adsorption of rotavirus and bacteriophage MS2 using glass fiber coated with hematite nanoparticles. *Water Research*, *43*(20), 5198–5208. <https://doi.org/10.1016/j.watres.2009.08.031>

- Hakim, A., & Kobayashi, M. (2018). Aggregation and charge reversal of humic substances in the presence of hydrophobic monovalent counter-ions: Effect of hydrophobicity of humic substances. *Colloids and Surfaces A: Physicochemical and Engineering Aspects*, 540(November 2017), 1–10. <https://doi.org/10.1016/j.colsurfa.2017.12.065>
- Harwood, V. J., Jiang, S., & Sobsey, M. D. (2015). Review of Coliphages as Possible Indicator Organisms of Fecal Contamination for Ambient Water Quality.
- Hashimoto, K., Matsuda, M., Inoue, D., & Ike, M. (2014). Bacterial community dynamics in a full-scale municipal wastewater treatment plant employing conventional activated sludge process. *Journal of Bioscience and Bioengineering*, 118(1), 64–71. <https://doi.org/10.1016/j.jbiosc.2013.12.008>
- Hennebert, P., Avellan, A., Yan, J., & Aguerre-Chariol, O. (2013). Experimental evidence of colloids and nanoparticles presence from 25 waste leachates. *Waste Management*, 33(9), 1870–1881. <https://doi.org/10.1016/j.wasman.2013.04.014>
- Hiradate, S., Yonezawa, T., & Takesako, H. (2006). Isolation and purification of hydrophilic fulvic acids by precipitation. *Geoderma*, 132(1–2), 196–205. <https://doi.org/10.1016/j.geoderma.2005.05.007>
- Hmaied, F., & Jebri, S. (2013). Use of Bacteriophages as Surrogate Indicators of Viruses in Water. In C. Denton & R. Crosby (Eds.), *Bacteriophages: Biology, Applications and Role in Health and Disease* (p. ebook). Sidi Thabet, Tunisie.
- Hoff, J. C., & Akin, E. W. (2018). Removal of Viruses from Raw Waters by Treatment Processes. In G. Berg (Ed.), *Viral Pollution of the Environment*. Baton Rouge: Taylor & Francis Group.
- Hu, X., Ren, C., Kang, W., Mu, L., Liu, X., Li, X., ... Zhou, Q. (2018). Characterization and toxicity of nanoscale fragments in wastewater treatment plant effluent. *Science of The Total Environment*, 626, 1332–1341. <https://doi.org/10.1016/j.scitotenv.2018.01.180>
- Israelachvili, J. N. (2011). *Intermolecular and Surface Forces: Third Edition*. *Intermolecular and Surface Forces: Third Edition*. <https://doi.org/10.1016/C2011-0-05119-0>
- IUPAC. (2002). No Title. Retrieved from http://old.iupac.org/reports/2001/colloid_2001/manual_of_s_and_t/node8.%0Ahtml

- Jiang, N., Shang, R., Heijman, S. G. J., & Rietveld, L. C. (2018). High-silica zeolites for adsorption of organic micro-pollutants in water treatment : A review. *Water Research*, *144*, 145–161. <https://doi.org/10.1016/j.watres.2018.07.017>
- Keller, A. A., & Lazareva, A. (2013). Predicted Releases of Engineered Nanomaterials: From Global to Regional to Local. *Environmental Science and Technology Letters*, *1*(1), 65–70. <https://doi.org/10.1021/ez400106t>
- Khan, I., Saeed, K., & Khan, I. (2017). Nanoparticles: Properties, applications and toxicities. *Arabian Journal of Chemistry*. <https://doi.org/10.1016/j.arabjc.2017.05.011>
- Kosmulski, M. (2009). pH-dependent surface charging and points of zero charge. IV. Update and new approach. *Journal of Colloid and Interface Science*, *337*(2), 439–448. <https://doi.org/10.1016/j.jcis.2009.04.072>
- Kumar, N., Zhao, C., Klaassen, A., Van den Ende, D., Mugele, F., & Siretanu, I. (2016). Characterization of the surface charge distribution on kaolinite particles using high resolution atomic force microscopy. *Geochimica et Cosmochimica Acta*, *175*, 100–112. <https://doi.org/10.1016/j.gca.2015.12.003>
- Langlet, J., Gaboriaud, F., Duval, J. F. L., & Gantzer, C. (2008). Aggregation and surface properties of F-specific RNA phages: Implication for membrane filtration processes. *Water Research*, *42*(10–11), 2769–2777. <https://doi.org/10.1016/j.watres.2008.02.007>
- Levine, A. D., Tchobanoglous, G., Asano, T., Journal, S., Pollution, W., Federation, C., & Jul, N. (1985). Characterization of the Size Distribution of Contaminants in Wastewater: Treatment and Reuse Implications. *Water Pollution Control Federation*, *57*(7), 805–816. <https://doi.org/10.2307/25042701>
- Levy, B. S., & Sidel, V. W. (2011). Water Rights and Water Fights : Preventing and Resolving Conflicts Before They Boil Over. *American Journal of Public Health*, *101*(5), 778–781. <https://doi.org/10.2105/AfPH.2010.194670>
- Li, L., Stoiber, M., Wimmer, A., Xu, Z., Lindenblatt, C., Helmreich, B., & Schuster, M. (2016). To What Extent Can Full-Scale Wastewater Treatment Plant Effluent Influence the Occurrence of Silver-Based Nanoparticles in Surface Waters? *Environmental Science and Technology*, *50*(12), 6327–6333. <https://doi.org/10.1021/acs.est.6b00694>
- Lin, K., & Marr, L. C. (2017). Aerosolization of Ebola Virus Surrogates in Wastewater

Systems. *Environmental Science and Technology*, 51(5), 2669–2675.
<https://doi.org/10.1021/acs.est.6b04846>

Madigan, M. T., & Martinko, J. P. (1996). *Brock Biology of Microorganisms* (8th ed.). New Jersey: Prentice-Hall International.

Mattle, M. J., Crouzy, B., Brennecke, M., R. Wigginton, K., Perona, P., & Kohn, T. (2011). Impact of virus aggregation on inactivation by peracetic acid and implications for other disinfectants. *Environmental Science and Technology*, 45(18), 7710–7717. <https://doi.org/10.1021/es201633s>

McNew, C. P., Kananizadeh, N., Li, Y., & LeBoeuf, E. J. (2017). The attachment of colloidal particles to environmentally relevant surfaces and the effect of particle shape. *Chemosphere*, 168, 65–79.
<https://doi.org/10.1016/j.chemosphere.2016.10.039>

Meissner, J., Prause, A., Bharti, B., & Findenegg, G. H. (2015). Characterization of protein adsorption onto silica nanoparticles: influence of pH and ionic strength. *Colloid and Polymer Science*, 293(11), 3381–3391. <https://doi.org/10.1007/s00396-015-3754-x>

Michen, B., & Graule, T. (2010). Isoelectric points of viruses. *Journal of Applied Microbiology*, 109(2), 388–397. <https://doi.org/10.1111/j.1365-2672.2010.04663.x>

Moore, B. E., Sagik, B. P., & J.F. Jr., M. (1975). Viral association with suspended solids. *Water Research*, 9(2), 197–203. [https://doi.org/10.1016/0043-1354\(75\)90009-3](https://doi.org/10.1016/0043-1354(75)90009-3)

Nel, A., Xia, T., Madler, L., & Li, N. (2006). Toxic Potential of Materials at the Nanolevel. *Science*, 311(5761), 622–627. <https://doi.org/10.1126/science.1114397>

Papadopoulos, A., Fatta, D., Parperis, K., Mentzis, A., Haralambous, K. J., & Loizidou, M. (2004). Nickel uptake from a wastewater stream produced in a metal finishing industry by combination of ion-exchange and precipitation methods. *Separation and Purification Technology*, 39(3), 181–188.
<https://doi.org/10.1016/j.seppur.2003.10.010>

Park, J. A., & Kim, S. B. (2015). DLVO and XDLVO calculations for bacteriophage MS2 adhesion to iron oxide particles. *Journal of Contaminant Hydrology*, 181, 131–140. <https://doi.org/10.1016/j.jconhyd.2015.01.005>

Roffey, R., Lantorp, K., Tegnell, A., & Elgh, F. (2002). Biological weapons and bioterrorism preparedness : importance of public-health awareness and international

- cooperation. *Clinical Microbiology & Infection*, 8(8), 522–528.
- Sakoda, A., Sakai, Y., Hayakawa, K., & Suzuki, M. (1997). Adsorption of viruses in water environment onto solid surfaces. *Water Science Technology*, 35(7), 107–114.
- Shen, Y., Kim, H., Tong, M., & Li, Q. (2011). Influence of solution chemistry on the deposition and detachment kinetics of RNA on silica surfaces. *Colloids and Surfaces B: Biointerfaces*, 82(2), 443–449. <https://doi.org/10.1016/j.colsurfb.2010.09.018>
- Shi, X., Li, Z., Chen, W., Qiang, L., Xia, J., Chen, M., ... Alvarez, P. J. J. (2016). Fate of TiO₂ nanoparticles entering sewage treatment plants and bioaccumulation in fish in the receiving streams. *NanoImpact*, 3–4, 96–103. <https://doi.org/10.1016/j.impact.2016.09.002>
- Shin, G. A., & Sobsey, M. D. (1998). Reduction of norwalk virus, poliovirus 1 and coliphage MS2 by monochloramine disinfection of water. *Water Science and Technology*, 38(12), 151–154. <https://doi.org/10.1128/AEM.69.7.3975>
- Shishovs, M., Rumnieks, J., Diebolder, C., Jaudzems, K., Andreas, L. B., Stanek, J., ... Tars, K. (2016). Structure of AP205 Coat Protein Reveals Circular Permutation in ssRNA Bacteriophages. *Journal of Molecular Biology*, 428, 4267–4279. <https://doi.org/10.1016/j.jmb.2016.08.025>
- Skripkin, E. A., Adhin, M. R., de Smit, M. H., & van Duin, J. (1990). Secondary structure of the central region of bacteriophage MS2 RNA. *Journal of Molecular Biology*, 211, 447–463.
- Stagg, C. H., Wallis, C., & Ward, C. H. (1977). Inactivation of Clay-Associated Bacteriophage MS-2 by Chlorine. *Applied and Environmental Microbiology*, 33(2), 385–391.
- Stumm, W., & Morgan, J. J. (1996). *Aquatic chemistry : chemical equilibria and rates in natural waters* (3rd ed.). New York: Wiley.
- Stuntz, S. (2018). *The Effect of MS2 Bacteriophage on the Activity and Performance of Activated Sludge*. Air Force Institute of Technology.
- Templeton, M. R., Andrews, R. C., & Hofmann, R. (2005). Inactivation of particle-associated viral surrogates by ultraviolet light. *Water Research*, 39(15), 3487–3500. <https://doi.org/10.1016/j.watres.2005.06.010>
- Timchak, E., & Gitis, V. (2012). A combined degradation of dyes and inactivation of

viruses by UV and UV/H₂O₂. *Chemical Engineering Journal*, 192, 164–170.
<https://doi.org/10.1016/j.cej.2012.03.054>

Tong, M., Shen, Y., Yang, H., & Kim, H. (2012). Deposition kinetics of MS2 bacteriophages on clay mineral surfaces. *Colloids and Surfaces B: Biointerfaces*, 92, 340–347. <https://doi.org/10.1016/j.colsurfb.2011.12.017>

Toropova, K., Basnak, G., Twarock, R., Stockley, P. G., & Ranson, N. A. (2008). The Three-dimensional Structure of Genomic RNA in Bacteriophage MS2: Implications for Assembly. *Journal of Molecular Biology*, 375(3), 824–836.
<https://doi.org/10.1016/j.jmb.2007.08.067>

U.S. Environmental Protection Agency. (2001). *Method 1601: Male-specific (F+) and Somatic Coliphage in Water by Two-step Enrichment Procedure*. Washington, D.C.

USAID. (2017). *U.S. Government Global Water Strategy*. Retrieved from https://www.usaid.gov/sites/default/files/documents/1865/Global_Water_Strategy_2017_final_508v2.pdf

Van De Velde, K., & Kiekens, P. (2000). Wettability and surface analysis of glass fibres. *Indian Journal of Fibre and Textile Research*, 25(March), 8–13.

van Oss, C. J. (2006). *Interfacial Forces in Aqueous Media*. Boca Raton: Taylor & Francis Group.

Walshe, G. E., Pang, L., Flury, M., Close, M. E., & Flintoft, M. (2010). Effects of pH, ionic strength, dissolved organic matter, and flow rate on the co-transport of MS2 bacteriophages with kaolinite in gravel aquifer media. *Water Research*, 44(4), 1255–1269. <https://doi.org/10.1016/j.watres.2009.11.034>

Wang, Q., Wang, P., & Yang, Q. (2018). Science of the Total Environment Occurrence and diversity of antibiotic resistance in untreated hospital wastewater. *Science of the Total Environment*, 621, 990–999. <https://doi.org/10.1016/j.scitotenv.2017.10.128>

Wang, R. Q., Gutierrez, L., Choon, N. S., & Croué, J. P. (2015). Hydrophilic interaction liquid chromatography method for measuring the composition of aquatic humic substances. *Analytica Chimica Acta*, 853(1), 608–616.
<https://doi.org/10.1016/j.aca.2014.09.026>

Water and Wastewater, & Sector Strategic Roadmap Work Group. (2017). *Roadmap to a Secure and Resilient Water and Wastewater Sector*.

- Water Environment Research Foundation. (2016). *Handling , Management , and Treatment of Bio-Contaminated Wastewater*. Alexandria.
- Weber Jr., W. J., & DiGiano, F. A. (1996). *Process Dynamics in Environmental Systems*. New York: John Wiley & Sons, Inc.
- Wienczek, K. M., Klapes, N. A., & Foegeding, P. M. (1990). Hydrophobicity of Bacillus and Clostridium spores. *Applied and Environmental Microbiology*, 56(9), 2600–2605. <https://doi.org/0099-2240/90/092600-06>
- Wu, X., Feng, Z., Yuan, B., Zhou, Z., Li, F., & Sun, W. (2018). Effects of solution chemistry on the sunlight inactivation of particles-associated viruses MS2. *Colloids and Surfaces B: Biointerfaces*, 162, 179–185. <https://doi.org/10.1016/j.colsurfb.2017.11.056>
- Yoon, R. H., Flinn, D. H., & Rabinovich, Y. I. (1997). Hydrophobic interactions between dissimilar surfaces. *Journal of Colloid and Interface Science*, 185(2), 363–370. <https://doi.org/10.1006/jcis.1996.4583>
- Zhang, W., & Zhang, X. (2015). Adsorption of MS2 on oxide nanoparticles affects chlorine disinfection and solar inactivation. *Water Research*, 69, 59–67. <https://doi.org/10.1016/j.watres.2014.11.013>
- Zhou, Z., & Gunter, W. D. (1992). The nature of the surface charge of kaolinite. *Clays and Clay Minerals*, 40(3), 365–368. <https://doi.org/10.1346/CCMN.1992.0400320>
- Zoli, C., Steinberg, L. J., Grabowski, M., & Hermann, M. (2018). Terrorist critical infrastructures , organizational capacity and security risk. *Safety Science*, 110(May), 121–130. <https://doi.org/10.1016/j.ssci.2018.05.021>

REPORT DOCUMENTATION PAGE			<i>Form Approved</i> <i>OMB No. 074-0188</i>		
<p>The public reporting burden for this collection of information is estimated to average 1 hour per response, including the time for reviewing instructions, searching existing data sources, gathering and maintaining the data needed, and completing and reviewing the collection of information. Send comments regarding this burden estimate or any other aspect of the collection of information, including suggestions for reducing this burden to Department of Defense, Washington Headquarters Services, Directorate for Information Operations and Reports (0704-0188), 1215 Jefferson Davis Highway, Suite 1204, Arlington, VA 22202-4302. Respondents should be aware that notwithstanding any other provision of law, no person shall be subject to a penalty for failing to comply with a collection of information if it does not display a currently valid OMB control number.</p> <p style="text-align: center;">PLEASE DO NOT RETURN YOUR FORM TO THE ABOVE ADDRESS.</p>					
1. REPORT DATE (DD-MM-YYYY) 21-03-2019		2. REPORT TYPE Master's Thesis		3. DATES COVERED (From - To) October 2017 - March 2019	
TITLE AND SUBTITLE Virus adsorption to colloids in water: Interactions between bacteriophage MS2, kaolinite, and fiberglass			5a. CONTRACT NUMBER DW-057-92440901-3		
			5b. GRANT NUMBER		
			5c. PROGRAM ELEMENT NUMBER		
6. AUTHOR(S) Ellis, Ashlee N., Captain, USAF			5d. PROJECT NUMBER 19V107		
			5e. TASK NUMBER		
			5f. WORK UNIT NUMBER		
7. PERFORMING ORGANIZATION NAMES(S) AND ADDRESS(S) Air Force Institute of Technology Graduate School of Engineering and Management (AFIT/ENV) 2950 Hobson Way, Building 640 WPAFB OH 45433-8865			8. PERFORMING ORGANIZATION REPORT NUMBER AFIT-ENV-MS-19-M-171		
9. SPONSORING/MONITORING AGENCY NAME(S) AND ADDRESS(ES) Matthew L. Magnuson, Ph.D. Environmental Protection Agency Office of Research and Development/National Homeland Security Research Center Water Infrastructure Protection Division MS NG-16 26 W. Martin Luther King Drive Cincinnati, OH 45268			10. SPONSOR/MONITOR'S ACRONYM(S) US EPA		
			11. SPONSOR/MONITOR'S REPORT NUMBER(S)		
12. DISTRIBUTION/AVAILABILITY STATEMENT DISTRIBUTION STATEMENT A. APPROVED FOR PUBLIC RELEASE; DISTRIBUTION UNLIMITED.					
13. SUPPLEMENTARY NOTES This material is declared a work of the U.S. Government and is not subject to copyright protection in the United States.					
14. ABSTRACT Virus adsorption to colloidal particles is an important issue for wastewater treatment plants accepting biohazardous waste. Colloids impact the transport of viruses, and provide protection against oxidants and other destructive mechanisms. This study investigated adsorption of bacteriophage MS2 to colloidal suspensions of kaolinite (KAO) and fiber glass (FG). Laboratory batch tests performed over a range of experimental conditions determined kinetic rate constants and characterized bond strength. Computational experiments assessed adsorption and aggregation of MS2. First order removal rate constants were faster than previously reported (between 2.5 - 2.8 min ⁻¹ and 0.4 - 2.8 min ⁻¹ for KAO and FG respectively). Evidence of MS2 adsorption was collected with fluorescent and bright field microscopic images, showing MS2 clusters associated with colloidal particles. After two-hours the 55.2% - 80.8% of the adsorbed MS2 was tightly bound in the FG experiment and 54.8% - 87.9% in the KAO experiment. This implies MS2 has a stronger affinity for KAO than FG. MS2 aggregation was also observed experimentally and predicted with XDLVO models. These results show colloids can quickly and strongly attach to clusters of viruses, leading to significant implications for management of biohazardous wastes at water recovery facilities.					
15. SUBJECT TERMS Adsorption, fluorescence, colloid, wastewater treatment, transport, MS2, aggregation, kinetic rate constant, XLDVO					
16. SECURITY CLASSIFICATION OF:			17. LIMITATION OF ABSTRACT	18. NUMBER OF PAGES 110	19a. NAME OF RESPONSIBLE PERSON Willie Harper, Jr, AFIT/ENV
a REPORT	b. ABSTRACT	c. THIS PAGE			19b. TELEPHONE NUMBER (Include area code) (937) 255-3636 ext. 4528
U	U	U	UU		

Standard Form 298 (Rev. 8-98)
Prescribed by ANSI Std. Z39-18